

1 **Characteristics of recessional moraines at a temperate glacier in**  
2 **SE Iceland: insights into patterns, rates and drivers of glacier**  
3 **retreat**

4 Benjamin M. P. Chandler \*, David J. A. Evans and David H. Roberts

5 Department of Geography, Durham University, Durham, UK

6 \* Correspondence to: Benjamin M. P. Chandler, School of Geography, Queen Mary University  
7 of London, Mile End Road, London, E1 4NS, UK. Email: [b.m.p.chandler@qmul.ac.uk](mailto:b.m.p.chandler@qmul.ac.uk)

8

9

10

11

12

13

14

15

16

17

18

19

20

21

22

23

24 **Abstract**

25

26 Icelandic glaciers are sensitive to climate variability on short-term timescales owing to their  
27 North Atlantic maritime setting, and have been undergoing ice-marginal retreat since the mid-  
28 1990s. Recent patterns, rates and drivers of ice-frontal retreat at Skálafellsjökull, SE Iceland,  
29 are examined using small-scale recessional moraines as a geomorphological proxy. These  
30 small-scale recessional moraines exhibit distinctive sawtooth planform geometries, and are  
31 constructed by a range of genetic processes associated with minor ice-margin re-advance,  
32 including (i) combined push/squeeze mechanisms, (ii) bulldozing of pre-existing proglacial  
33 material, and (iii) submarginal freeze-on. Remote-sensing investigations and lichenometric  
34 dating highlight sequences of annually-formed recessional moraines on the northern and central  
35 parts of the foreland. Conversely, moraines are forming on a sub-annual timescale at the  
36 southeastern Skálafellsjökull margin. Using annual moraine spacing as a proxy for annual ice-  
37 margin retreat rates (IMRRs), we demonstrate that prominent periods of glacier retreat at  
38 Skálafellsjökull are coincident with those at other Icelandic outlet glaciers, as well as those  
39 identified at Greenlandic outlet glaciers. Analysis of IMRRs and climate data suggests summer  
40 air temperature, sea surface temperature and the North Atlantic Oscillation have an influence  
41 on IMRRs at Skálafellsjökull, with the glacier appearing to be most sensitive to summer air  
42 temperature. On the basis of further climate data analyses, we hypothesise that sea surface  
43 temperature may drive air temperature changes in the North Atlantic region, which in turn  
44 forces IMRRs. The increase in sea surface temperature over recent decades may link to  
45 atmospheric-driven variations in North Atlantic subpolar gyre dynamics.

46

47 **Keywords:** recessional moraines; ice-marginal retreat; glacier-climate interactions;  
48 Skálafellsjökull; Iceland

49 **1. Introduction**

50

51 Iceland lies in a climatically important location in the North Atlantic, situated at the boundary  
52 between polar and mid-latitude atmospheric circulation cells and oceanic currents  
53 (Guðmundsson, 1997; Bradwell et al., 2006; Geirsdóttir et al., 2009). As a consequence of this  
54 maritime setting, the temperate glaciers of Iceland are particularly sensitive to climatic  
55 fluctuations on an annual to decadal scale, and have exhibited rapid rates of ice-marginal retreat  
56 and mass loss during the past decade (e.g. Jóhannesson, 1986; Sigurðsson and Jónsson, 1995;  
57 Aðalgeirsdóttir et al., 2006; Sigurðsson et al., 2007; Björnsson and Pálsson, 2008; Björnsson  
58 et al., 2013; Bradwell et al., 2013; Mernild et al., 2014; Phillips et al., 2014; Hannesdóttir et  
59 al., 2015a, b). Icelandic glacier termini variations during the observational period (since  
60 ~1930s) have previously been argued to be associated with fluctuations of summer air  
61 temperature (e.g. Boulton, 1986; Sigurðsson and Jónsson, 1995; Jóhannesson and Sigurðsson,  
62 1998; Bradwell, 2004a; Sigurðsson et al., 2007; Bradwell et al., 2013). However, there has  
63 been limited consideration of other climate variables (e.g. sea surface temperature and the  
64 North Atlantic Oscillation) and the complex interactions between them (e.g. Kirkbride, 2002;  
65 Mernild et al., 2014). This restricts current understanding of contemporary Icelandic glacier  
66 change and its wider significance. Thus, a thorough assessment of the patterns, rates and drivers  
67 of ice-frontal retreat currently evident in Iceland is of key importance.

68

69 Small-scale, annual ice-marginal fluctuations are manifest in the form of annual moraines in  
70 front of many active temperate glaciers in Iceland and elsewhere (Thórarinsson, 1967; Price,  
71 1970; Worsley, 1974; Sharp, 1984; Boulton, 1986; Matthews et al., 1995; Evans and Twigg,  
72 2002; Bradwell, 2004a; Schomacker et al., 2012; Bradwell et al., 2013; Reinardy et al., 2013;  
73 Hiemstra et al., 2015). According to previous studies, annual moraines are formed by short-

74 lived seasonal re-advances of the ice-front during a period of overall retreat (e.g. Andersen and  
75 Sollid, 1971; Boulton, 1986; Krüger, 1995). Provided recession during the summer (ablation  
76 season) is greater than advance during the winter (accumulation season) over consecutive  
77 years, a long sequence of inset, consecutively younger annual moraines may be formed  
78 (Boulton, 1986; Krüger, 1995; Bennett, 2001; Lukas, 2012). Consequently, annual moraines  
79 potentially record a seasonal signature of glacier response to climate variations, and have been  
80 subject to renewed interest over recent years (e.g. Bradwell, 2004a; Beedle et al., 2009; Lukas,  
81 2012; Bradwell et al., 2013; Reinardy et al., 2013).

82

83 Given the potential of annual moraines as a terrestrial climate archive, detailed examination of  
84 the characteristics of annual moraines on the forelands of Icelandic glaciers could yield  
85 valuable insights into the nature of, and controls on, recent ice-marginal retreat. In this study,  
86 we apply small-scale recessional moraines on the foreland of Skálafellsjökull, SE Iceland, as a  
87 geomorphological proxy to examine patterns, rates and drivers of ice-marginal retreat since the  
88 1930s. These recessional moraines have previously been argued to form on an annual basis in  
89 response to seasonally-driven processes (cf. Sharp, 1984, Evans and Orton, 2015), and this  
90 concept is re-examined in this paper. We integrate multiple methods at a range of spatial and  
91 temporal scales in order to examine the characteristics of the recessional moraines, wherefrom  
92 the significance of patterns and rates of recent ice-marginal retreat at Skálafellsjökull are  
93 assessed.

94

## 95 **2. Study site**

96

97 Skálafellsjökull is a non-surging piedmont outlet lobe draining the southeastern margin of the  
98 Vatnajökull ice-cap, flowing for ~24 km (Table 1) from the Breiðabunga plateau and

99 descending steeply onto a low elevation (20–60 m a.s.l.) foreland (Hannesdóttir et al., 2014,  
100 2015a, b; Evans and Orton, 2015). At its northern margin, the piedmont lobe is topographically  
101 confined by the Hafrafellsháls mountain spur, which reaches a maximum elevation of ~1008  
102 m a.s.l. (Evans and Orton, 2015). In the southern part of the foreland, the present-day glacier  
103 terminates near an area of heavily abraded, basalt bedrock outcrops on Hjallar. Two proglacial  
104 lakes front the contemporary Skálafellsjökull ice-margin, the largest being situated at the  
105 central sector of the margin (Figure 1). The development of ice-marginal lakes is a  
106 characteristic feature of the retreating southern Vatnajökull outlet glaciers (e.g. Howarth and  
107 Price 1969; Price and Howarth 1970; Evans et al. 1999a; Evans and Twigg 2002; Björnsson et  
108 al., 2001; Nick et al., 2007; Schomacker, 2010). Recent mapping of the surficial geology and  
109 glacial geomorphology (Evans and Orton, 2015) has demonstrated that the glacier foreland is  
110 characterised by the three diagnostic depositional domains of the active temperate landsystem:  
111 marginal morainic, subglacial and glaciofluvial/glaciolacustrine (cf. Krüger, 1994; Evans and  
112 Twigg, 2002; Evans, 2003, and references therein).

113  
114 Much debate remains regarding the veracity of the Skálafellsjökull Little Ice Age (LIA)  
115 maximum and its subsequent retreat pattern, with the application of different lichenometric  
116 dating techniques having resulted in contrasting age assignments (cf. Evans et al., 1999a;  
117 McKinzey et al., 2004, 2005; Evans and Orton, 2015). However, documentary and  
118 photographic evidence indicate Skálafellsjökull formerly coalesced with the neighbouring  
119 Heinabergsjökull on the coastal plain of Hornafjörður, and they remained confluent until  
120 sometime between 1929 and 1945 (Danish General Staff, 1904; Wadell, 1920; Roberts et al.,  
121 1933; Thórarinsson, 1943; Pálsson, 1945; Hannesdóttir et al., 2014). By the time of the US  
122 Army Map Service aerial photograph survey in 1945, the glaciers had separated. Ice-front  
123 measurements conducted at the glacier since the 1930s indicate Skálafellsjökull has undergone

124 similar fluctuations to other Vatnajökull outlet glaciers (Figure 2). The ice-front retreated  
125 during the period 1932–1957, with particularly rapid ice-marginal retreat occurring between  
126 1937 and 1942 ( $\sim 41 \text{ m a}^{-1}$ ). Since the 1970s, measurements have been sporadic, limiting  
127 understanding of the behaviour of this outlet glacier. Thus, the sequences of recessional  
128 (annual) moraines previously identified on the Skálafellsjökull foreland (Sharp, 1984; Evans  
129 and Orton, 2015) offer the opportunity to gain important insights into ice-frontal fluctuations.

130

### 131 **3. Methods**

132

#### 133 3.1. Geomorphological mapping

134

135 Geomorphological mapping was undertaken through a combination of remote-sensing and  
136 field-based approaches, providing a framework for exploring the characteristics of the  
137 recessional moraines at Skálafellsjökull. The remote-sensing data included high-resolution  
138 scans of 2006 colour aerial photographs (0.41 m Ground Sample Distance (GSD)),  
139 multispectral (8-band) WorldView-2 satellite imagery captured in June 2012 (2.0 m GSD) and  
140 associated panchromatic images (0.5 m GSD), along with a Digital Elevation Model (DEM)  
141 generated from Unmanned Aerial Vehicle (UAV) -captured imagery (spatial resolution: 0.09  
142 m). This approach of integrating multiple remote-sensing datasets, augmented by field  
143 mapping, has been applied in a variety of contemporary and ancient glacial landscapes (e.g.  
144 Bennett et al., 2010; Boston, 2012; Bradwell et al., 2013; Reinardy et al., 2013; Brynjólfsson  
145 et al., 2014; Darvill et al., 2014; Evans et al., 2014, 2015; Jónsson et al., 2014; Pearce et al.,  
146 2014; Schomacker et al., 2014). Further details on the image processing, mapping techniques  
147 and map production are presented elsewhere (Chandler et al., 2015).

148

149 3.2. Chronological techniques

150

151 A chronological framework for the recessional moraines was established using two approaches:  
152 (i) examination and cross-correlation of imagery spanning the period 1945–2012; and (ii)  
153 lichenometric surveys of a sub-sample of moraines. Lichenometric dating conducted in this  
154 study employed the largest lichen (LL) and size-frequency (SF) approaches, following the  
155 strategy previously applied to annual moraines elsewhere in SE Iceland (cf. Bradwell, 2001,  
156 2004a, b; Bradwell et al., 2013). This sampling approach involves measuring the longest axis  
157 of >200 thalli of lichen *Rhizocarpon* Section *Rhizocarpon* in fixed area quadrats on the ice-  
158 proximal slopes of moraines (cf. Bradwell, 2001, for further details). The longest axes were  
159 measured to the nearest millimetre using a ruler, with thalli less than 5 mm in diameter omitted  
160 from the surveys. Although callipers may have smaller *instrumental errors* (e.g. Karlén and  
161 Black, 2002), a *measurement error* of  $\pm 1$  mm is most realistic and a ruler was therefore deemed  
162 sufficient (cf. Innes, 1985; Osborn et al., 2015). Elongate and irregular thalli were measured  
163 regardless of their shape, whilst coalescent thalli were disregarded (Bradwell, 2001; 2004a, b).  
164 Sampling was restricted to the ice-proximal slopes as (i) the distal slope may, theoretically, be  
165 colonised prior to abandonment of the ice-proximal slope and stabilisation of the moraine, and  
166 (ii) the distal slope may incorporate re-worked material (e.g. Matthews, 1974; Erikstad and  
167 Sollid, 1986; Bradwell, 2004b). SF analysis was subsequently undertaken for each of the  
168 moraines to establish if the sampled lichens represent a single or composite lichen population  
169 (cf. Bradwell, 2001, 2004b; McKinzey et al., 2004, for further details). Where single  
170 populations were revealed by the SF analysis, estimates of the timing of lichen colonisation  
171 were calculated using the LL. Use of the LL approach is based on the assumption that the LL  
172 colonised soon after deposition and continued to grow during the period between colonisation  
173 and measurement (cf. Osborn et al., 2015). For comparison, three different lichenometric dating

174 curves previously constructed for SE Iceland were employed to derive possible moraine surface  
175 ages (Table 2; Figure 3). Estimates of the date of lichen colonisation calculated using the  
176 Bradwell (2001) age-size curve have been recalibrated to the survey date (2014) using the  
177 growth rates derived by Bradwell and Armstrong (2007). Corrections were only applied to  
178 lichen thalli between 15 and 50 mm where growth rates are broadly constant (cf. Bradwell et  
179 al., 2013).

180

### 181 3.3. Sedimentological techniques

182

183 Sedimentological analysis of manually-created exposures was undertaken to provide  
184 information on moraine genesis. Sedimentological investigations followed standard  
185 procedures, including section logging and description (Figure 4), lithofacies analysis and clast  
186 morphological analysis (cf. Benn and Ballantyne, 1993, 1994; Evans and Benn, 2004; Lukas  
187 et al., 2013). These procedures have been widely employed in investigations of moraine  
188 genesis, both in glaciated and glacierised environments, and have provided valuable insights  
189 into glacier dynamics (e.g. Price 1970; Krüger 1993, 1995, 1996; Bennett et al., 2004a, b;  
190 Evans and Hiemstra, 2005; Lukas, 2005a, b, 2007, 2012; Benn and Lukas, 2006; Benediktsson  
191 et al., 2008, 2009, 2010, 2015; Reinardy et al., 2013; Hiemstra et al., 2015). The moraine  
192 sampling strategy and section logging followed the procedures outlined by Lukas (2012) in a  
193 previous study of annual moraines.

194

### 195 3.4. Calculation of ice-margin retreat rates

196

197 Annual ice-margin retreat rates (IMRRs) were calculated for periods of annual moraine  
198 formation on the basis that annual moraine spacing equates to ice-margin retreat in any given

199 year (cf. Sharp, 1984; Bennett, 2001; Bradwell, 2004a; Lukas, 2012). Moraine crest-to-crest  
200 spacing was measured to the nearest metre along transects in *ArcMap*. For consistency in the  
201 measurement of moraine spacing, IMRRs were only calculated for the period covered by the  
202 remote-sensing data (up to June 2012), and the sub-metre resolution of the imagery (see Section  
203 3.1) was deemed sufficient for this purpose. As no part of the foreland contains a ‘complete’  
204 moraine sequence covering the whole period, a number of transects were used to create a  
205 composite record.

206

## 207 **4. Moraine characteristics**

208

### 209 4.1. Moraine distribution and geomorphology

210

211 Geomorphological mapping reveals a series of small-scale (<2 m in height) moraines  
212 distributed across the Skálafellsjökull foreland, with long, largely uninterrupted sequences of  
213 these moraines occurring on the northern and central parts of the foreland (Figure 5; cf.  
214 Chandler et al., 2015). Numerous small-scale moraines are also evident in close proximity to  
215 the southeastern margin of Skálafellsjökull (Figure 6). We initially term these features ‘minor  
216 moraines’ (cf. Ham and Attig, 2001; Bradwell, 2004a; Bradwell et al., 2013) in order to avoid  
217 attaching any genetic connotations, before examining moraine chronology and formation in  
218 subsequent sections.

219

220 The moraines on the northern and central parts of the foreland appear to be mostly continuous  
221 ridges that may extend up to ~530 m in length. However, these ridges may locally consist of a  
222 number of moraine fragments, ranging in length from ~3–20 m, which form part of longer  
223 chains (Figure 5). By contrast, the minor moraines in the southern part of the foreland are

224 predominantly discontinuous and fragmentary in nature, with longer, continuous moraine  
225 ridges being limited in number (Figure 6). Lateral spacing between moraine fragments ranges  
226 from ~3 m to 35 m. Fragments are occasionally separated by relict stream channels, indicative  
227 of post-depositional breaching of longer, continuous ridges by meltwater streams.

228

229 In planform, the moraines exhibit a distinctive ‘sawtooth’ or crenulate pattern (Figure 7).  
230 Complexities in the general planview geometry occur locally, with individual moraine ridges  
231 exhibiting bifurcations and cross-cutting patterns. Ponding occurs occasionally between  
232 moraines, particularly in the central parts of the foreland. The minor moraines are typically  
233 asymmetrical in cross-section, with cross-profiles displaying shorter, steeper distal slopes and  
234 longer, gently-sloping ice-proximal surface slopes. Individual minor moraines have heights  
235 ranging from ~0.2 m to 1.5 m, with moraine width being between ~2 m and 18 m. Moraine  
236 surfaces are largely covered by gravel to cobble sized material, though occasional large,  
237 angular boulders ( $a$ -axis >2 m) occur on the moraine surfaces or strewn between.

238

239 The minor moraines are frequently found in close association with flutings, which may drape  
240 the ice-proximal slopes of moraines in places (Figure 8). The flutings extend from the break of  
241 slope on the distal side of the moraines, forming lineated terrain that intervenes the moraines.  
242 On the reverse basalt bedrock slope in the southern part of the foreland, minor moraines and  
243 flutings are also found in association with an abundance of roches moutonnées: flutings often  
244 extend from the lee-side faces of roches moutonnées (cf. Evans and Orton, 2015). This area of  
245 the foreland is also characterised by a number of recessional meltwater channels and a  
246 contemporary meltwater stream running along the ice-margin. Locally, meltwater accumulates  
247 along parts of the southeastern margin to form a small ice-marginal lake. At the time of the

248 field investigations (May–June 2014), minor moraines could be found partially submerged by  
249 ponded and slow-moving meltwater at the ice-margin.

250

#### 251 *4.1.1. Morphometric characteristics*

252

253 The available dataset of mapped minor moraines ( $n = 3201$ ; Chandler et al., 2015), combined  
254 with the availability of a high-resolution DEM (spatial resolution: 0.09 m), allows the  
255 morphometry of the moraines to be explored. Moraine morphometry has been given limited  
256 treatment in the literature, with investigations restricted to a few studies (Matthews et al., 1979;  
257 Sharp 1984; Burki et al., 2009; Bradwell et al., 2013). However, examining moraine  
258 morphometry using similar approaches to those applied to other glacial landforms (e.g. Clark  
259 et al., 2009; Spagnolo et al., 2010, 2014; Stokes et al., 2013a; Storrar et al., 2014) may provide  
260 useful insights into glacier dynamics and debris transport (debris availability). Morphometric  
261 properties have been extracted from the mapped datasets (Chandler et al., 2015) in *ArcMap*,  
262 and are discussed below.

263

##### 264 *4.1.1.1. Length*

265

266 Moraine length exhibits a unimodal distribution and is highly positively skewed (4.54).  
267 Distributions are also leptokurtic, displaying an excess kurtosis of 36.14 (Figure 9A). The  
268 extracted values indicate that the majority of moraine fragments are less than 40 m in length  
269 (74.9%), with the mean and median lengths being 35.2 m ( $\sigma = 34.9$  m) and 25 m, respectively.  
270 Only 5.4% of the mapped moraines exceed 100 m in length. Thus, the analysis indicates that  
271 the minor moraines are largely fragmentary in nature.

272

#### 273 4.1.1.2. *Width*

274

275 Moraine width was obtained along 30 transects, 15 in zone A and 15 in zone B (see Figure 4),  
276 allowing variations in width along individual moraine ridges to be captured in the dataset.  
277 Similar to moraine length, moraine width exhibits a unimodal, leptokurtic distribution, with an  
278 excess kurtosis of 2.89 and a positive skewness value (1.39; Figure 9B). Moraine width in the  
279 two areas ranges between 1.4 m and 18.4 m, with a mean value of 5.7 m ( $\sigma = 2.8$  m) and a  
280 median of 5.2 m ( $n = 345$ ). Moraines predominantly display a width of 3–8 m, with 75.0% of  
281 moraines displaying a width within this range.

282

#### 283 4.1.1.3. *Surface area*

284

285 Moraine surface area, extracted from the database of mapped moraine polygons ( $n = 375$ ;  
286 Chandler et al., 2015), exhibits a unimodal, leptokurtic distribution with high positive skewness  
287 (3.02) and an excess kurtosis of 12.58 (Figure 9C). Moraine surface area values range between  
288 6 m<sup>2</sup> and 1739 m<sup>2</sup>, with the majority of moraines (68.5%) having surface areas of between 1  
289 and 200 m<sup>2</sup>. The mean surface area value for the dataset is 195 m<sup>2</sup> ( $\sigma = 219$  m<sup>2</sup>), whilst the  
290 median is 120 m<sup>2</sup>.

291

#### 292 4.1.1.4. *Variations between teeth and notches*

293

294 Using a sample of 50 cross-profiles, extracted from the DEM in zones A and B of the glacier  
295 foreland (see Figure 5), the width and height of each tooth and notch have been calculated.  
296 Moraine notches have a mean height of 0.7 m ( $\sigma = 0.3$  m), with values ranging between 0.2 m  
297 and 1.5 m. By comparison, teeth have a slightly lower mean value of 0.6 m ( $\sigma = 0.3$  m), with

298 the range of heights being 0.2–1.5 m. The width of teeth ranges between 3.7 m and 15.4 m,  
299 with a mean value of 8.6 m ( $\sigma = 3.1$  m) and a median of 8.2 m. Conversely, notches exhibit  
300 greater mean and median values of 9.7 m ( $\sigma = 1.9$  m) and 9.5 m, respectively. Notch width  
301 ranges between 6.0 m and 13.7 m. However, a Wilcoxon rank-sum (or Mann Whitney U) test  
302 indicates no statistically significant difference exists between the two independent sample  
303 distributions (Table 3).

304

## 305 4.2. Moraine chronology

306

### 307 *4.2.1. Remote-sensing and field observations*

308

309 Examination of an archive of remote-sensing data, spanning 1945–2012, indicates that  
310 sustained minor moraine formation occurred during the following periods: 1945–1964; 1969–  
311 1974; and 2006–2012. Minor moraines mapped in zone A (Figure 10) are evident on the oldest  
312 vertical aerial photograph, captured by the US Army Mapping Service in 1945, indicating  
313 minor moraines were also formed prior to 1945. The 1945 ice-margin is situated in close  
314 proximity to a minor moraine which appears to reflect the ice-front morphology, though the  
315 quality and resolution of the imagery is relatively poor. Aerial photographs were subsequently  
316 captured in 1947, and two minor moraines had formed during the interval between the two  
317 surveys. Based on the available aerial photographs, it is also evident that the entire suite of  
318 minor moraines in zone A were formed prior to September 1954, as the ice-margin had  
319 retreated from the area by this time (Figure 11). Furthermore, the higher-resolution 1954  
320 photograph reveals that the minor moraines are prominent features. The moraines display a  
321 more subdued appearance in later aerial photographs (e.g. 1969, 1979, 1982), implying that  
322 these features were formed not long prior to 1954. Examination of the available aerial

323 photographs and satellite imagery also indicates that this area of the foreland was not  
324 subsequently overridden by ice. However, formation dates cannot be confidently ascribed  
325 based solely on the remote-sensing data, due to (i) a lack of data between 1947 and 1954, and  
326 (ii) the presence of moraines which were formed prior to the earlier aerial photograph.

327

328 The suite of minor moraines mapped in zone B (see Figure 10) formed between 1954 and 1969  
329 based on the aerial photograph evidence (Figure 12). The northeastern and eastern parts of the  
330 sequence have been partially affected by meltwater activity, as well as the evolution and  
331 migration of the Kolgrima River. Minor moraines evident close to the 1954 ice-margin have  
332 been subject to post-depositional modification or have been obliterated altogether.  
333 Furthermore, the innermost (western) part of the moraine sequence has been affected by glacier  
334 re-advance, which occurred sometime between 1964 and 1969. Unfortunately, there is a  
335 paucity of ice-front measurement data during the 1960s and 1970s to verify the timing and  
336 magnitude of this re-advance. The ice-margin had, however, retreated from this area of the  
337 foreland by 1975, with the ice-marginal lake substantially increasing in size between 1969 and  
338 1975. On the basis of the available remote-sensing and ice-front measurement data, we  
339 confidently identify 8 annual moraines formed between 1957 and 1964 in this zone. Other  
340 minor moraines mapped in this sequence cannot be ascribed a date/frequency of formation with  
341 any certainty, due to the aforementioned issues.

342

343 The sequence of minor moraines in zone C (see Figure 10) formed some time during the period  
344 1945 and 1964, on the basis of aerial photograph evidence (Figure 13). The outermost moraine  
345 in this sequence is ascribed a formation date of 1945, with another 12 moraines subsequently  
346 formed prior to 1957. The 1957 ice-margin is situated in close proximity to a minor moraine in  
347 this sequence, suggesting formation during a small 1956/1957 winter re-advance. The four

348 aerial photographs captured during the period 1945–1957 show Skálafellsjökull was in overall  
349 retreat throughout this period, with no evidence of re-advance. This is supported by ice-front  
350 measurements which demonstrate Skálafellsjökull underwent ice-marginal retreat each year  
351 between 1945 and 1957, averaging  $\sim 28.5 \text{ m a}^{-1}$ . As the number of moraines ( $n = 13$ ) formed in  
352 this area between 1945 and 1957 is equivalent to the time elapsed, we interpret these features  
353 as annual moraines (cf. Krüger, 1995; Bradwell, 2004a; Krüger et al., 2010; Bradwell et al.,  
354 2013). The frequency and timing of moraine formation inside the 1957 moraine cannot  
355 confidently be established owing to a paucity of data. Moreover, examination of the 1969 aerial  
356 photograph reveals the glacier re-advanced onto this part of the foreland, introducing  
357 complexity.

358

359 A further sequence of minor moraine ridges is present on the northern part of the foreland in  
360 zone D, situated to the northwest of zone B (Figure 10). Based on the available photographic  
361 evidence, this suite was formed between 1969 and 1975 (Figure 14). As with the above  
362 sequences, these minor moraines are believed to represent annual moraines. Following 1975,  
363 Skálafellsjökull was relatively stable in this area of the foreland (Figure 14), with a cessation  
364 of minor moraine deposition. Minor moraine formation recommenced after 1989, with a series  
365 of moraines deposited inside a substantially larger moraine (height:  $\sim 9\text{--}10 \text{ m}$ ) in zone E (see  
366 Figure 10). However, the age of these features is unknown owing to a lack of remote-sensing  
367 data between 1989 and 2006. Furthermore, it is unknown whether additional moraines formed  
368 during this period and were then subsequently obliterated, either by glacier re-advance or  
369 glaciofluvial activity. Comparison of mapping from the 2006 aerial photographs and 2012  
370 satellite imagery shows that seven minor moraines (zone F; Figure 10), displaying distinctive  
371 sawtooth planform geometries, formed at the northeastern margin during this period (Figure

372 15). As the number of moraine ridges formed between 2006 and 2012 is equal to the number  
373 of years elapsed, we interpret these features as annual moraines.

374

375 At the southeastern margin, relatively few (<24) minor moraines were formed during the period  
376 1945–1969. Between 1979 and 1989 the southeastern margin was relatively stable and limited  
377 moraine formation occurred in this area (Figure 16). A number of minor moraines formed in  
378 this area following 1989 but due to a lack of data (remote sensing and ice-front measurements)  
379 for the 1990s, age estimates cannot confidently be assigned to these features. Mapping based  
380 on the 2006 and 2012 imagery indicates that numerous minor moraines have been formed in  
381 this part of the glacier foreland during 2006–2012 (Figure 17). Field investigations conducted  
382 between May and June 2014 identified a number of minor moraines that have formed since  
383 2012, and there is evidence of ongoing moraine formation. Since 2006, >9 minor moraines  
384 have formed, implying moraines have formed on a sub-annual basis. Sub-annual formation is  
385 supported by the geomorphology of these features, with small moraines identifiable in the field  
386 with heights of <20 cm. Owing to these complicating factors, minor moraines in this part of  
387 the glacier foreland cannot be ascribed age estimates with any confidence.

388

#### 389 4.2.2. *Lichenometric dating*

390

391 Lichenometric surveys were conducted in zone A (Figure 10) in order to establish the age of  
392 the minor moraines formed prior to the oldest aerial photograph (prior to 1945). The measured  
393 lichen populations have been plotted as log-normal plots of frequency against class size (Figure  
394 18) following the method outlined elsewhere (cf. Benedict, 1967, 1985; Bradwell, 2001). All  
395 lichen populations follow an approximate straight line and show strong negative correlations  
396 between lichen diameter and  $\log_{10}$  frequency, with  $r^2$  values ranging from 0.8580 to 0.9763

397 (Figure 18). Furthermore, the largest lichen in each population falls below the theoretical '1 in  
398 1000' diameter threshold in all cases (cf. Andersen and Sollid, 1971; Locke et al., 1979;  
399 Caseldine, 1991; Cook-Talbot, 1991; Bradwell, 2001, 2004b). Thus, the lichens constitute  
400 single SF populations and the LL in each population can therefore be applied to derive dates  
401 for the moraines.

402

403 Estimates of the timing of lichen colonisation for each ridge in zone A have been derived using  
404 a variety of dating curves (Gordon and Sharp, 1983; Bradwell, 2001, 2004b) for comparison  
405 (Table 4). The lichenometric survey on the ice-proximal slope of the outermost moraine (A1)  
406 recorded a LL of 36 mm and a single population ( $r^2 = 0.9618$ ,  $p < 0.0001$ , Figure 18A). Using  
407 this LL value and the age-size dating curve of Bradwell (2001), colonisation of the moraine  
408 surface is dated to  $1940 \pm 7$ . By comparison, the Gordon and Sharp (1983) age-size dating  
409 curve yields an older date of  $1929 \pm 9$ . Finally, the age-gradient curve of Bradwell (2004b)  
410 produces an estimate of  $1933 \pm 8$ . Based on the remote-sensing data, it is known that the ice-  
411 margin had retreated from moraine A1 prior to 1945 and that the glacier has not subsequently  
412 re-advanced into this part of the foreland. The lichenometric dating curves and photographic  
413 evidence therefore indicate that moraine ridge A1 formed in the date range 1920–1945.

414

415 In the 1945 aerial photograph, moraine A10 is situated in close proximity to the ice-margin and  
416 is hypothesised to have been formed during a small winter re-advance during 1944/1945. The  
417 lichenometric survey on moraine A10 recorded a LL value of 30 mm and revealed a single  
418 lichen population ( $r^2 = 0.9641$ ,  $p < 0.0001$ , Figure 18I). As such, the LL is not considered to  
419 be anomalous (cf. Bradwell, 2001). Estimates of the timing of colonisation, derived from the  
420 Bradwell (2001, 2004b) dating curves, are broadly consistent with the hypothesis of formation  
421 during a 1944/1945 winter re-advance: even the most well-calibrated lichenometric dating has

422 an optimum precision of only 5–10% (Innes, 1988; Noller and Locke, 2000). Comparison of  
423 the dates derived from the Gordon and Sharp (1983) dating curve with the available aerial  
424 photographs implies that this dating curve consistently overestimates the timing of moraine  
425 colonisation in this suite. Based on all the strands of evidence, we ascribe moraine A10 a  
426 formation date of winter 1944/1945.

427

428 Lichenometric investigations conducted on the ice-proximal slope of the innermost moraine  
429 (A15) yielded a LL of 24 mm, with the lichens comprising a single population ( $r^2 = 0.9219$ ,  $p$   
430  $= 0.0005$ , Figure 18N). The Bradwell (2001) age-size dating curve produces an estimate of  
431  $1959 \pm 6$  for the timing of colonisation. As with moraines A1 and A10, the Gordon and Sharp  
432 (1983) dating curve yields an older estimate ( $1941 \pm 7$ ). An estimate of  $1958 \pm 6$  is derived  
433 from the age-gradient curve of Bradwell (2004b). Based on the aerial photograph evidence, it  
434 is known that Skálafellsjökull retreated from this part of the foreland by 1954 and that moraine  
435 A15 formed after 1947. Additionally, there is no evidence of re-advance into this area. Using  
436 these strands of evidence, we deduce that moraine A15 formed sometime between 1947 and  
437 1954.

438

439 Notwithstanding the veracity of the timing of moraine formation, the dates derived using the  
440 Bradwell (2001) and Gordon and Sharp (1983) age-size dating curves appear to be broadly  
441 consistent with annual moraine formation in zone A. Conversely, the Bradwell (2004b) age-  
442 gradient curve yields inconsistent dates, implying the moraine suite is interspersed with  
443 apparently younger moraine ridges. It has previously been acknowledged by Bradwell (2004b)  
444 that it is unlikely that the age-gradient curve can be accurately used to date surfaces formed  
445 within the last ~70 years due to the exponential nature of the dating curve. Given that the minor  
446 moraines in zone A are believed to have formed between the ~1930s and early 1950s, this

447 appears to explain the apparently erroneous estimates derived using the age-gradient curve.  
448 Whilst the dates of moraine colonisation yielded from the Bradwell (2001) age-size dating  
449 curve are broadly consistent with annual formation, the location of control sites used in  
450 calibrating this curve may introduce errors into the precise dates obtained. The Bradwell (2001)  
451 age-size curve is based on measurements of independently dated surfaces which encompass a  
452 range of precipitation zones (cf. Evans et al., 1999a). As lichen growth rates are known to be  
453 influenced by local environmental factors such as precipitation (cf. Innes, 1985; Benedict,  
454 1990; Evans et al., 1999a; Bradwell and Armstrong, 2007; Armstrong, 2015, Osborn et al.,  
455 2015, and references therein), the dating curve may yield erroneous estimates for the timing of  
456 colonisation, particularly as Skálafellsjökull is situated in a zone of high precipitation (cf.  
457 Evans et al., 1999a). Meanwhile, Gordon and Sharp (1983) employed a different sampling  
458 strategy to that utilised in this study, with long axis measurements of the aggregated species  
459 *Rhizocarpon geographicum* undertaken in areas of 150 m<sup>2</sup> on the proximal side of moraines.  
460 As such, estimates of the timing of moraine colonisation derived from the Gordon and Sharp  
461 (1983) dating curve may have errors associated with them.

462

463 Despite the issues highlighted above, and excluding the dates derived from the Bradwell  
464 (2004b) dating curve, the lichenometric analysis and supporting evidence (remote-sensing data  
465 and field observations) appear to broadly support the hypothesis that the moraines formed  
466 annually. The formation of two moraines (A11 and A12) between the 1945 and 1947 aerial  
467 photograph surveys provides additional support for formation on an annual basis. Moreover,  
468 the geomorphological characteristics of the moraines are similar to other features interpreted  
469 as annual moraines in SE Iceland and elsewhere (e.g. Boulton, 1986; Krüger, 1995; Bradwell,  
470 2004a; Lukas, 2012; Bradwell et al., 2013; Reinardy et al., 2013), suggesting annual formation  
471 relating to minor re-advances of the Skálafellsjökull ice-margin during overall glacier

472 recession. Accepting that (i) moraine A10 formed during a small winter re-advance in  
473 1944/1945 based on the aerial photographic evidence and (ii) moraines in this suite formed on  
474 an annual basis, the suite of minor moraines in zone A are believed to have formed between  
475 winter 1935/1936 and 1949/1950 (Table 5). Nonetheless, some caution should be attached to  
476 these age estimates given the large errors associated with them (see Table 4) and the  
477 uncertainties in lichenometric dating (cf. Jochimsen, 1973; Worsley, 1981; Osborn et al., 2015,  
478 and references therein). Furthermore, it cannot be ruled out that some of the moraines may have  
479 formed in the same year, particularly given the recognition of sub-annual moraine formation  
480 elsewhere on the foreland.

481

### 482 4.3. Moraine sedimentology

483

#### 484 *4.3.1. Section descriptions and initial interpretations*

485

486 Sections were created through the width of four representative moraines in order to assess the  
487 genetic processes of moraine formation at Skálafellsjökull using sedimentological analysis.  
488 These moraine sections are considered to be a representative subsample of the facies  
489 associations evident within the recessional moraines on the foreland.

490

##### 491 *4.3.1.1. Moraine SKA-04*

492

493 This sawtooth moraine is located within the suite of moraines in zone A (64.27662°N,  
494 015.65767°W; Figure 1), with a natural exposure through the northern part of the moraine  
495 created by the Kolgrima River. It has a rounded top and is a 130 m long and 6 m wide, low-  
496 amplitude (~0.8 m high), symmetrical ridge with surface slopes dipping at angles of 18°. The

497 surface is strewn with a number of large boulders ( $a$ -axis >1.5 m). Based on remote-sensing  
498 observations and lichenometric analysis this moraine is believed to have formed during a winter  
499 re-advance in 1945/1946. It is largely composed of dark-grey/brown, massive, largely  
500 homogenous, structureless, matrix-supported diamicton, with moderate clast content (Dmm;  
501 Figure 19). The diamicton is firm, with a clayey-silty matrix, and is relatively difficult to  
502 excavate. On the distal side of the moraine, there is a zone of compact and fissile, matrix-  
503 supported diamicton (Dmm(s)). This zone of distinct fissility extends up to ~0.98 m in width  
504 at the base of the section, and reaches a maximum height of ~0.65 m. The fissility reflects the  
505 presence of sub-horizontal and anastomosing partings, which are interpreted as brittle shear  
506 structures (cf. Evans, 2000; Evans et al., 2006; Ó Cofaigh et al., 2011). A prominent, faceted  
507 and bullet-shaped boulder at the base of this section displays numerous upper surface striations.  
508 Morphological analysis of basalt clasts ( $n = 50$ ) sampled from the massive diamicton (Dmm)  
509 shows that the clasts are largely subangular to rounded (RA = 4; RWR = 28) and blocky in  
510 character ( $C_{40} = 16$ ), with low percentages of oblate and prolate clasts (Figure 19). These  
511 characteristics are consistent with active transport in a subglacial environment (cf. Benn and  
512 Ballantyne, 1993, 1994; Evans and Benn, 2004; Lukas, 2007). Based on the evidence  
513 presented, and the similarity of the diamictons with sediments interpreted as subglacial traction  
514 tills elsewhere in Iceland (e.g. Evans, 2000; Evans and Twigg, 2002; Evans and Hiemstra,  
515 2005; Evans et al., 2006; Benediktsson et al., 2008, 2009, 2010, 2015; Schomacker et al., 2012),  
516 we interpret the diamictons as subglacial traction tills (*sensu* Evans et al., 2006). Given the  
517 subglacial origin of the sediment and the moraine morphology (sawtooth planform: Figure 7),  
518 the simplest interpretation of moraine SKA-04 is as a push/squeeze moraine (cf. Price, 1970;  
519 Sharp, 1984; Bennett, 2001; Evans and Hiemstra, 2005). We argue that the gently sloping ice-  
520 proximal slope supports a partly submarginal origin for the moraine (extrusion of subglacial

521 traction till), and that the combination of squeezing and pushing at the ice-margin results in the  
522 distinctive sawtooth planform (cf. Price, 1970; Sharp, 1984).

523

#### 524 4.3.1.2. *Moraine SKA-07*

525

526 This section is through the northern face of a crenulate moraine situated in the southern part of  
527 the foreland (64.26811°N, 015.68353°W; Figure 1). The moraine is 32 m long, ~2.3 m wide  
528 and up to ~0.5 m high. It has no clearly developed crestline but has a rounded top and is  
529 asymmetrical, with a shorter, steeper distal slope (24°) and longer, gentler ice-proximal slope  
530 (20°). Based on the available aerial photographs and satellite imagery, moraine SKA-07 was  
531 most likely formed during the winter of 2006/2007. This moraine is largely composed of a  
532 dark-grey/brown, massive, clast-supported diamicton (Dcm), and contains clasts with  
533 maximum *a*-axis lengths of 15 cm (Figure 20). The diamicton is firm, and the matrix is  
534 dominated by silt and clay. Clasts sampled from this lithofacies are predominantly subangular  
535 to rounded (RA = 10; RWR = 16), with low percentages of angular and well-rounded clasts  
536 (Figure 20B). Moreover, the clasts are largely blocky in shape (C<sub>40</sub> = 16; Figure 20C). These  
537 morphological characteristics are consistent with active transport. The characteristics of the  
538 diamicton are similar to those of diamictons found within annual moraines on other Icelandic  
539 glacier forelands, and these have been interpreted as deformed and partially extruded subglacial  
540 sediments (cf. Price, 1970; Evans and Hiemstra, 2005). A prominent feature of SKA-07 is the  
541 deformed unit of fine sediments (Fl) on the distal side. These sorted sediments are interpreted  
542 as glaciofluvial sediments, resulting from submarginal fluvial processes, which were  
543 incorporated into the deforming subglacial sediments. Based on the available evidence,  
544 moraine SKA-07 is interpreted as being formed through submarginal deformation and  
545 extrusion of water-soaked tills through marginal crevasses and into crenulations or pecten of

546 the ice-margin (cf. Price, 1970; Sharp, 1984; Evans and Hiemstra, 2005). The extruded  
547 subglacial traction till is believed to subsequently undergo pushing, leading to the production  
548 of a sawtooth or crenulate push/squeeze moraine (cf. Sharp, 1984).

549

#### 550 *4.3.1.3. Moraine SKA-11*

551

552 The section through moraine SKA-11, a broadly linear feature situated near the present ice-  
553 margin (64.26721°N, 015.69118°W; Figure 1), is the most complex examined. Based on  
554 remote-sensing observations and field investigations, it is believed that this moraine formed  
555 some time during 2012/2013. The ridge has a well-defined crestline, and exhibits a slightly  
556 steeper distal (31°) than ice-proximal slope (29°). It is ~21 m long, ~2.8 m wide and up to ~0.8  
557 m high. An exposure created through the southwestern face of this moraine ridge reveals two  
558 lithofacies associations (LFAs) (Figure 21). LFA1 comprises stacked sequences of matrix-  
559 supported, stratified diamictons (Dms) and (crudely) horizontally-bedded granule and gravel  
560 units (GRh, G(h), Gh), with occasional interbeds of sorted sediments (Sm). This LFA occurs  
561 on the ice-proximal side and dips at an angle of ~29°, accordant with the ice-proximal surface  
562 slope. The diamictic facies in LFA1 displays a grey/brown colour and a loose, friable character,  
563 with layers of matrix-supported, stratified diamicton reaching a maximum thickness of ~19 cm.  
564 Individual layers of the (crudely) horizontally-bedded gravels reach maximum thicknesses of  
565 ~13 cm, whilst the horizontally-bedded granule to fine gravel unit reaches a maximum  
566 thickness of ~12 cm. The lower, crudely horizontally-bedded gravel (G(h)) is medium to coarse  
567 grade, whereas the uppermost horizontally-bedded gravel (Gh) is fine to medium grade gravel.  
568 A unit of massive, medium to coarse sand which reaches a maximum thickness of 4 cm is  
569 interbedded between the stratified diamicton and lower gravel lithofacies. LFA1 is interpreted  
570 as sediment slabs, incorporating submarginal fluvial and subglacial sediments, emplaced in the

571 moraine through glacier submarginal freeze-on (cf. Harris and Bothamley, 1984; Krüger, 1993,  
572 1994, 1995, 1996; Matthews et al., 1995; Evans and Hiemstra, 2005; Reinardy et al., 2013;  
573 Hiemstra et al., 2015). Further support of a subglacial origin is provided by morphological  
574 analysis of clasts sampled from the stratified diamicton (Dms), with the clasts mainly  
575 subangular to rounded and blocky in character (Figure 21B, C). These characteristics are  
576 consistent with active transport in the subglacial environment (cf. Benn and Ballantyne, 1993,  
577 1994; Evans and Benn, 2004; Lukas, 2007).

578

579 The remainder of moraine SKA-11 is formed of LFA2, which comprises a very loose, silty-  
580 sandy, massive, matrix-supported diamicton (Dmm), together with massive sand (Sm) and  
581 pods/lenses of massive and openwork gravels (Gm, Go). A large, prominent pod of medium to  
582 coarse, poorly sorted, massive gravel (Gm) occurs on the distal side, and reaches a maximum  
583 thickness of 28 cm. Layers/lenses of medium to coarse, massive sand (Sm) occur within this  
584 gravel unit, locally reaching thicknesses of 3 cm, but tapering out distally and proximally. The  
585 lowermost unit of massive sand includes out-sized clasts. A further lens of sorted sediment  
586 (Sm) occurs within the Dmm, locally extending up to 9 cm before tapering out distally. Lenses  
587 of massive and openwork gravel in LFA2 reach thicknesses of 6 cm. On the lower distal side  
588 of the section, lenses of massive granules and gravels dip approximately parallel to the surface  
589 slope at angles of 30–31°. In the upper distal side of the moraine, the gravel units appear to  
590 have undergone deformation. We suggest that the loose sediments that constitute LFA2 may  
591 relate to pushing of unfrozen glaciofluvial sediment in front of advancing frozen slabs (cf.  
592 Matthews et al., 1995; Evans and Hiemstra, 2005; Reinardy et al., 2013) and then subsequent  
593 gravitational collapse. The deformed lenses in the upper distal side of the section appear  
594 consistent with the interpretation that material was pushed up in front of the frozen-on sediment  
595 slabs.

596

597 4.3.1.4. *Moraine SKA-13*

598

599 Moraine SKA-13 has a distinctive morphology and appearance, which contrasts with that of  
600 the majority of moraines within the foreland; only one other moraine ridge was found to have  
601 similar characteristics. This moraine is situated close to the contemporary southeastern margin  
602 (64.26753°N, 015.68968°W; Figure 1) and is likely to have formed during a winter re-advance  
603 in 2013/2014, based on remote-sensing and field observations. This moraine is arcuate in  
604 planform and exhibits a sharp crestline, reaching ~31 m in length. In cross-section this ridge is  
605 ~1.0 m high and up to ~2.1 m wide, and displays an asymmetric cross-profile with an ice-  
606 proximal slope that is gentler (24°) than the distal slope (29°). The surface of this ridge is  
607 strewn with cobbles and boulders, the boulders having maximum *a*-axis lengths of ~0.75 m.  
608 The moraine is composed largely of a massive, matrix-supported diamicton (Dmm), which  
609 exhibits a red/brown colour and a high clay content (Figure 22). Clast shape data (Figure 22B,  
610 C) indicate that clasts from this diamicton are largely subangular to rounded (RA = 16; RWR  
611 = 20) and blocky (C<sub>40</sub> = 24), consistent with active transport of the material. This section is  
612 visually dominated by the edge-rounded, boulder-sized clasts sitting within the diamicton  
613 matrix, which reach maximum *a*-axis lengths of 0.35 m. Aside from the diamicton unit, a core  
614 of massive, poorly-sorted, medium to coarse gravel (Gm) is evident at the base of the ice-  
615 proximal side of the moraine. Although containing no sedimentary structures indicative of  
616 pushing, this moraine is interpreted as a push moraine, predominantly on the basis of its  
617 morphological similarity with push moraines elsewhere (cf. Worsley, 1974; Birnie, 1977;  
618 Matthews et al., 1979; Bennett, 2001; Benn and Evans, 2010). We argue that the lack of  
619 deformation structures reflects the clast/boulder-rich content of the constituent material. The  
620 massive gravel core is interpreted as evidence of re-working and incorporation of sediments

621 originally deposited by a proglacial stream. This, combined with the sharp, well-defined  
622 crestline and numerous large cobbles, indicates bulldozing of extant proglacial material by the  
623 ice-margin. The clast shape data (Figure 22B, C) suggests that this proglacial material is, at  
624 least in part, of subglacial origin.

625

#### 626 4.3.2. Covariance analysis

627

628 Covariance analysis was conducted on samples from each of the four moraine sections  
629 described above, following established procedures (Benn and Ballantyne, 1993, 1994; Benn,  
630 2004; Evans 2010; Brook and Lukas, 2012; Lukas et al., 2013). Only basalt clasts were sampled  
631 as lithology has been shown to have a primary role in determining clast shape (Lukas et al.,  
632 2013). Control samples from Fláajökull, an active temperate outlet of the southern margin of  
633 Vatnajökull (cf. Evans et al., 2015), were employed as reference. Fláajökull exhibits dominant  
634 subglacial and fluvial erosion and transport, with multiple and complex transfers of material  
635 between the subglacial and glaciofluvial realms (Lukas et al., 2013). This corresponds well  
636 with findings from Skálafellsjökull where Evans (2000) has found convincing stratigraphical  
637 evidence, in the form of a gravel outwash/subglacial traction till continuum, for these processes  
638 working at the base of the glacier. Comparison of the four samples with the control samples  
639 from Fláajökull, using covariance plots of both RA-C<sub>40</sub> and RWR-C<sub>40</sub>, suggests the diamicton  
640 units were derived from subglacial material (Figure 23). This confirms the initial interpretations  
641 of the clast shape data presented in the previous sections. Supporting evidence for a subglacial  
642 origin is provided by the presence of numerous striated and faceted clasts within the moraine  
643 sections. Thus, the clast-shape data indicates the dominance of subglacial processes, and  
644 strongly suggests the sediments exposed in section reflect transport in the subglacial traction  
645 zone (cf. Boulton, 1978; Benn, 1992; Benn and Ballantyne, 1994; Lukas, 2005a, b, 2007), even

646 though local dilution of the subglacial signature may be created wherever the glacier margin  
647 incorporated proglacial stream deposits.

648

## 649 **5. Significance of the moraines**

650

### 651 5.1. Synthesis of moraine sedimentology

652

653 The sedimentological data presented strongly suggest that the majority of moraines at  
654 Skálafellsjökull are formed through a combination of squeezing and bulldozing of subglacial  
655 sediments, though pre-existing proglacial sediments may be locally pushed into a moraine  
656 ridge. In limited instances submarginal sediment slabs may be emplaced in the moraines  
657 through subglacial freeze-on (*sensu* Krüger, 1994, 1995). The moraines are predominantly  
658 composed of subglacial traction tills (*sensu* Evans et al., 2006), with no apparent evidence for  
659 the incorporation of supraglacial debris flow deposits: the clast shape analysis is a particularly  
660 strong indicator of the dominance of subglacial transport pathways (Section 4.3.2; cf. Boulton,  
661 1978; Benn, 1992; Benn and Ballantyne, 1994; Lukas, 2005a, b, 2007). The absence of  
662 supraglacial debris within the moraines is attributed to the lack of appreciable debris cover on  
663 the glacier surface, with supraglacial debris point sources limited to isolated debris cones at the  
664 southeastern margin. Reworking of material on the distal side of moraines was evident in some  
665 sections, as reported in previous studies of Icelandic moraines (e.g. Sharp, 1984; Krüger, 1994,  
666 1995), though it was not ubiquitous.

667

668 Sedimentological evidence for the incorporation of submarginal sediments through freeze-on  
669 (*sensu* Krüger, 1994, 1995) was restricted to two moraine exposures, both situated in the  
670 southern part of the foreland. In this area, the glacier is retreating from a reverse bedrock slope

671 and exhibits a relatively thin and gently-sloping ice-front. Additionally, meltwater accumulates  
672 and flows along the southeastern margin, appearing to undercut the ice-front in places. We  
673 suggest that these topographic and glaciological characteristics provide propitious conditions  
674 for submarginal freeze-on of sediments. The relatively thin ice-margin and undercutting by  
675 meltwater allows the penetration of a winter freezing front, leading to freeze-on (cf. Krüger,  
676 1993, 1994, 1995, 1996; Matthews et al., 1995; Evans and Hiemstra, 2005; Reinardy et al.,  
677 2013; Hiemstra et al., 2015). Climatic factors may also exert some control over the localised  
678 occurrence of subglacial freeze-on of sediments at Skálafellsjökull, with the formation of  
679 moraine SKA-11 associated with below average winter/spring temperatures in 2012/2013.  
680 Thus, the combination of relatively cold winter conditions in particular years and the thin ice-  
681 margin provide favourable conditions for this mode of formation.

682

683 The topography and bedrock geology of the southern part of the foreland also has an important  
684 role in other genetic processes identified, with the reverse basalt bedrock slope preventing  
685 permeation of surface waters (meltwater) and generating an aquiclude. Consequently, surface  
686 waters flow back down the slope towards the ice-margin, accumulating in channels and ponds  
687 at the ice-front. This combination of topographic and geological factors results in highly  
688 saturated subglacial/submarginal sediments and high pore-water pressure. The presence of this  
689 viscous slurry and high pore-water pressure at the base of the glacier leads to submarginal  
690 deformation and ice-marginal squeezing (cf. Price, 1970; Sharp, 1984; Evans and Twigg, 2002;  
691 Evans and Hiemstra, 2005, Evans et al., 2015, and references therein). This extruded sediment  
692 is subsequently bulldozed into a moraine ridge by the ice-front (cf. Sharp, 1984). Deformable  
693 sediments are also manifest in the form of widespread flutings, which are found in close  
694 association with the recessional moraines. The close association of recessional moraines and  
695 flutings is a characteristic feature of active temperate glacial landsystems, and suggests that

696 these features are genetically linked (cf. Evans and Twigg, 2002; Evans, 2003). Formation of  
697 these moraines through push/squeeze mechanisms is consistent with a subglacial  
698 deformation/ploughing origin for the flutings: the moraines are partially submarginal in origin,  
699 with the ice-proximal side connected to the deforming layer that produces the flutings (cf.  
700 Price, 1970; Boulton, 1976; Sharp, 1984; Boulton and Hindmarsh, 1987; Benn, 1994; Boulton  
701 and Dobbie, 1998; Boulton et al., 2001).

702

703 The range of genetic processes identified at Skálafellsjökull is consistent with existing genetic  
704 models of moraine formation at Icelandic glaciers. In particular, push/squeeze moraines have  
705 been identified at a number of Icelandic outlet glaciers (cf. Price, 1970; Sharp, 1984; Evans  
706 and Twigg, 2002; Evans and Hiemstra, 2005). Additionally, the emplacement of frozen-on  
707 sediment slabs has been proposed for Icelandic moraine formation (cf. Krüger, 1993, 1994,  
708 1995, 1996; Evans and Hiemstra, 2005) and a similar genesis has also been posited for  
709 moraines at Norwegian outlet glaciers (Matthews et al., 1995; Reinardy et al., 2013; Hiemstra  
710 et al., 2015). However, the incidence of subglacial freeze-on is not widespread at  
711 Skálafellsjökull. Important differences between the range of processes identified herein and  
712 previous models of small-scale recessional (annual) moraine formation are as follows: (i) no  
713 evidence was found for snow-cover having a significant role in moraine genesis or post-  
714 depositional modification (Price, 1970; Birnie, 1977; Sharp, 1984); (ii) dead-ice incorporation  
715 as a result of inefficient bulldozing was not apparent, with no ice-cored moraines identified  
716 (Sharp, 1984; Lukas, 2012); (iii) there was no evidence for dead-ice incorporation as a result  
717 of isolation of an ice core beneath englacial debris bands (Sharp, 1984); and (iv) terrestrial ice-  
718 contact fans were not evident (Lukas, 2012). Of the moraine types previously identified at  
719 Skálafellsjökull by Sharp (1984), only push/squeeze moraines (Type A) have been observed.  
720 This difference may partly reflect changes in glacier dynamics, ice-margin

721 structure/morphology and/or climatic conditions. However, the occurrence of dead-ice  
722 incorporation (Types B and C) and the influence of snowbanks (Type D) cannot be entirely  
723 ruled out as (i) sedimentological investigations were undertaken part way through the ablation  
724 season (June), and (ii) moraine forming processes were not investigated at the northeastern  
725 margin. The absence of terrestrial ice-contact fans (Lukas, 2012) reflects the lack of appreciable  
726 supraglacial debris cover and limited availability of supraglacial point sources (cf. hochsandur  
727 fans; Krüger, 1997; Kjær et al., 2004).

728

729 Based on the sediment composition and structure of the moraines, we distinguish the following  
730 three categories of moraine-forming processes at Skálafellsjökull: (i) submarginal deformation  
731 and subsequent bulldozing of the extruded sediments (SKA-04 and SKA-07; Figure 24A); (ii)  
732 efficient bulldozing of pre-existing proglacial material (SKA-13; Figure 24B); and (iii)  
733 emplacement of frozen-on submarginal sediment slabs (SKA-11; Figure 24C).

734

#### 735 *5.1.1. Efficient bulldozing of extruded submarginal sediments*

736

737 This process is dominant throughout the foreland, occurring both on the portions of the foreland  
738 with a lower surface gradient and on the reverse bedrock slope in the south. Moreover, this  
739 sequence of events appears to apply best where the ice-front is relatively steep and where  
740 pecten is well-developed at the terminus. During the melt season, an increase in meltwater  
741 descending to the base of the glacier saturates the underlying subglacial materials and elevates  
742 porewater pressures (1; Figure 24A) (Andrews and Smithson, 1966; Price, 1970; Evans and  
743 Hiemstra, 2005). Where the glacier is situated on a reverse bedrock slope, runoff of surface  
744 water back down the slope also contributes to this process. The elevation of porewater pressures  
745 and saturation of the subglacial sediments leads to submarginal deformation and ice-marginal

746 squeezing (1; Figure 24A) (Price, 1970; Sharp, 1984; Evans and Twigg, 2002; Evans and  
747 Hiemstra, 2005). During the winter re-advance (2), the extruded sediments are bulldozed by  
748 the advancing ice-front, leading to ductile deformation and folding of sorted sediments  
749 incorporated within the moraine (e.g. SKA-07, Figure 20). As retreat commences in the spring  
750 (3), localised reworking of the moraine surface slopes may occur due to gravitational and  
751 glaciofluvial activity. The relative steepness of the ice-front ensures that efficient bulldozing  
752 occurs (*sensu* Lukas, 2012) and, therefore, no material slumps onto the glacier surface.  
753 Consequently, no dead-ice is incorporated within the moraine (3–4).

754

#### 755 *5.1.2. Efficient bulldozing of pre-existing proglacial sediments*

756

757 This sequence of events (Figure 24B) applies where Skálafellsjökull is retreating from the  
758 reverse bedrock slope in the southern part of the foreland, and where the ice-margin is relatively  
759 steep (1). Accumulation of meltwater along the southeastern ice-margin allows glaciofluvial  
760 deposition, whilst thin spreads of (immature) subglacial traction tills (*sensu* Evans et al., 2006)  
761 are also evident on the foreland. During the course of the winter re-advance (2), the proglacial  
762 material is bulldozed by the advancing glacier to form a ridge. Where the material is  
763 cobble/boulder-rich, as in SKA-13 (Figure 22), the sediments record limited evidence of having  
764 undergone proglacial deformation. Following initiation of ice-marginal retreat during the  
765 spring (3), the ice-proximal slope collapses due to loss of support and may undergo localised  
766 reworking. In the case of SKA-13, the cobble/boulder-rich composition of the moraine results  
767 in relatively steep surface slopes and limited action by gravitational processes. The steepness  
768 and bulldozing capabilities of the ice-margin ensure that no material is transferred onto the  
769 glacier surface (cf. Lukas, 2012). As a result, no glacier ice is cut-off from the active margin  
770 and buried within the moraine (3–4).

771

772 *5.1.3. Emplacement of sediment slabs through freeze-on*

773

774 The sequence of events reconstructed for SKA-11 (Figure 24C) occurs where the ice-margin  
775 is relatively thin and retreating from a reverse bedrock slope in the southern part of the foreland  
776 (1). Due to penetration of the winter freezing front (2), slabs of subglacial and glaciofluvial  
777 sediments become frozen to the underside of the glacier snout during winter re-advance (cf.  
778 Krüger, 1993, 1994, 1995, 1996; Matthews et al., 1995; Evans and Hiemstra, 2005; Reinardy  
779 et al., 2013; Hiemstra et al., 2015). As the ice-margin re-advances, the frozen-on sediment is  
780 moved as an integral part of the glacier sole and overrides the foreland (Krüger, 1995).  
781 Proglacial materials may also begin to build up and be pushed as the ice-front continues to re-  
782 advance (Reinardy et al., 2013). During the spring (3), this frozen-on sediment begins to melt  
783 out incrementally, forming a ridge containing diamicton, gravel and sand units dipping  
784 upglacier (see Figure 21; Krüger, 1993, 1995, 1996; Evans and Hiemstra, 2005; Reinardy et  
785 al., 2013). As the glacier continues to retreat during the summer (4), a moraine ridge comprising  
786 upglacier dipping sediment units is revealed. Localised reworking of the distal slope may occur  
787 through mass movement activity, as in the case of SKA-11 (see Figure 21). The genetic model  
788 outlined for SKA-11 is similar to that previously proposed for annual moraine formation  
789 elsewhere (Krüger, 1995; Reinardy et al., 2013).

790

791 *5.2. Influences on moraine geomorphology*

792

793 Recessional moraines on the foreland of Skálafellsjökull display a distinctive sawtooth or  
794 crenulate planform geometry, similar to that previously identified elsewhere (e.g. Andrews and  
795 Smithson, 1966; Price; 1970; Matthews et al., 1979; Evans and Twigg, 2002; Bradwell, 2004a;

796 Burki et al., 2009; Evans et al., 2015). This sawtooth planform geometry has previously been  
797 interpreted as reflecting formation along a glacier snout strongly indented by closely-spaced,  
798 longitudinal crevasses, which give rise to closely spaced re-entrants or pecten (Price, 1970;  
799 Matthews et al., 1979; Sharp, 1984; Burki et al., 2009; Evans et al., 2015). Given that  
800 recessional moraines at Skálafellsjökull form through a range of ice-marginal genetic  
801 processes, and predominantly through push/squeeze mechanisms, we suggest that the sawtooth  
802 planform of the moraines represents ice-margin morphology. Further support for this is  
803 provided by remote-sensing observations, with recessional moraines appearing to closely  
804 reflect the structure of the ice-margin.

805

806 The structure of the glacier reflects down-ice changes in hypsometry, from a topographically-  
807 confined icefall to an unconfined foreland, which result in changes in transverse tensional stress  
808 of the glacier surface layers and corresponding changes in the crevasse pattern. As the glacier  
809 flows out onto the unconfined foreland there is a reduction in transverse stress, with lateral  
810 extension of the ice and longitudinal compressive flow occurring (Nye, 1952; Benn and Evans,  
811 2010; Cuffey and Paterson, 2010). This change in the glacier stress field leads to the  
812 development of radial crevasses at the glacier snout, and hence the development of a pecten  
813 (Nye, 1952; Matthews et al., 1979; Burki et al., 2009; Benn and Evans, 2010; Cuffey and  
814 Paterson, 2010; Johnson et al., 2010). The distinctive sawtooth moraines at Skálafellsjökull  
815 therefore integrate the effects of both glacier structure and topography (Figure 25). A similar  
816 process-form regime has been identified at Fláajökull (Evans et al., 2015).

817

818 Previously it has been demonstrated that sawtooth moraines may exhibit statistically significant  
819 differences in the morphological characteristics of teeth and notches (Matthews et al., 1979).  
820 However, no statistically significant differences were identified in the height and width of

821 moraines at Skálafellsjökull, despite moraine geomorphology being strongly influenced by  
822 glacier structure and topography (cf. Matthews et al., 1979; Burki et al., 2009). The greater  
823 height of notches at Bødalsbreen, southern Norway, was argued to reflect the accumulation of  
824 bulldozed debris in the recesses formed by radial crevasses at the glacier snout, while the lower  
825 height of teeth was explained by debris spreading around the advancing protuberances of ice  
826 (Matthews et al., 1979). The differences between Skálafellsjökull and Bødalsbreen may reflect  
827 the following: (i) a difference in moraine genetic processes, with the Skálafellsjökull moraines  
828 predominantly being formed by bulldozing of extruded submarginal sediments rather than  
829 bulldozing of proglacial material; (ii) Skálafellsjökull may be a less effective bulldozer of  
830 material than Bødalsbreen; (iii) differences in glacier dynamics, with Skálafellsjökull being a  
831 piedmont lobe rather than a valley glacier; and/or (iv) the duration of moraine construction,  
832 with the moraines at Skálafellsjökull being formed during a single winter/spring re-advance  
833 rather than over a number of seasonal cycles. The difference in moraine genesis (i) is likely to  
834 exert a particularly important control, with the regular heights of annual moraines at  
835 Skálafellsjökull reflecting the amount of saturated subglacial sediment available for squeezing.  
836 Nonetheless, it is likely that the morphological differences reflect a combination of these  
837 intimately linked factors.

838

### 839 5.3. Patterns, rates and drivers of recent ice-marginal retreat

840

#### 841 *5.3.1. Patterns and rates of recent ice-marginal retreat*

842

843 As it has been established that moraines on the central and northern parts of the Skálafellsjökull  
844 foreland formed annually through a range of ice-marginal genetic processes, we interpret these  
845 features as representative of successive annual ice-marginal positions. The annual moraines

846 can therefore be employed to calculate IMRRs, equivalent to annual moraine crest-to-crest  
847 spacing (cf. Bradwell, 2004a; Lukas, 2012). IMRRs have been calculated for the periods 1936–  
848 1964, 1969–1974 and 2006–2011 (see Section 3.4). Moraines situated on the southern part of  
849 the foreland have not been used in calculations of IMRRs, due to (i) difficulties in ascribing  
850 dates of formation to the moraines (see Section 4.2), and (ii) the presence of a reverse bedrock  
851 slope which may control and/or modulate the rate of ice-marginal fluctuations at this part of  
852 the margin, superimposing another signal on the moraine sequence (Lukas, 2012).

853

854 Annual moraine spacing (IMRRs) indicates that Skálafellsjökull experienced ice-marginal  
855 retreat in every year between 1936 and 1964 (average:  $25.6 \text{ m a}^{-1}$ ), representing the longest  
856 sustained period of glacier recession during the ~80-year period examined. Ice-front retreat  
857 was particularly rapid during the late 1930s and early 1940s, before a reduction of IMRR values  
858 in the latter part of the 1940s (Figure 26A). More pronounced glacier recession again occurred  
859 during the mid-1950s, before rates of ice-margin retreat slowed in early 1960s. Remote-sensing  
860 observations suggest Skálafellsjökull subsequently re-advanced sometime during 1964–1969.  
861 The reversal in the trend of ice-marginal retreat during the 1960s appears to be a common  
862 pattern across all Icelandic non-surge-type glaciers, with many of them advancing to varying  
863 degrees during this period (cf. Sigurðsson and Jónsson, 1995; Sigurðsson, 1998; Sigurðsson et  
864 al., 2007). A short period of annual moraine formation occurred at the northeastern margin of  
865 Skálafellsjökull between 1969 and 1974, with IMRRs averaging  $9.9 \text{ m a}^{-1}$ . Following this  
866 period, annual moraine formation ceased at the ice-margin. Remote-sensing observations  
867 indicate that the glacier was relatively stable between 1975 and 1989. Unfortunately, there is a  
868 lack of ice-front measurements and remote-sensing data during the 1990s, but observations at  
869 other Icelandic non-surge-type glaciers indicate many of them re-advanced during the mid-  
870 1990s (e.g. Sigurðsson and Jónsson, 1995; Sigurðsson, 1998; Sigurðsson et al., 2007). Annual

871 moraine formation recommenced at the northeastern margin during winter 2005/2006, with  
872 ice-front recession continuing to the end of the imagery archive (June 2012).

873

874 The calculated IMRRs for Skálafellsjökull are comparable to those calculated from annual  
875 moraine spacing at other Icelandic outlet glaciers (cf. Bradwell, 2004a; Bradwell et al., 2013),  
876 demonstrating that Icelandic glaciers underwent similar change during the 20<sup>th</sup> Century. This  
877 is supported by ice-front measurements from all non-surge-type outlet glaciers in Iceland (cf.  
878 Sigurðsson et al., 2007). Elsewhere in the North Atlantic region, SE Greenland outlet glaciers  
879 underwent two pronounced recessional periods, occurring during 1933–1943 and 2000–2010  
880 (Bjørk et al., 2012; see also Howat et al., 2008; Thomas et al., 2009; Howat and Eddy, 2011;  
881 Mernild et al., 2012). These prominent periods of ice-front recession coincide with the periods  
882 of rapid Icelandic glacier retreat identified above (see also Bradwell, 2004a; Sigurðsson *et al.*,  
883 2007; Bradwell et al., 2013), implying that glaciers in the North Atlantic region may be  
884 responding to a regional external forcing mechanism, rather than local drivers. However,  
885 comparisons between Icelandic and Greenlandic outlet glaciers are somewhat complicated by  
886 differences in both size and terminal environment, with many Greenlandic glaciers terminating  
887 in a marine environment (cf. Bjørk et al., 2012). The response of marine-terminating glaciers  
888 to forcing may be strongly influenced by topography and bathymetry (e.g. Howat et al., 2008;  
889 Thomas et al., 2009; Carr et al., 2013, 2014, 2015).

890

### 891 *5.3.2. Drivers of recent ice-marginal retreat*

892

893 Previous studies of annual moraine spacing, both in Iceland and elsewhere, have demonstrated  
894 a temporal coincidence between IMRRs and air temperature anomalies (Boulton, 1986; Krüger,  
895 1995; Bradwell, 2004a; Beedle et al., 2009; Bradwell et al., 2013). However, such studies have

896 undertaken limited statistical treatment of other climate variables (e.g. precipitation, sea surface  
897 temperature). Presently, only two studies have examined the influence of precipitation on  
898 IMRRs calculated from annual moraine spacing (Beedle et al., 2009; Lukas, 2012).  
899 Furthermore, remote-sensing studies of ice-frontal retreat frequently present limited statistical  
900 analysis of driving mechanisms, often restricted to visual comparisons of time-series plots (e.g.  
901 Bjørk et al., 2012; Carr et al., 2013; Miles et al., 2013; Stokes et al., 2013b). We present  
902 statistical analysis of a wider array of climate variables, building on previous studies of annual  
903 moraine spacing (e.g. Bradwell, 2004a; Beedle et al., 2009; Lukas, 2012).

904

905 Visual comparison of time-series plots for IMRRs and key climate variables appear to show  
906 that periods of retreat (and annual moraine formation) are associated with elevated air  
907 temperature and sea surface temperature (Figure 26). Covariance analysis was conducted to  
908 examine the possible influence of AAT, SST, precipitation and the NAO on IMRRs in further  
909 detail (Table 6; Figure 27). This analysis focused on the summer and winter signatures as (i)  
910 Icelandic glaciers are thought to be particularly sensitive to variations in summer temperature  
911 (e.g. Bradwell, 2004a; Sigurðsson et al., 2007; Bradwell et al., 2013), (ii) accumulation season  
912 (winter) precipitation and NAO are believed to be important controls on glacier mass balance  
913 in the wider North Atlantic region (e.g. Nesje et al., 2000; Laumann and Nesje, 2009; Winkler  
914 et al., 2009; Marzeion and Nesje, 2012; Mernild et al., 2014), and (iii) it has been established  
915 that annual moraines at Skálafellsjökull are formed during the course of a winter re-advance.  
916 Indeed, no statistically significant relationships were identified for the annual, spring and  
917 autumn signatures (Table 6). The results of the covariance analysis reveal statistically  
918 significant relationships between IMRRs and the summer signatures of AAT ( $r^2 = 0.3464$ ,  $p <$   
919  $0.0001$ ), SST ( $r^2 = 0.1623$ ,  $p = 0.0010$ ) and the NAO ( $r^2 = 0.1310$ ,  $p = 0.0201$ ) (Figure 27).  
920 However, the analysis reveals no statistically significant relationships are evident between

921 IMRRs and the winter signatures of these climate variables (Figure 27; Table 6). In all cases,  
922 the covariance analysis indicated no statistically significant relationships exist between  
923 precipitation and IMRRs (Figure 27; Table 6).

924

925 Based on the analysis presented herein, it appears that Skálafellsjökull is most sensitive to inter-  
926 annual variations in summer AAT. This finding is in accordance with previous studies of  
927 Icelandic glaciers (e.g. Boulton, 1986; Krüger, 1995; Bradwell, 2004a; Sigurðsson et al., 2007;  
928 Bradwell et al., 2013). Furthermore, the temporal coincidence of summer AAT anomalies and  
929 IMRRs suggests that the glacier may have a very rapid reaction time (*sensu* Benn and Evans,  
930 2010), reacting to summer AAT fluctuations at a sub-annual timescale (cf. Bradwell et al.,  
931 2013). Variability in summer SST and the NAO also appear to have some influence on IMRRs,  
932 though to a lesser degree. Statistically significant relationships between SST and Icelandic  
933 termini variations have not hitherto been identified, though it has been identified as a potential  
934 driver of glacier change in SE Greenland (Bjørk et al., 2012). The positive correlation identified  
935 between summer NAO and IMRRs is the opposite of that demonstrated in Norway (Nesje et  
936 al., 2000), where positive NAO leads to overall increase in glacier mass. This is in agreement  
937 with general comparisons presented by Bradwell et al. (2006) from elsewhere in SE Iceland.  
938 Icelandic precipitation values have shown no apparent trend during the observational period  
939 (e.g. Sigurðsson and Jónsson, 1995; Hanna et al., 2004), and this is reflected in the lack of  
940 statistically significant relationships between precipitation and IMRRs. Moreover, the annual  
941 moraines at Skálafellsjökull reflect seasonally-driven submarginal processes active in a given  
942 year (see Section 5.1). As such, processes in the accumulation zone (influence of precipitation)  
943 do not directly impact moraine construction and are, therefore, not reflected in the  
944 annual/seasonal signal recorded by the moraines.

945

946 Although statistically significant relationships have been identified, it should be recognised  
947 that SE Iceland climate is highly complex. Statistical analysis of the inter-annual variability of  
948 atmospheric and oceanic climate variables in SE Iceland shows complex atmosphere-ocean  
949 interactions, with SST in particular appearing to exert an influence on AAT (Figure 28).  
950 Consequently, it may be difficult to unravel the influence of individual climate variables on  
951 ice-frontal variations. In addition to these interactions, there may be underlying longer-term  
952 (decadal to multi-decadal) climate signals, with multiple periodicities reinforcing or  
953 modulating each other. As such, unravelling the composite climate signal recorded in the  
954 Skálafellsjökull moraine record, and establishing the principal drivers of ice-marginal retreat,  
955 is not entirely straightforward (cf. Kirkbride and Brazier, 1998; Kirkbride and Winkler, 2012,  
956 and references therein). This complexity is reflected in the relatively low  $r^2$  values discussed  
957 above. Further potential confounding factors in extracting a climate signal from the annual  
958 moraine record at Skálafellsjökull relate to internal glacier dynamics, glacier structure and the  
959 presence of the reverse bedrock slope in the southern part of the foreland, which are difficult  
960 to quantify.

961

962 Despite these difficulties, the coincidence of periods of pronounced glacier recession at the  
963 study site with those at glaciers across Iceland (e.g. Sigurðsson, 1998; Bradwell, 2004a;  
964 Sigurðsson et al., 2007; Bradwell et al., 2013) implies glacier change forced by a common,  
965 regional mechanism. Furthermore, annual moraine spacing (IMRRs) and ice-front  
966 measurements have been shown to correspond to periods of elevated summer temperature  
967 elsewhere in Iceland (Boulton, 1986; Krüger, 1995; Sigurðsson and Jónsson, 1995; Bradwell,  
968 2004a; Sigurðsson et al., 2007; Bradwell et al., 2013). Thus, we consider summer AAT  
969 variability an important driver of IMRRs at Skálafellsjökull. Moreover, the coincidence of the  
970 periods of Icelandic glacier recession and pronounced Greenlandic ice-frontal retreat (cf. Björk

971 et al., 2012) suggests there may be a common mechanism in the North Atlantic region. We  
972 hypothesise that the mutual driver could be SST variability, with SSTs driving AAT change,  
973 which in turn forces IMRRs. The most recent period of warming and ice-marginal retreat may  
974 be associated with atmospherically-driven weakening and shrinking of the subpolar North  
975 Atlantic gyre (cf. Häkkinen and Rhines, 2004; Hátún et al., 2005; Lohmann et al., 2008; Bersch  
976 et al., 2007; Robson et al., 2012; Barrier et al., 2015, and references therein), a mechanism  
977 which has previously been implicated in forcing Greenlandic glacier fluctuations (Straneo and  
978 Heimbach, 2013). Nevertheless, further evidence from Icelandic glaciers is required to test the  
979 links between SST, AAT and IMRRs. It does, however, seem unlikely that there is a direct link  
980 between SST variability and IMRRs at Skálafellsjökull given the low coefficient of  
981 determination ( $r^2 = 0.1623$ ,  $p = 0.0010$ ).

982

983 Based on the climate variables analysed in this study and the associated  $r^2$  values, we have  
984 developed a sensitivity ranking for Skálafellsjökull (Table 7) which could be applied in the  
985 examination of ice-frontal retreat at other Icelandic glaciers. The variables with the highest  
986 ranking could be tested initially, before further statistical analysis is undertaken. Applying  
987 similar approaches to those used in this study, combined with a systematic approach to IMRR  
988 analysis, at other Icelandic glaciers would provide valuable data to test the hypothesis that  
989 glacier fluctuations in the North Atlantic region are driven by a common forcing mechanism.

990

#### 991 5.4. Recessional moraines as climate proxies

992

993 This study has built on previous studies of annual moraines and considered a greater range of  
994 climate variables in the analysis of IMRRs (cf. Boulton, 1986; Krüger, 1995; Bradwell, 2004a;  
995 Beedle et al., 2009; Lukas, 2012; Bradwell et al., 2013). Nonetheless, there are a number of

996 issues associated with utilising recessional (annual) moraines as climatic indicators, and these  
997 warrant further discussion. A principal issue with utilising annual moraines to examine IMRRs  
998 and extract climate signals is establishing a chronological framework. Previous studies have  
999 employed lichenometric dating to establish the timing of moraine formation (e.g. Bradwell,  
1000 2004a; Bradwell *et al.*, 2013), whilst many accept the features as annual moraines purely on  
1001 the basis of remote-sensing data (e.g. Beedle *et al.*, 2009; Lukas, 2012; Reinardy *et al.*, 2013).  
1002 In this study, moraine chronology was examined through the integration of remote-sensing  
1003 observations, ice-front measurements and lichenometric dating. This approach is effective  
1004 where the data from each of these techniques overlaps, and particularly during time periods  
1005 with a high frequency of imagery. However, problems may arise when attempting to establish  
1006 the date of formation for moraines older than the earliest aerial photograph. Examination of  
1007 ice-frontal fluctuations (and annual moraines) in Iceland benefits from the availability of a vast  
1008 inventory of historical maps and documents, imagery and ice-front measurements (cf.  
1009 Thórarinsson, 1943; Boulton, 1986; Bradwell, 2004a; Sigurðsson, 2005; Sigurðsson *et al.*,  
1010 2007; Bradwell *et al.*, 2013; Hannesdóttir *et al.*, 2014, and references therein). Elsewhere such  
1011 data may not be available, presenting a potential problem when attempting to establish a  
1012 chronological framework for annual moraines. As highlighted previously, even the most well-  
1013 calibrated lichenometric dating has an optimum precision of only 5–10% (Innes, 1988; Noller  
1014 and Locke, 2000). Moreover, the use of lichenometric dating is associated with a number of  
1015 uncertainties (e.g. Jochimsen, 1973; Worsley, 1981; Osborn *et al.*, 2015), which brings into  
1016 question the validity of ages ascribed purely on the basis of this technique.

1017

1018 A further complication is the possibility that moraine formation occurs on a sub-annual basis,  
1019 as demonstrated in the southern part of the foreland (Section 4.2.1). This challenges the concept  
1020 of annual moraines, and implies that ‘annual moraines’ may be an inappropriate classification.

1021 We suggest that grouplets of recessional moraines may form in the same year where  
1022 submarginal processes active over a single seasonal cycle are recorded as multiple ridges,  
1023 rather than as a single composite push/squeeze moraine (cf. Krüger, 1995; Evans and Hiemstra,  
1024 2005). Even where the number of moraines formed in a given time period is equivalent to the  
1025 time elapsed, some of these features may have formed during a single seasonal cycle.  
1026 Evidently, this would introduce errors into the calculations of IMRRs and the subsequent  
1027 analysis of driving mechanisms. Without the availability of remote-sensing data at numerous  
1028 intervals throughout each year during the period of moraine formation, it is difficult to establish  
1029 definitively whether or not these features are annual moraines.

1030

1031 It has previously been argued that annual moraine sequences in the geological record, once  
1032 identified, could be employed to extract high-resolution palaeoclimatic information (Bradwell,  
1033 2004a). However, given the difficulties in establishing the chronology of recessional moraines  
1034 formed during historical times, it seems highly unlikely that moraines could be identified as  
1035 annual features in the geological record and subsequently used to make high resolution  
1036 palaeoclimatic inferences. Indeed, the range of geochronological techniques typically  
1037 employed in a palaeoglaciological context are frequently associated with substantial errors (cf.  
1038 Lukas et al., 2007; Fuchs and Owen, 2008; Balco, 2011, Small et al., 2012; Hughes et al., 2015;  
1039 Osborn et al., 2015; Stokes et al., 2015, and references therein) and age estimates may  
1040 contradict the geomorphological evidence (e.g. Boston et al., 2015; cf. Gheorghiu et al., 2012;  
1041 Gheorghiu and Fabel, 2013). The resolution and errors associated with these geochronological  
1042 techniques would preclude the dating of annual moraines. Given these potential issues, we  
1043 argue that it is unlikely that annual moraines could reliably be employed in a high resolution  
1044 palaeoclimatic context (cf. Boulton, 1986; Krüger, 1995). Nonetheless, seasonal push moraines  
1045 have been identified in the ancient landform record through the use of a landsystems approach

1046 and modern analogues (e.g. Evans et al., 1999b, Ham and Attig, 2001, Evans et al., 2014). In  
1047 this way, these features have been employed to suggest glacier dynamics driven by seasonal  
1048 climate variability.

1049

1050 Aside from chronological issues, depositional and erosional censoring may affect the integrity  
1051 of moraine sequences and reduce their climatic representativeness (cf. Gibbons et al., 1984;  
1052 Kirkbride and Brazier, 1998; Kirkbride and Winkler, 2012; Barr and Lovell, 2014, and  
1053 references therein). Both self- and external censoring processes (*sensu* Kirkbride and Winkler,  
1054 2012) may impact recessional moraine sequences to varying degrees. Particularly significant  
1055 processes may include (i) localised glacier overriding and superimposition of moraines  
1056 (obliterative overlap) (e.g. Price, 1970; Sharp, 1984; Evans and Twigg, 2002; Lukas, 2005a, b;  
1057 Benn and Lukas, 2006; Evans et al., 2015), (ii) melting of debris-covered ice in ice-cored  
1058 moraines (cf. Andersen and Sollid, 1971; Sharp, 1984; Krüger and Kjær, 2000; Lukas et al.,  
1059 2005; Schomacker and Kjær, 2007, 2008; Schomacker, 2008; Lukas, 2011, 2012; Reinardy et  
1060 al., 2013), and (iii) external censoring by glaciofluvial processes, which are a prominent feature  
1061 of active temperate glacial landsystems (cf. Evans and Twigg, 2002; Evans, 2003; Evans and  
1062 Orton, 2015; Evans et al., 2015, and references therein). The efficacy of these self-censoring  
1063 and external censoring processes can have important implications for the integrity  
1064 (preservation) of recessional moraine sequences, introducing uncertainties into calculations of  
1065 IMRRs and subsequent analysis of drivers of ice-marginal retreat.

1066

1067 Despite the highlighted issues, we argue that annual moraine sequences do afford a valuable  
1068 tool for examining ice-frontal retreat in contemporary glacial environments (cf. Bradwell,  
1069 2004a; Beedle et al., 2009; Lukas, 2012; Bradwell et al., 2013). Provided that issues relating to  
1070 the integrity of the sequences can be minimised, and annual formation can confidently be

1071 ascribed, annual moraines can provide valuable insights into patterns, rates and drivers of ice-  
1072 marginal retreat. Landsystem imprints in ancient records (e.g. Evans et al., 1999b, 2014) can  
1073 also indicate rapid, potentially seasonal, responses of glacier/ice-sheet margins, despite the low  
1074 temporal resolution in some settings. Nevertheless, there are issues surrounding the frequency  
1075 of moraine formation, and our understanding of ice-marginal dynamics and moraine formation  
1076 at active temperate glaciers would benefit from repeat surveying/monitoring of ice-fronts  
1077 during a single year. This could be achieved through relatively low-cost UAV surveys or time-  
1078 lapse photography, which are becoming increasingly popular in glaciology and glacial  
1079 geomorphology (e.g. Amundson et al., 2010; Kristensen and Benn, 2012; Walter et al., 2012;  
1080 Evans et al., 2015; Ryan et al., 2015).

1081

## 1082 **6. Conclusions**

1083

1084 In this study we applied small-scale recessional moraines on the foreland of Skálafellsjökull,  
1085 SE Iceland, as a geomorphological proxy to examine recent patterns, rates and drivers of ice-  
1086 marginal retreat at this outlet glacier. Suites of small-scale, recessional moraines are distributed  
1087 across the glacier foreland, and exhibit distinctive sawtooth planform geometries.  
1088 Chronological investigations of the moraines, which integrated remote-sensing observations  
1089 and lichenometric dating, indicated annual moraine formation on the northern and central parts  
1090 of the foreland. These annual moraines formed during three key periods: 1936–1964; 1969–  
1091 1974; and from 2006 onwards. However, recessional moraines on the southern foreland appear  
1092 to be forming on a sub-annual basis, indicating that ‘annual moraines’ is an inappropriate  
1093 classification in some cases. Sedimentological investigations of a representative sub-sample of  
1094 moraines on the foreland revealed that moraines form through a range of ice-marginal  
1095 processes, with push/squeeze mechanisms being dominant. Furthermore, glacier structure was

1096 identified as a key factor in annual moraine formation and geomorphology. The  
1097 geomorphological, chronological and sedimentological data therefore indicated that these  
1098 moraines represent successive annual ice-frontal positions. Thus, these annual moraines  
1099 provided a framework for exploring patterns, rates and drivers of ice-marginal retreat at  
1100 Skálafellsjökull.

1101

1102 Calculation of IMRRs, on the basis of annual moraine spacing, indicated pronounced retreat  
1103 occurred at Skálafellsjökull during the 1930s and early 1940s, the early 1950s and from 2006  
1104 onwards. These pronounced periods of retreat coincide with those exhibited elsewhere in  
1105 Iceland and the wider North Atlantic region, implying a regional driving mechanism may be  
1106 forcing IMRRs. Covariance analysis of IMRRs at Skálafellsjökull and climate data suggested  
1107 summer AAT, SST and NAO have an influence on IMRRs, with the glacier appearing to be  
1108 most sensitive to summer air temperature. Based on the climate data analysis conducted in this  
1109 research, it has been hypothesised that SST may drive air temperature changes in the North  
1110 Atlantic region, which in turn forces IMRRs. The increase in SST over recent decades may  
1111 result from an atmospheric-driven weakening in the North Atlantic subpolar gyre. However,  
1112 further data is required to test the links between SST, AAT and IMRRs.

1113

1114

1115

1116

1117

1118

1119

1120

1121 **Acknowledgements**

1122

1123 We are grateful to Oddur Sigurðsson and Trausti Jónsson (both Icelandic Meteorological  
1124 Office), who kindly provided ice-front measurements and assisted with the compilation of  
1125 meteorological data, respectively. Thanks are due to the UK Meteorological Office and British  
1126 Atmospheric Data Centre for granting access to the HadSST2 dataset. Marek Ewertowski is  
1127 thanked for his assistance with remote-sensing aspects of this research, whilst Alex Clayton is  
1128 thanked for kindly providing access to UAV-captured imagery. Sven Lukas and Cianna  
1129 Wyshnytzky provided valuable discussion on annual moraines, and Cianna is also thanked for  
1130 comments on an earlier draft of this paper. BMPC would like to thank Hannah Bickerdike,  
1131 Jonathan Chandler and Bertie Miles for field assistance. Regína Hreinsdóttir (National Park  
1132 Warden, South Territory) kindly granted permission to undertake fieldwork within the  
1133 Vatnajökull National Park. The research was conducted under RANNÍS Agreement 4/2014.  
1134 Fieldwork in Iceland was supported by a Van Mildert College Principal's Award and QRA  
1135 New Research Workers' Award, awarded to BMPC. This study was conducted whilst BMPC  
1136 was in receipt of a Van Mildert College Postgraduate Award at Durham University. Thorough  
1137 and constructive reviews by Kurt Kjær and Ívar Örn Benediktsson improved the clarity of this  
1138 contribution.

1139

1140

1141

1142

1143

1144

1145

1146 **References**

1147

1148 Aðalgeirsdóttir, G., Jóhannesson, T., Björnsson, H., Pálsson, F., Sigurðsson, O., 2006. Response of  
1149 Hofsjökull and southern Vatnajökull, Iceland, to climate change. *J. Geophys. Res.* 111, F03001.

1150 doi: <http://dx.doi.org/10.1029/2005JF000388>

1151 Amundson, J.M., Fahnestock, M., Truffer, M., Brown, J., Lüthi, M.P., Motyka, R.J., 2010. Ice mélange  
1152 dynamics and implications for terminus stability, Jakobshavn Isbræ, Greenland. *J. Geophys.*

1153 *Res.: Earth Surf.* 115, F01005. doi: <http://dx.doi.org/10.1029/2009JF001405>

1154 Andersen, J.L., Sollid, J.L., 1971. Glacial chronology and glacial geomorphology in the marginal zones  
1155 of the glaciers Midtdalsbreen and Nigardsbreen, south Norway. *Nor. Geogr. Tidsskr.* 25, 1–38.

1156 doi: <http://dx.doi.org/10.1080/00291957108551908>

1157 Andrews, D.E., Smithson, B.B., 1966. Till fabric of the cross-valley moraines of north-central Baffin  
1158 Island, North West Territories, Canada. *Geol. Soc. Am. Bull.* 77, 271–290. doi:

1159 [http://dx.doi.org/10.1130/0016-7606\(1966\)77\[271:TFOTCM\]2.0.CO;2](http://dx.doi.org/10.1130/0016-7606(1966)77[271:TFOTCM]2.0.CO;2)

1160 Armstrong, R.A., 2015. The Influence of Environmental Factors on the Growth of Lichens in the Field.

1161 In: Upreti, D.K., Divakar, P.K., Shukla, V., Bajpai., R. (eds.), *Recent Advances in Lichenology*.  
1162 Springer, New Delhi, pp. 1–18.

1163 Balco, G., 2011. Contributions and unrealized potential contributions of cosmogenic-nuclide exposure  
1164 dating to glacier chronology, 1990–2010. *Quat. Sci. Rev.* 30, 3–27. doi:

1165 <http://dx.doi.org/10.1016/j.quascirev.2010.11.003>

1166 Barr, I.D., Lovell, H., 2014. A review of topographic controls on moraine distribution. *Geomorphol.*  
1167 226, 44–64. doi: <http://dx.doi.org/10.1016/j.geomorph.2014.07.030>

1168 Barrier, N., Deshayes, J., Treguier, A.-M., Cassou, C., 2015. Heat budget in the North Atlantic subpolar  
1169 gyre: Impacts of atmospheric weather regimes on the 1995 warming event. *Prog. Oceanogr.*

1170 130, 75–90. doi: <http://dx.doi.org/10.1016/j.pocean.2014.10.001>

1171 Beedle, M.J., Menounos, B., Luckman, B.H., Wheate, R., 2009. Annual push moraines as climate  
1172 proxy. *Geophys. Res. Lett.* 36, L20501. doi: <http://dx.doi.org/10.1029/2009GL039533>

- 1173 Benedict, J.B., 1967. Recent glacial history of an alpine area in the Colorado Front Range, USA. I.  
1174 Establishing a lichen growth curve. *J. Glaciol.* 6, 817–832.
- 1175 Benedict, J.B., 1985. Arapaho Pass. Glacial geology and archaeology at the crest of the Colorado Front  
1176 Range. Centre for Mountain Archaeology Research Report No. 3. Ward, Colorado.
- 1177 Benedict J.B., 1990. Experiments on lichen growth. I. Seasonal patterns and environmental controls.  
1178 *Arct. Alp. Res.* 22(3), 244–254. doi: <http://dx.doi.org/10.2307/1551587>
- 1179 Benediktsson, Í.Ö., Ingólfsson, Ó., Schomacker, A., Kjær, K.H., 2009. Formation of submarginal and  
1180 proglacial end moraines: implications of ice-flow mechanism during the 1963–64 surge of  
1181 Brúarjökull, Iceland. *Boreas* 38(3), 440–457. doi: <http://dx.doi.org/10.1111/j.1502-3885.2008.00077.x>
- 1182
- 1183 Benediktsson, Í.Ö., Möller, P., Ingólfsson, Ó., van der Meer, J.J.M., Kjær, K.H., Krüger, J., 2008.  
1184 Instantaneous end moraine and sediment wedge formation during the 1890 surge of  
1185 Brúarjökull. Iceland. *Quat. Sci. Rev.* 27, 209–234. doi:  
1186 <http://dx.doi.org/10.1016/j.quascirev.2007.10.007>
- 1187 Benediktsson, Í.Ö., Schomacker, A., Lokrantz, H., 2010. The 1890 surge end moraine at  
1188 Eyjabakkajökull, Iceland: A re-assessment of a classic glaciotectionic locality. *Quat. Sci. Rev.*  
1189 29, 484–506. doi: <http://dx.doi.org/10.1016/j.quascirev.2009.10.004>
- 1190 Benediktsson, Í.Ö., Schomacker, A., Johnson, M.D., Geiger, A.J., Ingólfsson, Ó., Guðmundsdóttir,  
1191 E.R., 2015. Architecture and structural evolution of an early Little Ice Age terminal moraine at  
1192 the surge-type glacier Múlajökull, Iceland. *J. Geophys. Res.: Earth Surf.* 120(9), 1895–1910.  
1193 doi: <http://dx.doi.org/10.1002/2015JF003514>
- 1194 Benn, D.I., 1992. The genesis and significance of ‘hummocky moraine’: evidence from the Isle of Skye,  
1195 Scotland. *Quat. Sci. Rev.* 11, 781–99. doi: [http://dx.doi.org/10.1016/0277-3791\(92\)90083-K](http://dx.doi.org/10.1016/0277-3791(92)90083-K)
- 1196 Benn, D.I., 1994. Fluted moraine formation and till genesis below a temperate glacier: Slettmarkbreen,  
1197 Jotunheimen, Norway. *Sedimentol.* 41, 279–292. doi: <http://dx.doi.org/10.1111/j.1365-3091.1994.tb01406.x>
- 1198
- 1199 Benn, D.I., 2004. Clast morphology. In: Evans, D.J.A., Benn, D.I. (eds.), 2004. *A Practical Guide to*  
1200 *the Study of Glacial Sediments*. Arnold, London, pp. 78–92.

- 1201 Benn, D.I., Ballantyne, C.K., 1993. The description and representation of particle shape. *Earth Surf.*  
1202 *Process. Landf.* 18, 665–72. doi: <http://dx.doi.org/10.1002/esp.3290180709>
- 1203 Benn, D.I., Ballantyne, C.K., 1994. Reconstructing the transport history of glacial sediments: a new  
1204 approach based on the co-variance of clast shape indices. *Sediment. Geol.* 91, 215–27. doi:  
1205 [http://dx.doi.org/10.1016/0037-0738\(94\)90130-9](http://dx.doi.org/10.1016/0037-0738(94)90130-9)
- 1206 Benn, D.I., Evans, D.J.A., 2010. *Glaciers and Glaciation (Second Edition)*. Hodder Education, London,  
1207 802 pp.
- 1208 Benn, D.I., Lukas, S., 2006. Younger Dryas glacial landsystems in North West Scotland: an assessment  
1209 of modern analogues and palaeoclimatic implications. *Quat. Sci. Rev.* 25, 2390–2408. doi:  
1210 <http://dx.doi.org/10.1016/j.quascirev.2006.02.015>
- 1211 Bennett, G.L., Evans, D.J.A., Carbonneau, P., Twigg, D.R., 2010. Evolution of a debris-charged glacier  
1212 landsystem, Kvíárjökull, Iceland. *J. Maps* 6(1), 40–67. doi:  
1213 <http://dx.doi.org/10.4113/jom.2010.1114>
- 1214 Bennett, M.R., 2001. The morphology, structural evolution and significance of push moraines. *Earth-*  
1215 *Sci. Rev.* 53, 197–236. doi: [http://dx.doi.org/10.1016/S0012-8252\(00\)00039-8](http://dx.doi.org/10.1016/S0012-8252(00)00039-8)
- 1216 Bennett, M.R., Huddart, D., Waller, R.I., Midgley, N.G., Gonzalez, S., Tomio, A., 2004a. Styles of ice-  
1217 marginal deformation at Hagafellsjökull-Eystri, Iceland during the 1998/99 winter-spring  
1218 surge. *Boreas* 33, 97–107. doi: <http://dx.doi.org/10.1111/j.1502-3885.2004.tb01132.x>
- 1219 Bennett, M.R., Huddart, D., Waller, R.I., Cassidy, N., Tomio, A., Zukowskyj, P., Midgley, N.G., Cook,  
1220 S.J., Gonzalez, S., Glasser, N.F., 2004b. Sedimentary and tectonic architecture of a large push  
1221 moraine: a case study from Hagafellsjökull-Eystri, Iceland. *Sediment. Geol.* 172, 269–292. doi:  
1222 <http://dx.doi.org/10.1016/j.sedgeo.2004.10.002>
- 1223 Bersch, M., Yashayaev, I., Koltermann, K.P., 2007. Recent changes of the thermohaline circulation in  
1224 the subpolar North Atlantic. *Ocean Dyn.* 57, 223–235. doi: [http://dx.doi.org/10.1007/s10236-](http://dx.doi.org/10.1007/s10236-007-0104-7)  
1225 [007-0104-7](http://dx.doi.org/10.1007/s10236-007-0104-7)
- 1226 Birnie, R.V., 1977. A snow-bank push mechanism for the formation of some “annual” moraine ridges.  
1227 *J. Glaciol.* 18, 77–85.

- 1228 Bjørk, A.A., Kjær, K.H., Korsgaard, N.J., Khan, S.A., Kjeldsen, K.K., Andresen, C.S., Box, J.E.,  
1229 Larsen, N.K., Funder, S., 2012. An aerial view of 80 years of climate-related glacier  
1230 fluctuations in southeast Greenland. *Nat. Geosci.* 5, 427–432. doi:  
1231 <http://dx.doi.org/10.1038/ngeo1481>
- 1232 Björnsson, H., Pálsson, F., 2008. Icelandic glaciers. *Jökull* 58, 365–386.
- 1233 Björnsson, H., Pálsson, F., Guðmundsson, S., 2001. Jökulsárlón at Breiðamerkursandur, Vatnajökull,  
1234 Iceland: 20th century changes and future outlook. *Jökull* 50, 1–18.
- 1235 Björnsson, H., Pálsson, F., Guðmundsson, S., Magnússon, E., Adalgeirsdóttir, G., Jóhannesson, T.,  
1236 Berthier, E., Sigurðsson, O., Thorsteinsson, T., 2013. Contribution of Icelandic ice caps to sea  
1237 level rise: Trends and variability since the Little Ice Age. *Geophys. Res. Lett.* 40, 1546–1550.  
1238 doi: <http://dx.doi.org/10.1002/grl.50278>
- 1239 Boston, C.M., 2012. A glacial geomorphological map of the Monadhliath Mountains, Central Scottish  
1240 Highlands. *J. Maps* 8(4), 437–444. doi: <http://dx.doi.org/10.1080/17445647.2012.743865>
- 1241 Boston, C.M., Lukas, S., Carr, S.J., 2015. A Younger Dryas plateau icefield in the Monadhliath,  
1242 Scotland, and implications for regional palaeoclimate. *Quat. Sci. Rev.* 108, 139–162. doi:  
1243 <http://dx.doi.org/10.1016/j.quascirev.2014.11.020>
- 1244 Boulton, G.S., 1976. The origin of glacially fluted surfaces: observations and theory. *J. Glaciol.* 17,  
1245 287–309.
- 1246 Boulton, G.S., 1978. Boulder shapes and grain-size distributions of debris as indicators of transport  
1247 paths through a glacier and till genesis. *Sedimentol.* 25(6), 773–799. doi:  
1248 <http://dx.doi.org/10.1111/j.1365-3091.1978.tb00329.x>
- 1249 Boulton, G.S., 1986. Push moraines and glacier-contact fans in marine and terrestrial environments.  
1250 *Sedimentol.* 33, 677–698. doi: <http://dx.doi.org/10.1111/j.1365-3091.1986.tb01969.x>
- 1251 Boulton, G.S., Dobbie, K.E., 1998. Slow flow of granular aggregates: the deformation of sediments  
1252 beneath glaciers. *Philos. Trans. R. Soc. Lond. A* 356(1747), 2713–2745. doi:  
1253 <http://dx.doi.org/10.1098/rsta.1998.0294>

- 1254 Boulton, G.S., Dobbie, K.E., Zatsepin, S., 2001. Sediment deformation beneath glaciers and its coupling  
1255 to the subglacial hydraulic system. *Quat. Int.* 86, 3–28. doi: <http://dx.doi.org/10.1016/S1040->  
1256 [6182\(01\)00048-9](http://dx.doi.org/10.1016/S1040-6182(01)00048-9)
- 1257 Boulton, G.S., Hindmarsh, R.C.A., 1987. Sediment deformation beneath glaciers: rheology and  
1258 sedimentological consequences. *J. Geophys. Res.: Solid Earth* 92, 9059–9082. doi:  
1259 <http://dx.doi.org/10.1029/JB092iB09p09059>
- 1260 Bradwell, T. 2001. A new lichenometric dating curve for southeast Iceland. *Geogr. Ann.* 83A, 91–101.  
1261 doi: <http://dx.doi.org/10.1111/j.0435-3676.2001.00146.x>
- 1262 Bradwell, T., 2004a. Annual moraines and summer temperatures at Lambatungnajökull, Iceland. *Arct.,*  
1263 *Antarct., Alp. Res.* 36, 502–508. doi: <http://dx.doi.org/10.1657/1523->  
1264 [0430\(2004\)036\[0502:AMASTA\]2.0.CO;2](http://dx.doi.org/10.1657/1523-0430(2004)036[0502:AMASTA]2.0.CO;2)
- 1265 Bradwell, T., 2004b. Lichenometric dating in southeast Iceland: the size-frequency approach. *Geogr.*  
1266 *Ann.* 86A, 31–41. doi: <http://dx.doi.org/10.1111/j.0435-3676.2004.00211.x>
- 1267 Bradwell, T., Armstrong, R.A., 2007. Growth rates of *Rhizocarpon geographicum*: a review with new  
1268 data from Iceland. *J. Quat. Sci.* 22, 311–320. doi: <http://dx.doi.org/10.1002/jqs.1058>
- 1269 Bradwell, T., Dugmore, D.J., Sugden, D.E., 2006. The Little Ice Age glacier maximum in Iceland and  
1270 the North Atlantic Oscillation: evidence from Lambatungnajökull, southeast Iceland. *Boreas*  
1271 35, 61–80. doi: <http://dx.doi.org/10.1111/j.1502-3885.2006.tb01113.x>
- 1272 Bradwell, T., Sigurðsson, O., Everest, J., 2013. Recent, very rapid retreat of a temperate glacier in SE  
1273 Iceland. *Boreas* 42, 959–973. <http://dx.doi.org/10.1111/bor.12014>
- 1274 Brook, M.S., Lukas, S., 2012. A revised approach to discriminating sediment transport histories in  
1275 glacial sediments in a temperate alpine environment: a case study from Fox Glacier, New  
1276 Zealand. *Earth Surf. Process. Landf.* 37, 895–900. doi: <http://dx.doi.org/10.1002/esp.3250>
- 1277 Brynjólfsson, S., Schomacker, A., Ingólfsson, Ó., 2014. Geomorphology and the Little Ice Age extent  
1278 of the Drangajökull ice cap, NW Iceland, with focus on its three surge-type outlets.  
1279 *Geomorphol.* 213, 292–304. doi: <http://dx.doi.org/10.1016/j.geomorph.2014.01.019>

- 1280 Burki, V., Larsen, E., Fredin, O., Margreth, A., 2009. The formation of sawtooth moraine ridges in  
1281 Bødalen, western Norway. *Geomorphol.* 105, 182–192. doi:  
1282 <http://dx.doi.org/10.1016/j.geomorph.2008.06.016>
- 1283 Carr J.R., Stokes C.R., Vieli A., 2014. Recent retreat of major outlet glaciers on Novaya Zemlya,  
1284 Russian Arctic, influenced by fjord geometry and sea-ice conditions. *J. Glaciol.* 60(219), 155–  
1285 170.
- 1286 Carr J.R., Vieli A., Stokes C.R., 2013. Climatic, oceanic and topographic controls on marine-  
1287 terminating outlet glacier behavior in north-west Greenland at seasonal to interannual  
1288 timescales. *J. Geophys. Res.* 118(3), 1210–1226. <http://dx.doi.org/10.1002/jgrf.20088>
- 1289 Carr J.R., Vieli A., Stokes C.R., Jamieson S.S.R., Palmer S.J., Christoffersen P., Dowdeswell J.A., Nick  
1290 F.M., Blankenship D.D., Young D.A., 2015. Basal topographic controls on rapid retreat of  
1291 Humboldt Glacier, northern Greenland. *J. Glaciol.* 61(225), 137–150.
- 1292 Caseldine, C.J., 1991. Lichenometric dating, lichen population studies and Holocene glacial history in  
1293 Tröllaskagi, northern Iceland. In: Maizels, J.K. and Caseldine, C. (eds.), *Environmental Change*  
1294 *in Iceland: Past and Present. Glaciology and Quaternary Geology.* Kluwer Academic  
1295 Publishers. Dordrecht pp. 219–233.
- 1296 Chandler, B.M.P., Evans, D.J.A., Roberts, D.H., Ewertowski, M.W., Clayton, A.I., 2015. Glacial  
1297 geomorphology of the Skálafellsjökull foreland, Iceland: A case study of ‘annual’ moraines. *J.*  
1298 *Maps*, in press. doi: <http://dx.doi.org/10.1080/17445647.2015.1096216>
- 1299 Clark, C.D., Hughes, A.L.C., Greenwood, S.L., Spagnolo, M., Ng, F.S.L., 2009. Size and shape  
1300 characteristics of drumlins, derived from a large sample, and associated scaling laws. *Quat. Sci.*  
1301 *Rev.* 28, 677–692. doi: <http://dx.doi.org/10.1016/j.quascirev.2008.08.035>
- 1302 Cook-Talbot, J.D., 1991. Sorted circles, relative-age dating and palaeoenvironmental reconstruction in  
1303 an alpine periglacial environment, eastern Jotunheim, Norway: Lichenometric and weathering-  
1304 based approaches. *The Holocene* 1, 128–141. doi:  
1305 <http://dx.doi.org/10.1177/095968369100100205>
- 1306 Cuffey, K.M., Paterson, W.S.B., 2010. *The Physics of Glaciers (Fourth Edition).* Butterworth-  
1307 Heinemann, Burlington, MA, USA and Kidlington, Oxford, UK, 693 pp.

- 1308 Danish General Staff, 1904. Sheet 96-NA, 1:50.000. The topographic department of the Danish General  
1309 Staff, Copenhagen.
- 1310 Darvill, C.M., Stokes, C.R., Bentley, M.R., Lovell, H., 2014. A glacial geomorphological map of the  
1311 southernmost ice lobes of Patagonia: the Bahía Inútil – San Sebastián, Magellan, Otway,  
1312 Skyring and Río Gallegos lobes. *J. Maps* 10(3), 500–520. doi:  
1313 <http://dx.doi.org/10.1080/17445647.2014.890134>
- 1314 Erikstad, L., Sollid, J.L., 1986. Neoglaciation in South Norway using lichenometric methods. *Nor.*  
1315 *Geogr. Tidsskr.* 40(2), 85–105. doi: <http://dx.doi.org/10.1080/00291958608552159>
- 1316 Evans, D.J.A., 2000. A gravel outwash/deformation till continuum, Skálafellsjökull, Iceland.  
1317 *Geografiska Annaler* 82A(4), 499–512. doi: <http://dx.doi.org/10.1111/j.0435->  
1318 [3676.2000.00137.x](http://dx.doi.org/10.1111/j.0435-3676.2000.00137.x)
- 1319 Evans, D.J.A., 2003. Ice-Marginal Terrestrial Landsystems: Active Temperate Glacier Margins. In:  
1320 Evans, D.J.A. (ed.), *Glacial Landsystems*. Arnold, London, pp. 12–43.
- 1321 Evans, D.J.A., 2010. Controlled moraine development and debris transport pathways in polythermal  
1322 plateau icefields: examples from Tungnafellsjökull, Iceland. *Earth Surf. Process. Landf.* 35,  
1323 1430–1444. doi: <http://dx.doi.org/10.1002/esp.1984>
- 1324 Evans, D.J.A., Archer, S., Wilson, D.J.H. 1999a. A comparison of the lichenometric and Schmidt  
1325 hammer dating techniques based on data from the proglacial areas of some Icelandic glaciers.  
1326 *Quat. Sci. Rev.* 18, 13–41. doi: [http://dx.doi.org/10.1016/S0277-3791\(98\)00098-5](http://dx.doi.org/10.1016/S0277-3791(98)00098-5)
- 1327 Evans, D.J.A., Benn, D.I. (eds.), 2004. *A Practical Guide to the Study of Glacial Sediments*. Arnold,  
1328 London, 266 pp.
- 1329 Evans, D.J.A., Ewertowski, M., Orton, C., 2015. Fláajökull (north lobe), Iceland: active temperate  
1330 piedmont lobe glacial landsystem. *J. Maps*, in press. doi:  
1331 <http://dx.doi.org/10.1080/17445647.2015.1073185>
- 1332 Evans, D.J.A., Hiemstra, J.F., 2005. Till deposition by glacier submarginal, incremental thickening.  
1333 *Earth Surf. Process. Landf.* 30, 1633–1662. doi: <http://dx.doi.org/10.1002/esp.1224>

- 1334 Evans, D.J.A., Lemmen, D.S., Rea, B.R., 1999b. Glacial landsystems of the southwest Laurentide Ice  
1335 Sheet: modern Icelandic analogues. *J. Quat. Sci.* 14(7), 673–691. doi:  
1336 [http://dx.doi.org/10.1002/\(SICI\)1099-1417\(199912\)14:7<673::AID-JQS467>3.0.CO;2-#](http://dx.doi.org/10.1002/(SICI)1099-1417(199912)14:7<673::AID-JQS467>3.0.CO;2-#)
- 1337 Evans, D.J.A., Orton, C., 2015. Heinabergsjökull and Skalafellsjökull, Iceland: Active Temperate  
1338 Piedmont Lobe and Outwash Head Glacial Landsystem. *J. Maps* 11(3), 415–431. doi:  
1339 <http://dx.doi.org/10.1080/17445647.2014.919617>
- 1340 Evans D.J.A., Phillips E.R., Hiemstra J.F., Auton C.A., 2006. Subglacial till: Formation, sedimentary  
1341 characteristics and classification. *Earth-Sci. Rev.* 78(1–2), 115–176. doi:  
1342 <http://dx.doi.org/10.1016/j.earscirev.2006.04.001>
- 1343 Evans, D.J.A., Twigg, D.R., 2002. The active temperate glacial landsystem: a model based on  
1344 Breiðamerkurjökull and Fjallsjökull, Iceland. *Quat. Sci. Rev.* 21, 2143–2177. doi:  
1345 [http://dx.doi.org/10.1016/S0277-3791\(02\)00019-7](http://dx.doi.org/10.1016/S0277-3791(02)00019-7)
- 1346 Evans, D.J.A., Young, N.J.P., Ó Cofaigh, C., 2014. Glacial geomorphology of terrestrial-terminating  
1347 fast flow lobes/ice stream margins in the southwest Laurentide Ice Sheet. *Geomorphol.* 204,  
1348 86–113. doi: <http://dx.doi.org/10.1016/j.geomorph.2013.07.031>
- 1349 Fuchs, M., Owen, L.A., 2008. Luminescence dating of glacial and associated sediments: review,  
1350 recommendations and future directions. *Boreas* 37, 636–659. doi:  
1351 <http://dx.doi.org/10.1111/j.1502-3885.2008.00052.x>
- 1352 Geirsdóttir, A., Miller, G.H., Axford, Y., Olafsdottir, S., 2009. Holocene and latest Pleistocene climate  
1353 and glacier fluctuations in Iceland. *Quat. Sci. Rev.* 28, 2107–2118. doi:  
1354 <http://dx.doi.org/10.1016/j.quascirev.2009.03.013>
- 1355 Gheorghiu, D.M., Fabel, D., 2013. Revised surface exposure ages in the southeast part of the  
1356 Monadhliath Mountains, Scotland. In: Boston, C.M., Lukas, S., Merritt, J.W. (eds.), *The*  
1357 *Quaternary of the Monadhliath Mountains and the Great Glen: Field Guide*. Quaternary  
1358 Research Association, London, pp. 183–189.

- 1359 Gheorghiu, D.M., Fabel, D., Hansom, J.D., Xu, S., 2012. Lateglacial surface exposure dating in the  
1360 Monadhliath Mountains, Central Highlands, Scotland. *Quat. Sci. Rev.* 41, 132–146. doi:  
1361 <http://dx.doi.org/10.1016/j.quascirev.2012.02.022>
- 1362 Gibbons, A.B., Megeath, J.D., Pierce, K.L., 1984. Probability of moraine survival in a succession of  
1363 glacial advances. *Geol.* 12, 327–330. doi: [http://dx.doi.org/10.1130/0091-7613\(1984\)](http://dx.doi.org/10.1130/0091-7613(1984)12<327:POMSIA>2.0.CO;2)  
1364 [12<327:POMSIA>2.0.CO;2](http://dx.doi.org/10.1130/0091-7613(1984)12<327:POMSIA>2.0.CO;2)
- 1365 Gordon, J. E., Sharp, M. 1983. Lichenometry in dating recent glacial landforms and deposits, southeast  
1366 Iceland. *Boreas* 12, 191–200. doi: <http://dx.doi.org/10.1111/j.1502-3885.1983.tb00312.x>
- 1367 Graham, D.J., Midgley, N.G., 2000. Graphical representation of particle shape using triangular  
1368 Diagrams: an Excel spreadsheet method. *Earth Surf. Process. Landf.* 25, 1473–1477. doi:  
1369 [http://dx.doi.org/10.1002/1096-9837\(200012\)25:13<1473::AID-ESP158>3.0.CO;2-C](http://dx.doi.org/10.1002/1096-9837(200012)25:13<1473::AID-ESP158>3.0.CO;2-C)
- 1370 Guðmundsson, H.J., 1997. A review of the Holocene environmental history of Iceland. *Quat. Sci. Rev.*  
1371 16, 81–92. doi: [http://dx.doi.org/10.1016/S0277-3791\(96\)00043-1](http://dx.doi.org/10.1016/S0277-3791(96)00043-1)
- 1372 Häkkinen, S., Rhines, P.B., 2004. Decline of subpolar North Atlantic circulation during the 1990s. *Sci.*  
1373 304, 555–559. doi: <http://dx.doi.org/10.1126/science.1094917>
- 1374 Ham, N.R., Attig, J.W., 2001. Minor end moraines of the Wisconsin Valley Lobe, north-central  
1375 Wisconsin, USA. *Boreas* 30, 31–41. doi: [http://dx.doi.org/10.1111/j.1502-](http://dx.doi.org/10.1111/j.1502-3885.2001.tb00986.x)  
1376 [3885.2001.tb00986.x](http://dx.doi.org/10.1111/j.1502-3885.2001.tb00986.x)
- 1377 Hanna, E., Jónsson, T., Box, J.E., 2004. An analysis of Icelandic climate since the nineteenth century.  
1378 *Int. J. Climatol.* 24, 1193–1210. doi: <http://dx.doi.org/10.1002/joc.1051>
- 1379 Hannesdóttir, H., Aðalgeirsdóttir, G., Jóhannesson, T., Guðmundsson, S., Crochet, P.,  
1380 Ágústsson, H., Pálsson, F., Magnússon, E., Sigurðsson, S.Þ., Björnsson, H., 2015a.  
1381 Downscaled precipitation applied in modelling of mass balance and the evolution of southeast  
1382 Vatnajökull, Iceland. *J. Glaciol.* 61(228), 799–813. doi: [http://dx.doi.org/](http://dx.doi.org/10.3189/2015JoG15J024)  
1383 [10.3189/2015JoG15J024](http://dx.doi.org/10.3189/2015JoG15J024)
- 1384 Hannesdóttir, H., Björnsson, H., Pálsson, F., Aðalgeirsdóttir, G., Guðmundsson, S., 2014. Variations of  
1385 southeast Vatnajökull ice cap (Iceland) 1650–1900 and reconstruction of the glacier surface

- 1386 geometry at the Little Ice Age maximum. *Geogr. Ann.: Ser. A, Phys. Geogr.*, in press. doi:  
1387 <http://dx.doi.org/10.1111/geoa.12064>
- 1388 Hannesdóttir, H., Björnsson, H., Pálsson, F., Aðalgeirsdóttir, G., Guðmundsson, S., 2015b.  
1389 Area, volume and mass changes of southeast Vatnajökull ice cap, Iceland, from the  
1390 Little Ice Age maximum in the late 19th century to 2010. *The Cryosphere* 9, 565–585.  
1391 doi: <http://dx.doi.org/10.5194/tc-9-565-2015>
- 1392 Hátún, H., Sandø, A.B., Drange, H., Hansen, B., Valdimarsson, H., 2005. Influence of the Atlantic  
1393 subpolar gyre on the thermohaline circulation. *Sci.* 309, 1841–1844. doi:  
1394 <http://dx.doi.org/10.1126/science.1114777>
- 1395 Harris, C., Bothamley, K. 1984. Englacial deltaic sediments as evidence for basal freezing and marginal  
1396 shearing, Leirbreen, southern Norway. *J. Glaciol.* 30, 30–34.
- 1397 Hiemstra, J.F., Matthews, J.A., Evans, D.J.A., Owen, G., 2015. Sediment fingerprinting and the mode  
1398 of formation of singular and composite annual moraine ridges at two glacier margins,  
1399 Jotunheimen, southern Norway. *The Holocene* 25(11), 1772–1785. doi:  
1400 <http://dx.doi.org/10.1177/0959683615591359>
- 1401 Howarth, P.J., Price, R.J., 1969. The proglacial lakes of Breiðamerkurjökull and Fjallsjökull, Iceland.  
1402 *Geogr. J.* 135, 573–581.
- 1403 Howat, I.M., Eddy, A., 2011. Multi-decadal retreat of Greenland’s marine-terminating glaciers. *J.*  
1404 *Glaciol.* 57(203), 389–396.
- 1405 Howat, I.M., Joughin, I., Fahnestock, M., Smith, B.E., Scambos, T.A., 2008. Synchronous retreat and  
1406 acceleration of southeast Greenland outlet glaciers 2000–06: ice dynamics and coupling to  
1407 climate. *J. Glaciol.* 54(187), 646–660.
- 1408 Hughes, A.L.C., Gyllencreutz, R., Lohne, Ø.S., Mangerud, J., Svendsen, J.I., 2015. The last Eurasian  
1409 Ice Sheets e a chronological database and time-slice reconstruction, DATED-1. *Boreas*, in  
1410 press. doi: <http://dx.doi.org/10.1111/bor.12142>
- 1411 Hurrell, J.W., NCAR Staff [National Center for Atmospheric Research Staff], 2014. Hurrell North  
1412 Atlantic Oscillation (NAO) Index (station-based). Available at:

- 1413 [https://climatedataguide.ucar.edu/climate-data/hurrell-north-atlantic-oscillation-naoindex-](https://climatedataguide.ucar.edu/climate-data/hurrell-north-atlantic-oscillation-naoindex-station-based)  
1414 [station-based](https://climatedataguide.ucar.edu/climate-data/hurrell-north-atlantic-oscillation-naoindex-station-based)
- 1415 Innes, J.L., 1985. Lichenometry. *Prog. Phys. Geogr.* 9(2), 187–254. doi:  
1416 <http://dx.doi.org/10.1177/030913338500900202>
- 1417 Innes, J.L., 1988. The use of lichens in dating. In: Galun, M. (ed.), *CRC Handbook of Lichenology*,  
1418 Volume III. CRC Press, Boca Raton, pp. 75–91.
- 1419 Jochimsen, M., 1973. Does the size of lichen thalli really constitute a valid measure for dating glacial  
1420 deposits? *Arct. Alp. Res.* 5(4), 417–424.
- 1421 Jóhannesson, T., 1986. The response time of glaciers in Iceland to changes in climate. *Ann. Glaciol.* 8,  
1422 100–101.
- 1423 Jóhannesson, T., Sigurðsson, O., 1998. Interpretation of glacier variations in Iceland 1930–1995. *Jökull*  
1424 45, 27–33.
- 1425 Johnson, M.D., Schomacker, A., Benediktsson, I.Ö., Geiger, A.J., Ferguson, A., Ingólfsson, Ó., 2010.  
1426 Active drumlin field revealed at the margin of Múlajökull, Iceland: a surge-type glacier. *Geol.*  
1427 38, 943–946. doi: <http://dx.doi.org/10.1130/G31371.1>
- 1428 Jónsson, S.A., Schomacker, A., Benediktsson, Í.Ö., Ingólfsson, Ó., Johnson, M.D., 2014. The drumlin  
1429 field and the geomorphology of the Múlajökull surge-type glacier, central Iceland.  
1430 *Geomorphol.* 207, 213–220. doi: <http://dx.doi.org/10.1016/j.geomorph.2013.11.007>
- 1431 Karlén, W., Black, J.L., 2002. Estimates of lichen growth-rate in northern Sweden. *Geogr. Ann.* 84(3–  
1432 4), 225–232. doi: <http://dx.doi.org/10.1111/j.0435-3676.2002.00177.x>
- 1433 Kirkbride, M.P. 2002. Icelandic climate and glacier fluctuations through the termination of the ‘Little  
1434 Ice Age’. *Polar Geogr.* 26(2), 116–133. doi: <http://dx.doi.org/10.1080/789610134>
- 1435 Kirkbride, M.P., Brazier, V., 1998. A critical evaluation of the use of glacier chronologies in climatic  
1436 reconstruction, with reference to New Zealand. In: Owen, L.A. (ed.), *Mountain Glaciation.*  
1437 *Quaternary Proceedings N6, Supplement 1 to Journal of Quaternary Science Volume 13.* Wiley,  
1438 Chichester, pp. 55–64.

- 1439 Kirkbride, M.P., Winkler, S., 2012. Correlation of Late Quaternary moraines: impact of climate  
1440 variability, glacier response, and chronological resolution. *Quat. Sci. Rev.* 46, 1–29. doi:  
1441 <http://dx.doi.org/10.1016/j.quascirev.2012.04.002>
- 1442 Kjær, K.H., Sultan, L., Krüger, J., Schomacker, A., 2004. Architecture and sedimentation of outwash  
1443 fans in front of the Mýrdalsjökull ice cap, Iceland. *Sediment. Geol.* 172, 139–163. doi:  
1444 <http://dx.doi.org/10.1016/j.sedgeo.2004.08.002>
- 1445 Kristensen, L., Benn, D.I., 2012. A surge of the glaciers Skobreen-Paulabreen, Svalbard, observed by  
1446 time-lapse photographs and remote sensing data. *Polar Res.* 31, 11106. doi:  
1447 <http://dx.doi.org/10.3402/polar.v31i0.11106>
- 1448 Krüger, J., 1993. Moraine ridge formation along a stationary ice front in Iceland. *Boreas* 22, 101–109.  
1449 doi: <http://dx.doi.org/10.1111/j.1502-3885.1993.tb00169.x>
- 1450 Krüger, J., 1994. Glacial processes, sediments, landforms and stratigraphy in the terminus region of  
1451 Mýrdalsjökull, Iceland. *Folia Geogr. Danica* 21, 1–233.
- 1452 Krüger, J., 1995. Origin, chronology and climatological significance of annual moraine ridges at  
1453 Mýrdalsjökull, Iceland. *The Holocene* 5, 420–427. doi:  
1454 <http://dx.doi.org/10.1177/095968369500500404>
- 1455 Krüger, J., 1996. Moraine ridges formed from subglacial frozen-on sediment slabs and their  
1456 differentiation from push moraines. *Boreas* 25, 57–63. doi: [http://dx.doi.org/10.1111/j.1502-](http://dx.doi.org/10.1111/j.1502-3885.1996.tb00835.x)  
1457 [3885.1996.tb00835.x](http://dx.doi.org/10.1111/j.1502-3885.1996.tb00835.x)
- 1458 Krüger, J., 1997. Development of minor outwash fans at Kötlujökull, Iceland. *Quat. Sci. Rev.* 16, 649–  
1459 659. doi: [http://dx.doi.org/10.1016/S0277-3791\(97\)00013-9](http://dx.doi.org/10.1016/S0277-3791(97)00013-9)
- 1460 Krüger, J., Kjaer, K.H., 2000. De-icing progression in ice-cored moraines in a humid, sub-polar climate.  
1461 *The Holocene* 10, 737–747. doi: <http://dx.doi.org/10.1191/09596830094980>
- 1462 Krüger, J., Schomacker, A., Benediktsson, Í.Ö., 2010. Ice-marginal environments: geomorphic and  
1463 structural genesis of marginal moraines at Mýrdalsjökull. In: Schomacker, A., Krüger, J., Kjær,  
1464 K. (eds.), *The Mýrdalsjökull Ice Cap, Iceland. Glacial processes, sediments and landforms on*  
1465 *active volcano. Developments in Quaternary Sciences* 13, pp. 79–104.

- 1466 Laumann, T., Nesje, A., 2009. A simple method of simulating the future frontal position of  
1467 Briksdalsbreen, western Norway. *The Holocene* 19, 221–228. doi:  
1468 <http://dx.doi.org/10.1177/0959683608100566>
- 1469 Locke, W.W., Andrews, J.T., Webber, P.J., 1979. A manual for lichenometry. British  
1470 Geomorphological Research Group, Technical Bulletin 26, 1–47.
- 1471 Lohmann, K., Drange, H., Bentsen, M., 2008. Response of the North Atlantic subpolar gyre to persistent  
1472 North Atlantic oscillation like forcing. *Clim. Dyn.* 32, 273–285. doi:  
1473 <http://dx.doi.org/10.1007/s00382-008-0467-6>
- 1474 Lukas S. 2005a. A test of the englacial thrusting hypothesis of 'hummocky' moraine formation – case  
1475 studies from the north-west Highlands, Scotland. *Boreas* 34, 287–307. doi:  
1476 <http://dx.doi.org/10.1111/j.1502-3885.2005.tb01102.x>
- 1477 Lukas, S., 2005b. Younger Dryas moraines in the NW Highlands of Scotland: genesis, significance and  
1478 potential modern analogues. Unpublished PhD thesis, University of St Andrews, UK.
- 1479 Lukas, S., 2007. Early-Holocene glacier fluctuations in Krundalen, south central Norway: palaeo-  
1480 glacier dynamics and palaeoclimate. *The Holocene* 17, 585–598. doi:  
1481 <http://dx.doi.org/10.1177/0959683607078983>
- 1482 Lukas, S., 2011. Ice-cored Moraines. In: Singh, V., Singh, P., Haritashya, U.K. (eds.), *Encyclopaedia*  
1483 *of Snow, Ice and Glaciers*. Springer, Heidelberg, pp. 616–618.
- 1484 Lukas, S., 2012. Processes of annual moraine formation at a temperate alpine valley glacier: insights  
1485 into glacier dynamics and climatic controls. *Boreas* 41(3), 463–480. doi:  
1486 <http://dx.doi.org/10.1111/j.1502-3885.2011.00241.x>
- 1487 Lukas, S., Benn, D.I., Boston, C.M., Brook, M.S., Coray, S., Evans, D.J.A., Graf, A., Kellerer-  
1488 Pirklbauer-Eulenstein, A., Kirkbride, M.P., Krabbendam, M., Lovell, H., Machiedo, M., Mills,  
1489 S.C., Nye, K., Reinardy, B.T.I., Ross, F.H., Signer, M., 2013. Clast shape analysis and clast  
1490 transport paths in glacial environments: A critical review of methods and the role of lithology.  
1491 *Earth-Sci. Rev.* 121, 96–116. doi: <http://dx.doi.org/10.1016/j.earscirev.2013.02.005>

- 1492 Lukas, S., Nicholson, L.I., Ross, F.H., Humlum, O., 2005. Formation, meltout processes and landscape  
1493 alteration of high-arctic ice-cored moraines: examples from Nordenskiöld Land, central  
1494 Spitsbergen. *Polar Geogr.* 29, 157–187. doi: <http://dx.doi.org/10.1080/789610198>
- 1495 Lukas, S., Spencer, J.Q.G., Robinson, R.A.J., Benn, D.I., 2007. Problems associated with luminescence  
1496 dating of Late Quaternary glacial sediments in the NW Scottish Highlands. *Quat. Geochronol.*  
1497 2, 243–248. doi: <http://dx.doi.org/10.1016/j.quageo.2006.04.007>
- 1498 Marzeion, B., Nesje, A., 2012. Spatial patterns of North Atlantic oscillation influence on mass balance  
1499 variability of European glaciers. *The Cryosphere* 6, 661–673. doi: [http://dx.doi.org/10.5194/tc-](http://dx.doi.org/10.5194/tc-6-661-2012)  
1500 [6-661-2012](http://dx.doi.org/10.5194/tc-6-661-2012)
- 1501 Matthews, J.A., 1974. Families of lichenometric dating curves from the Storbreen Gletschervorfeld,  
1502 Jotunheimen, Norway. *Nor. Geogr. Tidsskr.* 28(4), 215–235. doi:  
1503 <http://dx.doi.org/10.1080/00291957408551968>
- 1504 Matthews, J.A., Cornish, R., Shakesby, R.A., 1979. “Saw-tooth” moraines in front of Bødalsbreen,  
1505 southern Norway. *J. Glaciol.* 88, 535–546.
- 1506 Matthews, J.A., McCarroll, D., Shakesby, R.A., 1995. Contemporary terminal-moraine ridge formation  
1507 at a temperate glacier: Styggedalsbreen, Jotunheimen, southern Norway. *Boreas* 24, 129–139.  
1508 doi: <http://dx.doi.org/10.1111/j.1502-3885.1995.tb00633.x>
- 1509 McKinzey, K.M., Orwin, J.F., Bradwell, T., 2004. Re-dating the moraines at Skálafellsjökull and  
1510 Heinabergsjökull using different lichenometric methods: implications for the timing of the  
1511 Icelandic Little Ice Age maximum. *Geogr. Ann.* 86A, 319–355. doi:  
1512 <http://dx.doi.org/10.1111/j.0435-3676.2004.00235.x>
- 1513 McKinzey, K.M., Orwin, J.F., Bradwell, T., 2005. A revised chronology of key Vatnajökull (Iceland)  
1514 outlet glaciers during the Little Ice Age. *Ann. Glaciol.* 42, 171–179. doi:  
1515 <http://dx.doi.org/10.3189/172756405781812817>
- 1516 Mernild, S.H., Hanna, E., Yde, J.C., Seidenkrantz, M.-S., Wilson, R., Knudsen, N.T., 2014.  
1517 Atmospheric and oceanic influence on mass balance of northern North Atlantic region land-  
1518 terminating glaciers. *Geogr. Ann.* 96A(4), 561–577. doi: <http://dx.doi.org/10.1111/geoa.12053>

- 1519 Mernild, S.H., Malmros, J.K., Yde, J.C., Knudsen, N.T., 2012. Multi-decadal marine and land-  
1520 terminating glacier retreat in Ammassalik region, Southeast Greenland. *The Cryosphere* 6, 625–  
1521 639. doi: <http://dx.doi.org/10.5194/tc-6-625-2012>
- 1522 Miles, B.W.J., Stokes, C.R., Vieli, A., Cox, N.J., 2013. Rapid, climate-driven changes in outlet glaciers  
1523 on the Pacific coast of East Antarctica. *Nat.* 500, 563–566. doi:  
1524 <http://dx.doi.org/10.1038/nature12382>
- 1525 Nesje, A., Lie, Ø., Dahl, S.O., 2000. Is the North Atlantic Oscillation reflected in Scandinavian glacier  
1526 mass balance records? *J. Quat. Sci.* 15, 587–601. doi: [http://dx.doi.org/10.1002/1099-  
1527 1417\(200009\)15:6<587::AID-JQS533>3.0.CO;2-2](http://dx.doi.org/10.1002/1099-1417(200009)15:6<587::AID-JQS533>3.0.CO;2-2)
- 1528 Nick, F.M., van der Kwast, J., Oerlemans, J., 2007. Simulation of the evolution of Breidamerkurjökull  
1529 in the late Holocene. *J. Geophys. Res.: Solid Earth* 112(B1), B01103. doi:  
1530 <http://dx.doi.org/10.1029/2006JB004358>
- 1531 Noller, J.S., Locke, W.W., 2000. Lichenometry. In: Noller, J.S., Sowers, J.M., Lettis, W.R. (eds.),  
1532 Quaternary Geochronology: Methods and Applications. American Geophysical Union,  
1533 Washington DC, pp. 261–272.
- 1534 Nye, J.F., 1952. The mechanics of glacier flow. *J. Glaciol.* 2(12), 82–93.
- 1535 Ó Cofaigh, C., Evans, D.J.A., Hiemstra, J.F., 2011. Formation of a stratified subglacial ‘till’ assemblage  
1536 by ice-marginal thrusting and glacier overriding. *Boreas* 40(1), 1–14. doi:  
1537 <http://dx.doi.org/10.1111/j.1502-3885.2010.00177.x>
- 1538 Osborn, G., McCarthy, D., LaBrie, A., Burke, R., 2015. Lichenometric dating: Science or pseudo-  
1539 science? *Quat. Res.* 83(1), 1–12. doi: <http://dx.doi.org/10.1016/j.yqres.2014.09.006>
- 1540 Pálsson, S., 1945. *Ferðabók Sveins Pálssonar. Dagbækur og ritgerðir 1791–1794* [The Travel Book of  
1541 Sveinn Pálsson. Dairies and Essays 1791–1794]. Snælandsútgáfan, Reykjavík.
- 1542 Pearce, D., Rea, B.R., Bradwell, T., McDougall, D., 2014. Glacial geomorphology of the Tweedsmuir  
1543 Hills, Central Southern Uplands, Scotland. *J. Maps* 10(3), 457–465. doi:  
1544 <http://dx.doi.org/10.1080/17445647.2014.886492>
- 1545 Phillips, E., Finlayson, A., Bradwell, T., Everest, J., Jones, L., 2014. Structural evolution triggers a  
1546 dynamic reduction in active glacier length during rapid retreat: Evidence from Falljökull, SE

1547 Iceland. *J. Geophys. Res.: Earth Surf.* 119, 2194–2208. doi:  
1548 <http://dx.doi.org/10.1002/2014JF003165>  
1549  
1550 Price, R.J., 1970. Moraines at Fjallsjökull, Iceland. *Arct. Alp. Res.* 2, 27–42.  
1551 Price, R.J., Howarth, P.J., 1970. The evolution of the drainage system (1904–1965) in front of  
1552 Breðamerkurjökull, Iceland. *Jökull* 20, 27–37.  
1553 Rayner, N.A., Brohan, P., Parker, D.E., Folland, C.K., Kennedy, J.J., Vanicek, M., Ansell, T.J., Tett,  
1554 S.F.B., 2006. Improved Analyses of Changes and Uncertainties in Sea Surface Temperature  
1555 Measured In Situ since the Mid-Nineteenth Century: The HadSST2 Dataset. *J. Clim.* 19, 446–  
1556 469. doi: <http://dx.doi.org/10.1175/JCLI3637.1>  
1557 Reinardy, B.T.I., Leighton, I., Marx, P.J., 2013. Glacier thermal regime linked to processes of annual  
1558 moraine formation at Midtdalsbreen, southern Norway. *Boreas* 42(4), 896–911. doi:  
1559 <http://dx.doi.org/10.1111/bor.12008>  
1560 Roberts, B., Beckett, J.A., Lewis, W.V., Anderson, F.W., Fleming, W.L.S., Falk, P., 1933. The  
1561 Cambridge Expedition to Vatnajökull, 1932. *The Geogr. J.* 81(4), 289–308.  
1562 Robson, J., Sutton, R., Lohmann, K., Smith, D., Palmer, M.D., 2012. Causes of the rapid warming of  
1563 the North Atlantic Ocean in the mid-1990s. *J. Clim.* 25, 4116–4134. doi:  
1564 <http://dx.doi.org/10.1175/JCLI-D-11-00443.1>  
1565 Ryan, J.C., Hubbard, A.L., Todd, J., Carr, J.R., Box, J.E., Christoffersen, P., Holt, T.O., Snooke, N.,  
1566 2015. Repeat UAV photogrammetry to assess calving front dynamics at a large outlet glacier  
1567 draining the Greenland Ice Sheet. *The Cryosphere*, 9, 1–11. doi: [http://dx.doi.org/10.5194/tc-](http://dx.doi.org/10.5194/tc-9-1-2015)  
1568 [9-1-2015](http://dx.doi.org/10.5194/tc-9-1-2015)  
1569 Schomacker, A., 2008. What controls dead-ice melting under different climate conditions? A  
1570 discussion. *Earth-Sci. Rev.* 90(3–4), 103–113. doi:  
1571 <http://dx.doi.org/10.1016/j.earscirev.2008.08.003>  
1572 Schomacker, A., 2010. Expansion of ice-marginal lakes at the Vatnajökull ice cap, Iceland, from 1999  
1573 to 2009. *Geomorphol.* 119, 232–236. doi: <http://dx.doi.org/10.1016/j.geomorph.2010.03.022>

- 1574 Schomacker, A., Benediktsson, Í.Ö., Ingólfsson, Ó., 2014. The Eyjabakkajökull glacial landsystem,  
1575 Iceland: Geomorphic impact of multiple surges. *Geomorphol.* 218, 98–107. doi:  
1576 <http://dx.doi.org/10.1016/j.geomorph.2013.07.005>
- 1577 Schomacker, A., Benediktsson, Í.Ö., Ingólfsson, Ó., Friis, B., Korsgaard, N.J., Kjær, K.H., Keiding,  
1578 J.K., 2012. Late Holocene and modern glacier changes in the marginal zone of Sólheimajökull,  
1579 South Iceland. *Jökull*, 62, 111–130.
- 1580 Schomacker A., Kjær K.H., 2007. Origin and de-icing of multiple generations of ice-cored moraines at  
1581 Brúarjökull, Iceland. *Boreas* 36, 411–425. doi: <http://dx.doi.org/10.1080/03009480701213554>
- 1582 Schomacker A., Kjær K.H., 2008. Quantification of dead-ice melting in ice-cored moraines at the high-  
1583 Arctic glacier Holmströmbreen, Svalbard. *Boreas* 37, 211–225. doi:  
1584 <http://dx.doi.org/10.1111/j.1502-3885.2007.00014.x>
- 1585 Sharp, M.J., 1984. Annual moraine ridges at Skálafellsjökull, southeast Iceland. *J. Glaciol.* 30, 82–93.
- 1586 Sigurðsson, O., 1998. Glacier variations in Iceland 1930–1995: from the database of the Iceland  
1587 Glaciological Society. *Jökull* 45, 3–25.
- 1588 Sigurðsson, O., 2005. Variations of termini of glaciers in Iceland in recent centuries and their connection  
1589 with climate. In: Caseldine, C., Russell, A., Harðardóttir, J., Knudsen, Ó. (eds.), *Iceland –*  
1590 *Modern Processes and Past Environments. Developments in Quaternary Sciences* 5, 241–255.
- 1591 Sigurðsson, O., Jónsson, T. 1995. Relation of glacier variations to climate changes in Iceland. *Ann.*  
1592 *Glaciol.* 21, 263–270.
- 1593 Sigurðsson, O., Jónsson, T., Jóhannesson, T., 2007. Relation between glacier-termini variations and  
1594 summer temperatures in Iceland since 1930. *Ann. Glaciol.* 42, 395–401. doi:  
1595 <http://dx.doi.org/10.3189/172756407782871611>
- 1596 Small, D., Rinterknecht, V., Austin, W., Fabel, D., Miguens-Rodriguez, M., Xu, S., 2012. In situ  
1597 cosmogenic exposure ages from the Isle of Skye, northwest Scotland: implications for the  
1598 timing of deglaciation and readvance from 15 to 11 ka. *J. Quat. Sci.* 27(2), 150–158. doi:  
1599 <http://dx.doi.org/10.1002/jqs.1522>
- 1600 Spagnolo, M., Clark, C.D., Ely, J.C., Stokes, C.R., Anderson, J.B., Andreassen, K., Graham, A.G.C.,  
1601 King, E.C., 2014. Size, shape and spatial arrangement of megascale glacial lineations from a

1602 large and diverse dataset. *Earth Surf. Process. Landf.* 39, 1432–1448. doi:  
1603 <http://dx.doi.org/10.1002/esp.3532>

1604 Spagnolo, M., Clark, C.D., Hughes, A.L.C., Dunlop, P., Stokes, C.R., 2010. The planar shape of  
1605 drumlins. *Sediment. Geol.* 232, 119–129. doi: <http://dx.doi.org/10.1016/j.sedgeo.2010.01.008>

1606 Stokes, C.R., Shahgedanova, M., Evans, I.S., Popovin, V.V., 2013b. Accelerated loss of alpine glaciers  
1607 in the Kodar Mountains, south-eastern Siberia. *Glob. Planet. Chang.* 101, 82–96. doi:  
1608 <http://dx.doi.org/10.1016/j.gloplacha.2012.12.010>

1609 Stokes, C.R., Spagnolo, M., Clark, C.D., O'Cofaigh, C., Lian, O.B., Dunstone, R.B., 2013a. Formation  
1610 of mega-scale glacial lineations on the Dubawnt Lake Ice Stream bed: 1. size, shape and spacing  
1611 from a large remote sensing dataset. *Quat. Sci. Rev.* 77, 190–209. doi:  
1612 <http://dx.doi.org/10.1016/j.quascirev.2013.06.003>

1613 Stokes, C.R., Tarasov, L., Blomdin, R., Cronin, T.M., Fisher, T.G., Gyllencreutz, R., Hättestrand, C.,  
1614 Heyman, J., Hindmarsh, R.C.A., Hughes, A.L.C., Jakobsson, M., Kirchner, N., Livingstone,  
1615 S.J., Margold, M., Murton, J.B., Noormets, R., Peltier, W.R., Peteet, D.M., Piper, D.J.W.,  
1616 Preusser, F., Renssen, H., Roberts, D.H., Roche, D.M., Saint-Ange, F., Stroeven, A.P., Teller,  
1617 J.T., 2015. On the reconstruction of palaeo-ice sheets: Recent advances and future challenges.  
1618 *Quat. Sci. Rev.* 125, 15–49. doi: <http://dx.doi.org/10.1016/j.quascirev.2015.07.016>

1619 Storrar, R.D., Stokes, C.R., Evans, D.J.A., 2014. Morphometry and pattern of a large sample (>20,000)  
1620 of Canadian eskers and implications for subglacial drainage beneath ice sheets. *Quat. Sci. Rev.*  
1621 105, 1–25. doi: <http://dx.doi.org/10.1016/j.quascirev.2014.09.013>

1622 Straneo, F., Heimbach, P., 2013. North Atlantic warming and the retreat of Greenland's outlet glaciers.  
1623 *Nat.* 504, 36–43. doi: <http://dx.doi.org/10.1038/nature12854>

1624 Thomas, R., Frederick, E., Krabill, W., Manizade, S., Martin, C., 2009. Recent changes on Greenland  
1625 outlet glaciers. *J. Glaciol.* 55(189), 147–162.

1626 Thórarinnsson, S., 1943. Oscillations of the Icelandic glaciers in the last 250 years. *Geogr. Ann.* 25, 1–  
1627 54.

1628 Thórarinnsson, S., 1967. Washboard moraines in front of Skeiðarárjökull. *Jökull* 17, 311–312.

- 1629 Wadell, H., 1920: Vatnajökull. Some studies and observations from the greatest glacial area in Island.  
1630 Geogr. Ann. 4, 300–323.
- 1631 Walter, J.I., Box, J.E., Tulaczyk, S., Brodsky, E.E., Howat, I.M., Yushin, A., Brown, A., 2012. Oceanic  
1632 mechanical forcing of a marine-terminating Greenland glacier. Ann. Glaciol. 53(60), 181–192.  
1633 doi: <http://dx.doi.org/10.3189/2012AoG60A083>
- 1634 Winkler, S., Elvehøy, H., A. Nesje, A., 2009. Glacier fluctuations of Jostedalsbreen, western Norway,  
1635 during the past 20 years: The sensitive response to maritime mountains glaciers. The Holocene  
1636 19, 395–414. doi: <http://dx.doi.org/10.1177/0959683608101390>
- 1637 Worsley, P., 1974. Recent "annual" moraine ridges at Austre Okstindbreen, Okstindan, north Norway.  
1638 J. Glaciol. 13(68), 265–277.
- 1639 Worsley, P., 1981. Lichenometry. In: Goudie, A. (Ed.), Geomorphological Techniques. George Allen  
1640 and Unwin Ltd., London, pp. 302–305.
- 1641
- 1642
- 1643
- 1644
- 1645
- 1646
- 1647
- 1648
- 1649
- 1650
- 1651
- 1652
- 1653
- 1654

1655 **Figure captions**

1656

1657 Figure 1: Satellite images showing the location of Skálafellsjökull, SE Iceland. (A) Landsat 7  
1658 ETM+ scene (August 2006) displayed as a natural colour image (Bands 3, 2 and 1). The box  
1659 marks the location of Figure 1B. (B) Multispectral satellite image from the WorldView-2  
1660 sensor, *European Space Imaging* (June 2012). The boxes show the areas covered by the  
1661 geomorphological map excerpts presented in Figures 5 and 6. Also shown are the locations of  
1662 four sediment sections that were investigated in this study (SKA-04, -07, -11 and -13). Note  
1663 that moraines SKA-11 (2012/2013) and SKA-13 (2013/2014) were formed after this imagery  
1664 was captured. Scale and orientation are given by the Eastings and Northings. Projection: WGS  
1665 1984 / UTM Zone 28N (ESPG: 32628). Modified from Chandler et al. (2015).

1666

1667 Figure 2: Glacier termini variations for a selection of Vatnajökull outlet glaciers, taken from  
1668 the database of *Jöklarannsóknafélag Íslands* (the Icelandic Glaciological Society). The dashed  
1669 lines and question marks indicate periods where no measurements were undertaken at  
1670 Skálafellsjökull (see text for description).

1671

1672 Figure 3: Lichenometric dating curves for SE Iceland, compiled from various sources. The  
1673 corrected Bradwell (2001) curvilinear age-size curve is shown by the red line (see text for  
1674 explanation). Note the negative population gradient axis for the Bradwell (2004b) age-gradient  
1675 curve.

1676

1677 Figure 4: Lithofacies codes and symbols used in the section logs. Modified from Evans and  
1678 Benn (2004) and Lukas (2005a, 2012).

1679

1680 Figure 5: Extract from glacial geomorphological mapping by Chandler et al. (2015), showing  
1681 the distribution of minor moraines on the northern and central parts of the Skálafellsjökull  
1682 foreland. Boxes marked A and B show areas that have been used in more detailed  
1683 morphometric analysis (Section 4.1.1). The location of section SKA-04 is also indicated.  
1684 Mapping is based on 2012 imagery captured by the WorldView-2 satellite and supplied by  
1685 *European Spacing Imaging* (ID: 103001001A462900). Map projection is WGS 1984 / UTM  
1686 Zone 28N (ESPG: 32628).

1687  
1688 Figure 6: Extract from glacial geomorphological mapping by Chandler et al. (2015), showing  
1689 the distribution of minor moraines on the southern Skálafellsjökull foreland. The location of  
1690 section SKA-07 is also indicated. Mapping is based on 2012 imagery captured by the  
1691 WorldView-2 satellite and supplied by *European Spacing Imaging* (ID: 103001001A462900).  
1692 Map projection is WGS 1984 / UTM Zone 28N (ESPG: 32628).

1693  
1694 Figure 7: Annotated field photograph illustrating the characteristic ‘sawtooth’ planform of  
1695 moraines on the foreland of Skálafellsjökull, with down-ice pointing ‘teeth’ and upglacier  
1696 pointing ‘notches’. This moraine has been subject to sedimentological investigations, and the  
1697 location of a river cliff section through the moraine is indicated (SKA-04; see Section 4.3.1.1).  
1698 The boulder marked A has an  $a$ -axis of  $\sim 1.5$  m.

1699  
1700 Figure 8: UAV-captured image showing the close association of minor moraines and flutings  
1701 at the 2013 Skálafellsjökull ice-front. The flutings drape the ice-proximal slopes of the  
1702 moraines and form lineated terrain that intervenes the ridges. The alignment of the flutings  
1703 indicates the glacier maintains approximately the same flow trajectories year on year. Image  
1704 courtesy of Alex Clayton.

1705

1706 Figure 9: Histograms and summary statistics for moraine (A) length; (B) width; and (C) surface  
1707 area. Box-and-whisker plots show the 25th and 75th percentiles (grey box), and the 5th and  
1708 95th percentiles (whisker ends). The mean (horizontal line) is also shown. Morphometric  
1709 analyses are based on mapping presented by Chandler et al. (2015). See text for explanation.

1710

1711 Figure 10: Geomorphological map showing the location of the different zones of moraines on  
1712 the central and parts of the foreland described in the text, along with the locations of the  
1713 quadrats for the lichenometric surveys (numbered dots). The results of the lichenometric  
1714 surveys conducted at the locations A1, A10 and A15 are described in the text. See Figure 5 for  
1715 Key.

1716

1717 Figure 11: Aerial photograph extracts of the Skálafellsjökull foreland showing moraines in  
1718 zone A (north-orientated). Photographs were captured by *Landmælingar Íslands* in (A) 1947  
1719 and (B) 1954.

1720

1721 Figure 12: Aerial photograph extracts showing the retreat of Skálafellsjökull and formation of  
1722 minor moraines in zone B during the period 1954–1969 (north-orientated). Extracts from 1969  
1723 and 1975 illustrate the rapid retreat of the ice-margin and expansion of the ice-marginal lake.  
1724 Aerial photography was supplied by *Landmælingar Íslands* (National Land Survey of Iceland).

1725

1726 Figure 13: Aerial photograph extracts showing the retreat of the Skálafellsjökull and formation  
1727 of minor moraines in zone C, situated on the northern part of the glacier foreland (north-  
1728 orientated). Aerial photography was supplied by *Landmælingar Íslands* (National Land Survey  
1729 of Iceland).

1730

1731 Figure 14: Aerial photograph extracts showing the evolution of the glacier foreland and  
1732 deposition of moraines at the northeastern margin of Skálafellsjökull (north-orientated). These  
1733 moraines are situated in zone D (Figure 10). Note the relatively stable ice-margin between 1975  
1734 and 1989. Aerial photography was supplied by *Landmælingar Íslands* (National Land Survey  
1735 of Iceland).

1736

1737 Figure 15: Extracts from geomorphological mapping presented by Chandler et al. (2015),  
1738 illustrating the retreat of the Skálafellsjökull northeastern margin and deposition of moraines  
1739 between 2006 and 2012. (A) Extract of geomorphological mapping based on 2006 aerial  
1740 photographs. (B) Mapping based on 2012 satellite imagery, with the 2006 ice-margin position  
1741 shown by the solid red line. See Figure 5 for Key.

1742

1743 Figure 16: Aerial photograph extracts showing the stability of the southeastern ice-margin  
1744 during the period 1979–1989 (north-orientated). Aerial photography was supplied by  
1745 *Landmælingar Íslands* (National Land Survey of Iceland).

1746

1747 Figure 17: Extracts from geomorphological mapping presented by Chandler et al. (2015),  
1748 illustrating the retreat of the Skálafellsjökull southeastern margin and deposition of moraines  
1749 between 2006 and 2012. (A) Extract of geomorphological mapping based on 2006 aerial  
1750 photographs. (B) Mapping based on 2012 satellite imagery, with the 2006 ice-margin position  
1751 shown by the solid red line. See Figure 6 for Key.

1752

1753 Figure 18: Lichen size-frequency (SF) plots for moraines in zone A of the Skálafellsjökull  
1754 foreland (see Figure 10). The analysis indicate that the lichens constitute single SF populations.

1755

1756 Figure 19: (A) Log of the exposure created through moraine SKA-04. Shape (B) and roundness  
1757 (C) characteristics of clasts sampled from the massive, matrix-supported diamicton (Dmm).  
1758 Ternary diagrams and indices were derived using a modified version of TriPlot (Graham and  
1759 Midgley, 2000). Roundness classes for the frequency distribution plots follow the scheme of  
1760 Benn and Ballantyne (1994). See text for description of section. For Key see Figure 4.

1761

1762 Figure 20: (A) Log of the exposure created through moraine SKA-07. Results of clast shape  
1763 (B) and roundness (C) analyses conducted on clasts from the massive, clast-supported  
1764 diamicton (Dcm). See text for description. For Key see Figure 4.

1765

1766 Figure 21: (A) Log of the exposure created through moraine SKA-11. Results of clast shape  
1767 (B) and roundness (C) analyses conducted on clasts from the stratified, matrix-supported  
1768 diamicton (Dms). See text for description. For Key see Figure 4.

1769

1770 Figure 22: Log of the exposure created through moraine SKA-13. Shape (B) and roundness (C)  
1771 characteristics of clasts sampled from the massive, matrix-supported diamicton (Dmm). See  
1772 text for description. For Key see Figure 4.

1773

1774 Figure 23: Covariance plots displaying the RA-index plotted against the  $C_{40}$ -index (A) and the  
1775 RWR-index plotted against the  $C_{40}$ -index (B) for the various control samples and moraine  
1776 sections. Samples from the moraines suggest they contain subglacially-sourced material.

1777

1778 Figure 24: Schematic models of the general processes of annual moraine genesis at  
1779 Skálafellsjökull, as reconstructed from representative sections on the glacier foreland. (A)

1780 Efficient bulldozing of extruded submarginal sediments (SKA-04 and SKA-07). (B) Efficient  
1781 bulldozing of pre-existing proglacial sediments (SKA-13); and (C) Emplacement of sediment  
1782 slabs through subglacial freeze-on (SKA-11). For a detailed explanation of the processes, see  
1783 Sections 5.1.1–5.1.3.

1784

1785 Figure 25: Simple schematic diagram showing an idealised piedmont outlet lobe and structures  
1786 on the glacier surface. (1) Crevasses formed in longitudinal extension; (2) longitudinal  
1787 compression at the foot of the icefall produces transverse foliation; (3) crevasses formed as a  
1788 result of longitudinal compressive flow; (4) radial crevasses develop at the glacier snout due to  
1789 lateral extension and longitudinal compressive flow; and (5) planform geometry of annual  
1790 moraines, formed through a combination of squeeze and push processes, reflects the ice-margin  
1791 morphology and structure. Diagram not to scale.

1792

1793 Figure 26: Annual ice-margin retreat rates (IMRRs) at Skálafellsjökull (A) compared with  
1794 variability in key climate variables. Gaps in the IMRR record reflect periods where annual  
1795 moraine production ceased at the ice-margin. Solid lines in B–E show 5-year moving averages.  
1796 Climate variables in B–D are reported as deviations from the respective 1961–1990 averages.  
1797 Ambient air temperature (AAT) and precipitation data are from Hólar í Hornafirði  
1798 ( $64^{\circ}17.995'N$ ,  $15^{\circ}11.402'W$ ; 16.0 m a.s.l.), the nearest long-term weather station to  
1799 Skálafellsjökull (*Veðurstofa Íslands*). Sea surface temperature (SST) values are based on the  
1800 average between latitudes  $57.5$ – $67.5^{\circ}N$  and longitudes  $7.5$ – $17.5^{\circ}W$ , and were extracted from  
1801 the HadSST2 dataset (Rayner et al., 2006). North Atlantic Oscillation (NAO) index values were  
1802 obtained from the station-based Hurrell NAO database (Hurrell and NCAR Staff, 2014).

1803

1804 Figure 27: Covariance plots showing variations in the summer (1<sup>st</sup> June–30<sup>th</sup> September) and  
1805 winter (1<sup>st</sup> December–31<sup>st</sup> March) signatures of ambient air temperature (AAT: A and B),  
1806 precipitation (C and D), sea surface temperature (SST: E and F) and the North Atlantic  
1807 Oscillation (NAO: G and H). Climate variables in A–F are reported as deviations from the  
1808 respective 1961–1990 averages. Note that precipitation anomalies are based on monthly  
1809 averages rather total precipitation for each season. Values for 1945 are excluded from the  
1810 analysis of SST owing to a lack of SST data. Seasons follow the convention of *Veðurstofa*  
1811 *Íslands* (the Icelandic Meteorological Office; cf. Hanna et al., 2004).

1812

1813 Figure 28: Covariance plots comparing inter-annual variability in showing variations in: (A)  
1814 ambient air temperature (AAT) and sea surface temperature (SST); (B) AAT and the North  
1815 Atlantic Oscillation (NAO) index; (C) precipitation and SST; (D) precipitation and AAT; (E)  
1816 precipitation and the NAO index; and (F) the NAO index and SST. Values of AAT, SST and  
1817 precipitation are expressed as deviations from the respective 1961–1990 averages. Note that  
1818 precipitation anomalies and NAO index values are based on averages of monthly values.

1819

1820

1821

1822

1823

1824

1825

1826

1827

1828

1829

1830

1831

1832

1833 **Tables**

1834

1835 Table 1: Characteristics of Skálafellsjökull in 2010. Source: Hannesdóttir et al. (2015a, b).

1836

Volume (km <sup>3</sup> )	Area (km <sup>2</sup> )	Length (km)	Mean thickness (m)	Ice divide (m a.s.l.)	Surface slope (°)	AAR (%)	Snowline range 2007–2011 (m)
33.3	100.6	24.4	331	1490	3.1	0.68	910–1020

1837

1838 Table 2: Summary of lichenometric methods used to calibrate lichen dating curves employed in this study. Modified from McKinzey et al. (2004).

1839

Reference	Survey date	Location	Lichen species	Lichen parameter measured	Number of lichens measured <sup>a</sup>	Survey area (m <sup>2</sup> )	Calibration surfaces	Calibration method	Oldest surface (Date AD)	Eccesis (years) <sup>b</sup>	Growth rate (mm/yr)
Gordon and Sharp (1983)	1980	Skálafells-jökull	<i>R. geog.</i>	Long axis	1	150	Moraines	Largest lichen	1887	15	0.987
Bradwell (2001)	1999	SE Iceland	<i>R. Section R.</i> (includes <i>R. geog.</i> )	Long axis	~300	30	Glacial bedrock Moraines Rockfall Lava flow Jökulhlaup deposit	Largest lichen	1727	-	-
Bradwell (2004b)	1999	SE Iceland	<i>R. Section R.</i> (includes <i>R. geog.</i> )	Long axis	~300	30	Glacial bedrock Moraines Rockfall Lava flow Jökulhlaup deposit	Largest lichen Size-frequency population gradient	1727	-	-

1840

1841 <sup>a</sup> Number of lichens used to derive surface age e.g. 5 = the 5 largest lichens were averaged to determine surface age

1842 <sup>b</sup> Time lag for a lichen spore to arrive on and successfully colonise a surface

1843

1844

1845

1846 Table 3: Wilcoxon rank-sum test to examine the statistical significance of differences between  
 1847 the morphological characteristics of teeth and notches.

1848

Moraine	Sample size		Mean		Standard Deviation		Significance of differences
	<i>Teeth</i>	<i>Notches</i>	<i>Teeth</i>	<i>Notches</i>	<i>Teeth</i>	<i>Notches</i>	
Height (m)	26	24	0.6	0.7	0.3	0.3	Not significant
Width (m)	26	24	8.6	9.7	3.1	1.9	Not significant

1849

1850

1851

1852

1853

1854

1855

1856

1857

1858

1859

1860

1861

1862

1863

1864

1865

1866

1867

1868

1869

1870

1871

1872

1873 Table 4: Estimates of the date of moraine colonisation in zone A (see Figure 9) derived from a  
 1874 variety of dating curves developed for SE Iceland.

1875

Moraine	LL diameter (mm)	Gradient (-ve)	Date of surface (AD)		
			Gordon and Sharp (1983) curve <sup>c, d</sup>	Bradwell (2001) curve <sup>c</sup>	Bradwell (2004b) curve <sup>c</sup>
MOR A1	36	0.0690	1929 ± 9	1940 ± 7	1933 ± 8
MOR A2	34	0.0671	1931 ± 8	1943 ± 7	1931 ± 8
MOR A3	31	0.0910	1934 ± 8	1948 ± 7	1951 ± 6
MOR A4	32	0.0814	1933 ± 8	1946 ± 7	1944 ± 7
MOR A5	31	0.0855	1934 ± 8	1948 ± 7	1947 ± 7
MOR A6	31	0.0819	1934 ± 8	1948 ± 7	1946 ± 7
MOR A7	30	0.0675	1935 ± 8	1949 ± 6	1931 ± 7
MOR A8 <sup>a</sup>	-	-	-	-	-
MOR A9 <sup>b</sup>	30	0.0929	1935 ± 8	1949 ± 6	-
MOR A10	30	0.0780	1935 ± 8	1949 ± 6	1941 ± 7
MOR A11	29	0.0861	1936 ± 8	1951 ± 6	1948 ± 7
MOR A12	27	0.1000	1938 ± 8	1954 ± 6	1956 ± 7
MOR A13	28	0.0806	1937 ± 8	1953 ± 6	1944 ± 7
MOR A14	26	0.1125	1939 ± 8	1957 ± 6	1962 ± 5
MOR A15	24	0.1040	1941 ± 7	1959 ± 6	1958 ± 6

1876

1877 <sup>a</sup> Unable to identify sufficient lichen in fixed area quadrat; <sup>b</sup> Less than 200 lichen above modal class therefore not  
 1878 used to generate 'age-gradient' date; <sup>c</sup> All dates reported with 10% error (Innes 1988; Noller and Locke 2001); <sup>d</sup>  
 1879 Age estimates incorporate ecesis.

1880

1881

1882

1883

1884

1885

1886

1887

1888 Table 5: Formation dates for moraines in zone A of the Skálafellsjökull foreland (see Figure  
1889 9) as deduced from remote sensing observations and lichenometric analysis.

1890

---

Moraine	Date of surface (AD)
MOR A1	1935/1936
MOR A2	1936/1937
MOR A3	1937/1938
MOR A4	1938/1939
MOR A5	1939/1940
MOR A6	1940/1941
MOR A7	1941/1942
MOR A8	1942/1943
MOR A9	1943/1944
MOR A10	1944/1945
MOR A11	1945/1946
MOR A12	1946/1947
MOR A13	1947/1948
MOR A14	1948/1949
MOR A15	1949/1950

---

1891

1892

1893

1894

1895

1896

1897

1898

1899

1900

1901

1902

1903

1904

1905

1906

1907 Table 6: Summary of least regression analyses conducted to examine the potential influence of  
 1908 various climate variables on IMRRs at Skálafellsjökull. Seasons follow the convention of  
 1909 *Veðurstofa Íslands* (the Icelandic Meteorological Office; cf. Hanna et al., 2004). We follow the  
 1910 common convention in testing the statistical significance of the relationships\*.  
 1911

Climate variable	Annual		Spring		Summer		Autumn		Winter	
	$r^2$	$p$	$r^2$	$p$	$r^2$	$p$	$r^2$	$p$	$r^2$	$p$
AAT	0.0262	0.0262	0.0024	0.7630	0.3464	<0.0001	0.0284	0.2923	0.0242	0.3340
Precipitation	0.0013	0.8236	0.0004	0.9037	0.0484	0.1671	0.0014	0.8186	0.0552	0.1394
SST	0.0433	0.8378	0.0177	0.4066	0.1623	0.0010	0.0355	0.2380	0.0012	0.8300
NAO	0.0011	0.8378	0.0452	0.1823	0.1310	0.0201	0.0018	0.7904	0.0633	0.1125

1912  
 1913 \*  $p < 0.05$  indicates a statistically significant fit between the regression line and the data;  $p < 0.01$  indicates a  
 1914 highly statistically significant fit; and  $p < 0.001$  indicates a very highly statistically significant fit.  
 1915

1916  
 1917  
 1918  
 1919  
 1920  
 1921  
 1922  
 1923  
 1924  
 1925  
 1926  
 1927  
 1928  
 1929  
 1930  
 1931  
 1932  
 1933  
 1934  
 1935  
 1936  
 1937

1938 Table 7: Sensitivity ranking for Skálafellsjökull, SE Iceland. The ranking is based on the  $r^2$   
 1939 values for each of the linear regression models.

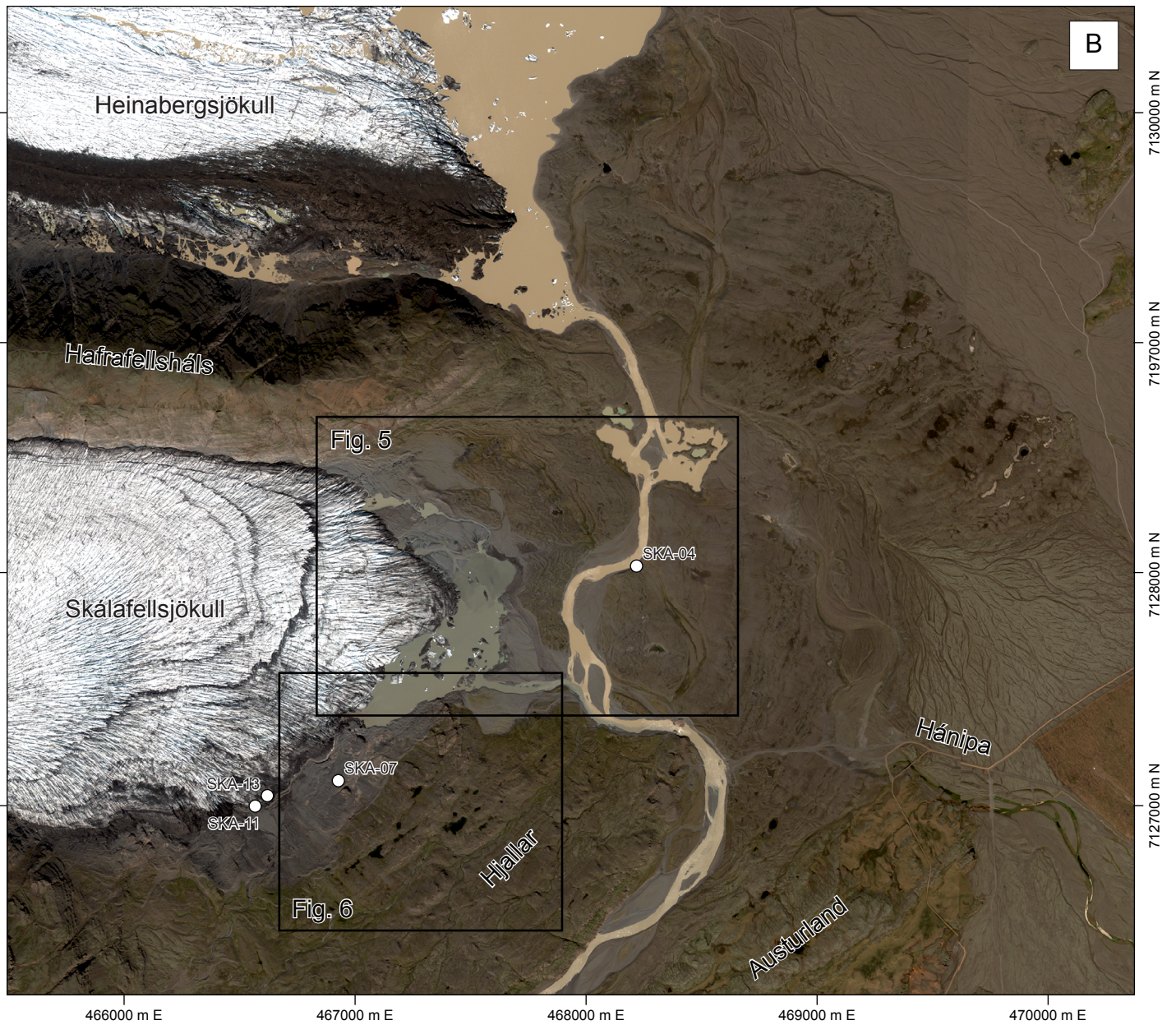
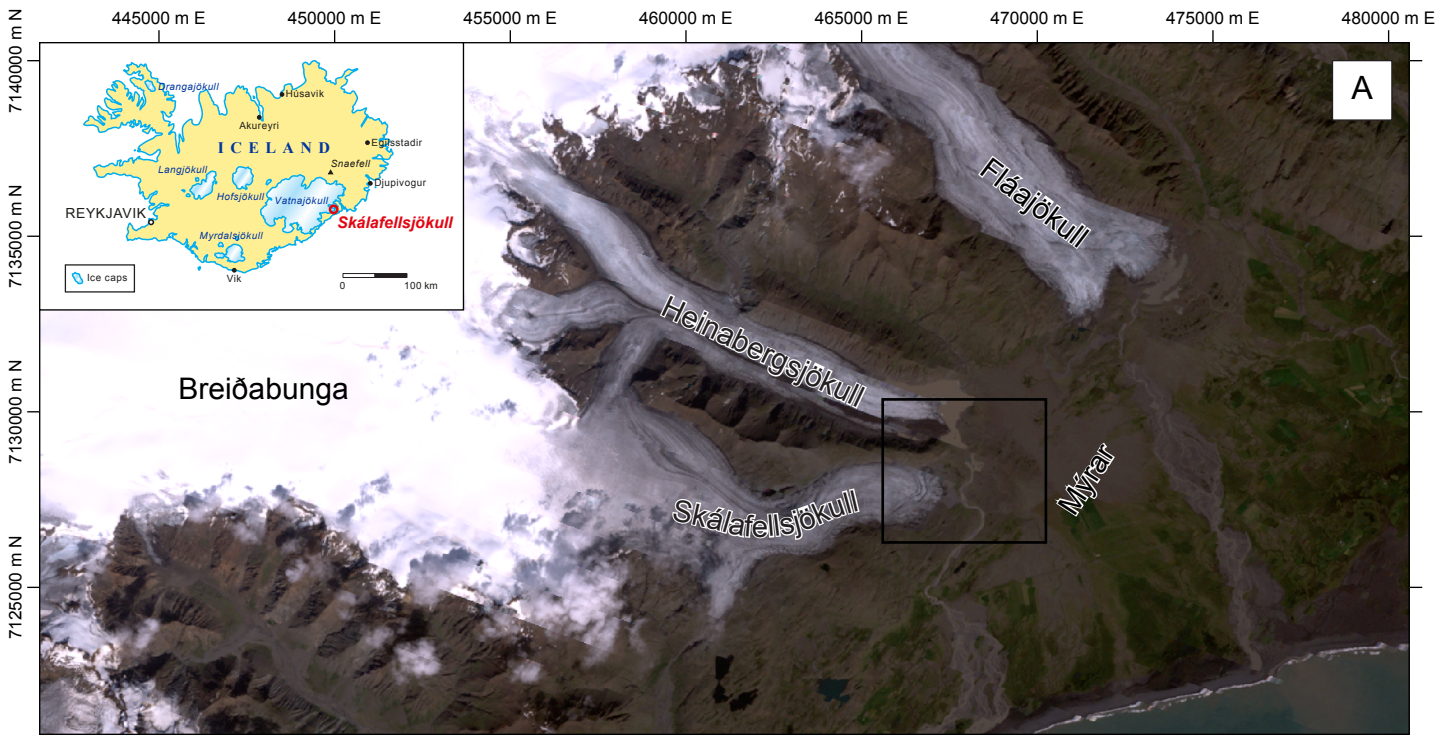
1940

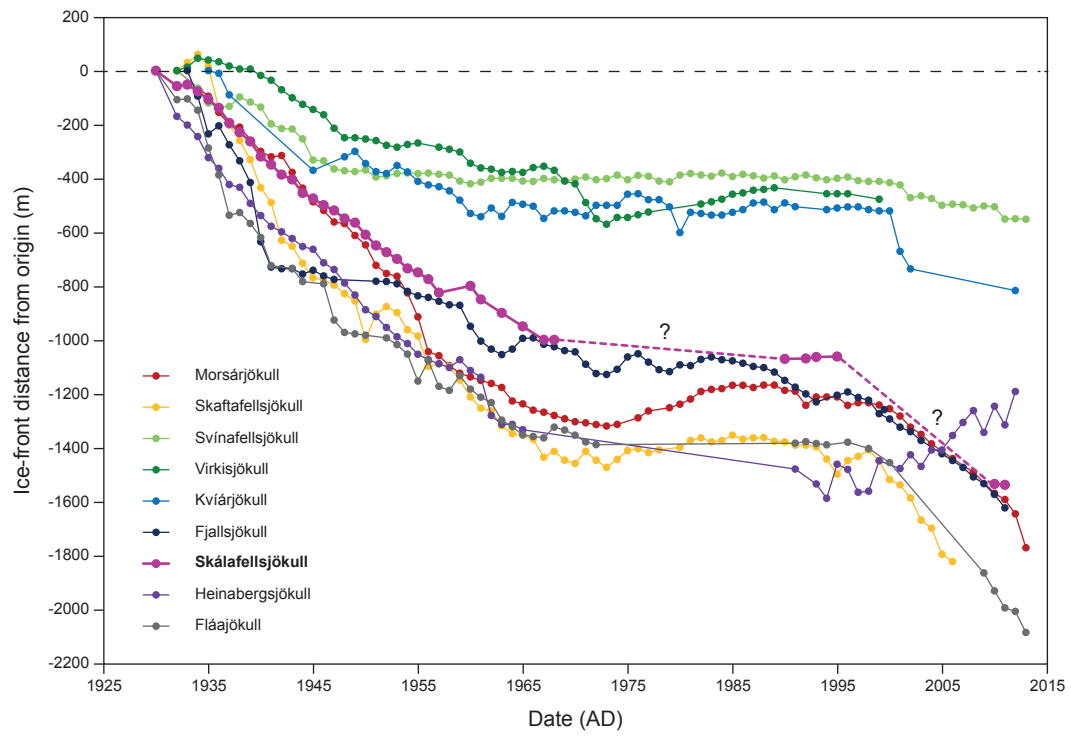
Climate variable	Annual		Spring		Summer		Autumn		Winter	
	$r^2$ value	Rank								
AAT	0.0262	11	0.0024	14	0.3464	1	0.0284	10	0.0242	12
Precipitation	0.0013	17	0.0004	20	0.0484	6	0.0014	16	0.0552	5
SST	0.0433	8	0.0177	13	0.1623	2	0.0355	9	0.0012	18
NAO	0.0011	19	0.0452	7	0.1310	3	0.0018	15	0.0633	4

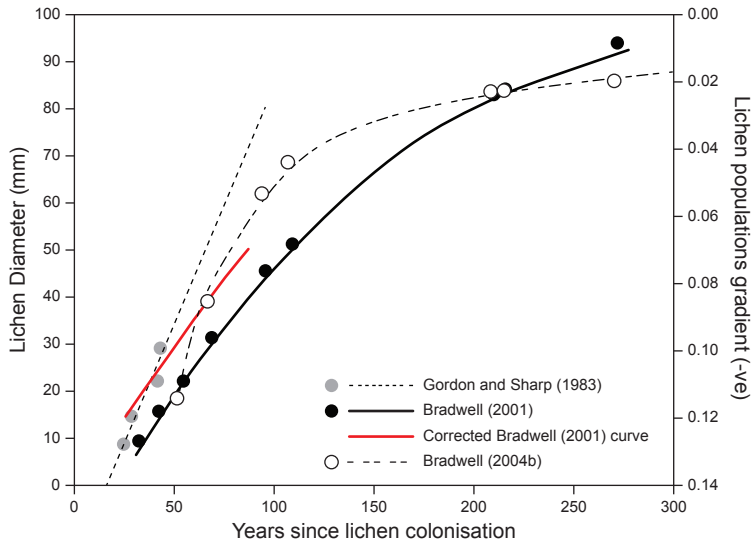
1941

1942

1943







**Lithofacies codes**

*Diamicton*

- Dc- Clast-supported
- Dm- Matrix-supported
- D-m Massive
- D-s Stratified
- (s) Evidence of shearing

*Gravel (8-256 mm)*

- Gm Massive
- Gh Horizontally-bedded
- G(h) Crudely horizontally-bedded
- Go Openwork

*Granules (2-8 mm)*

- GRm Massive
- GRh Horizontally-bedded
- GR(h) Crudely horizontally-bedded

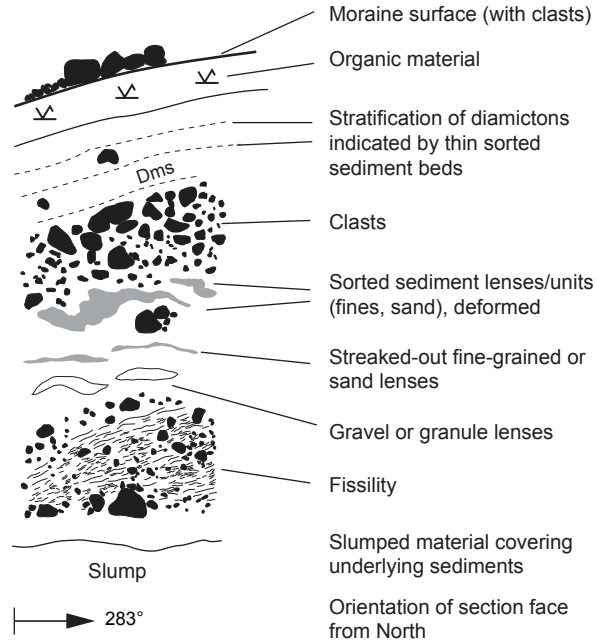
*Sand (0.063-2 mm)*

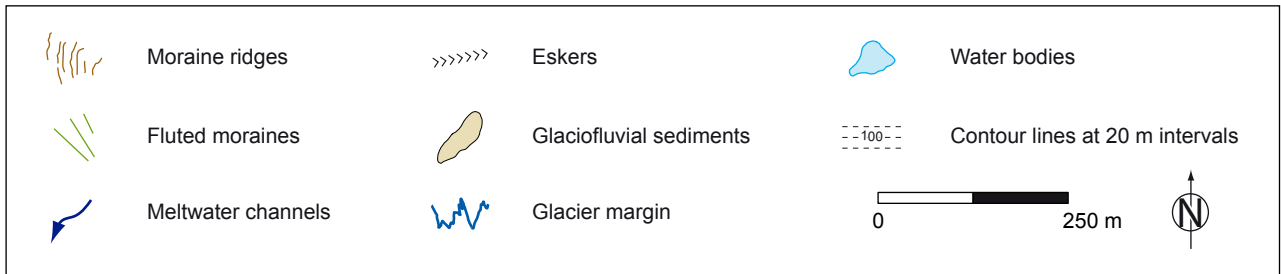
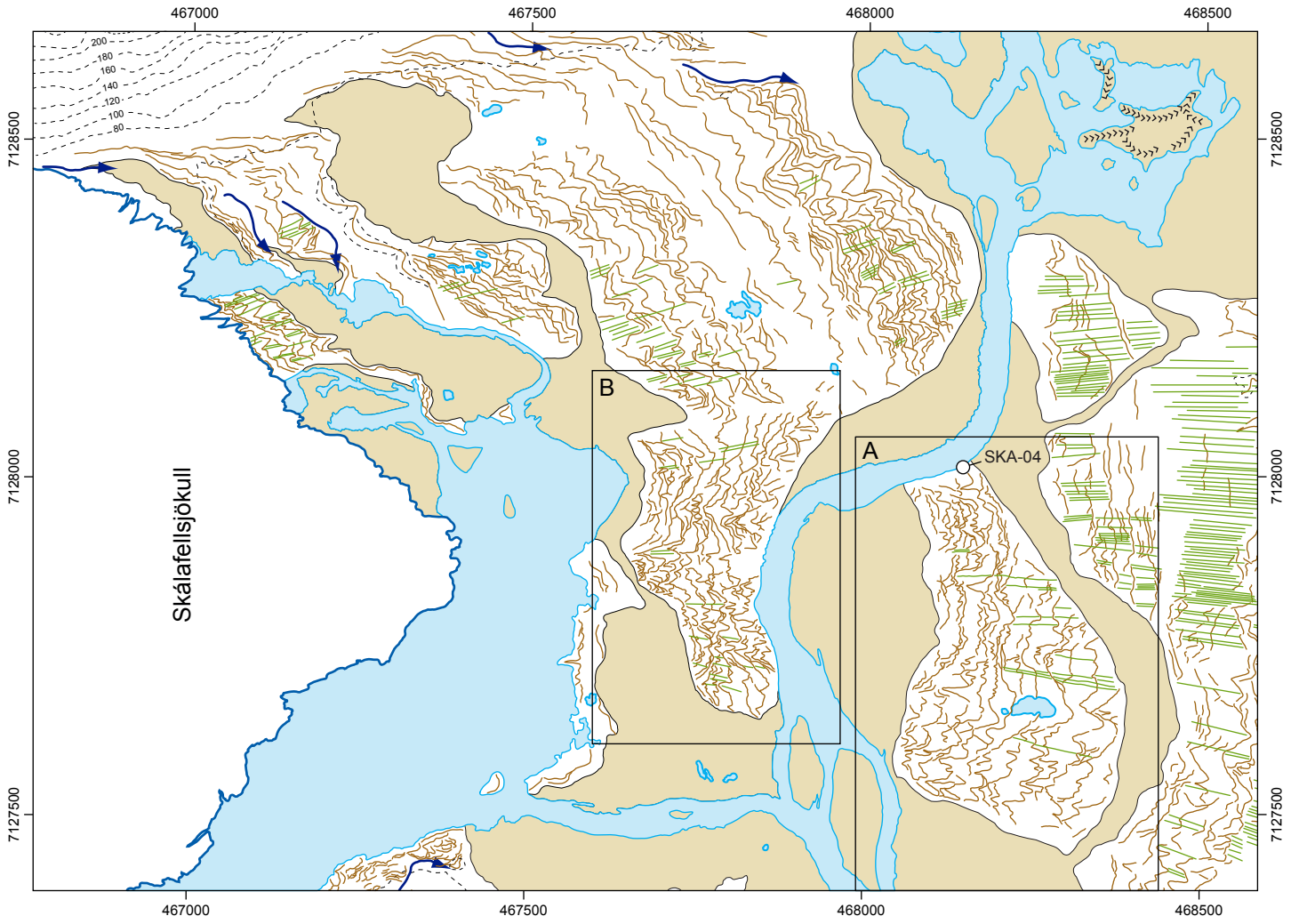
- Sm Massive

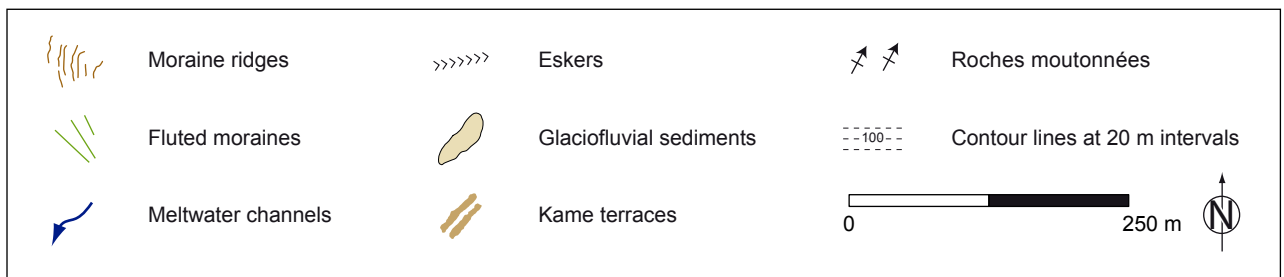
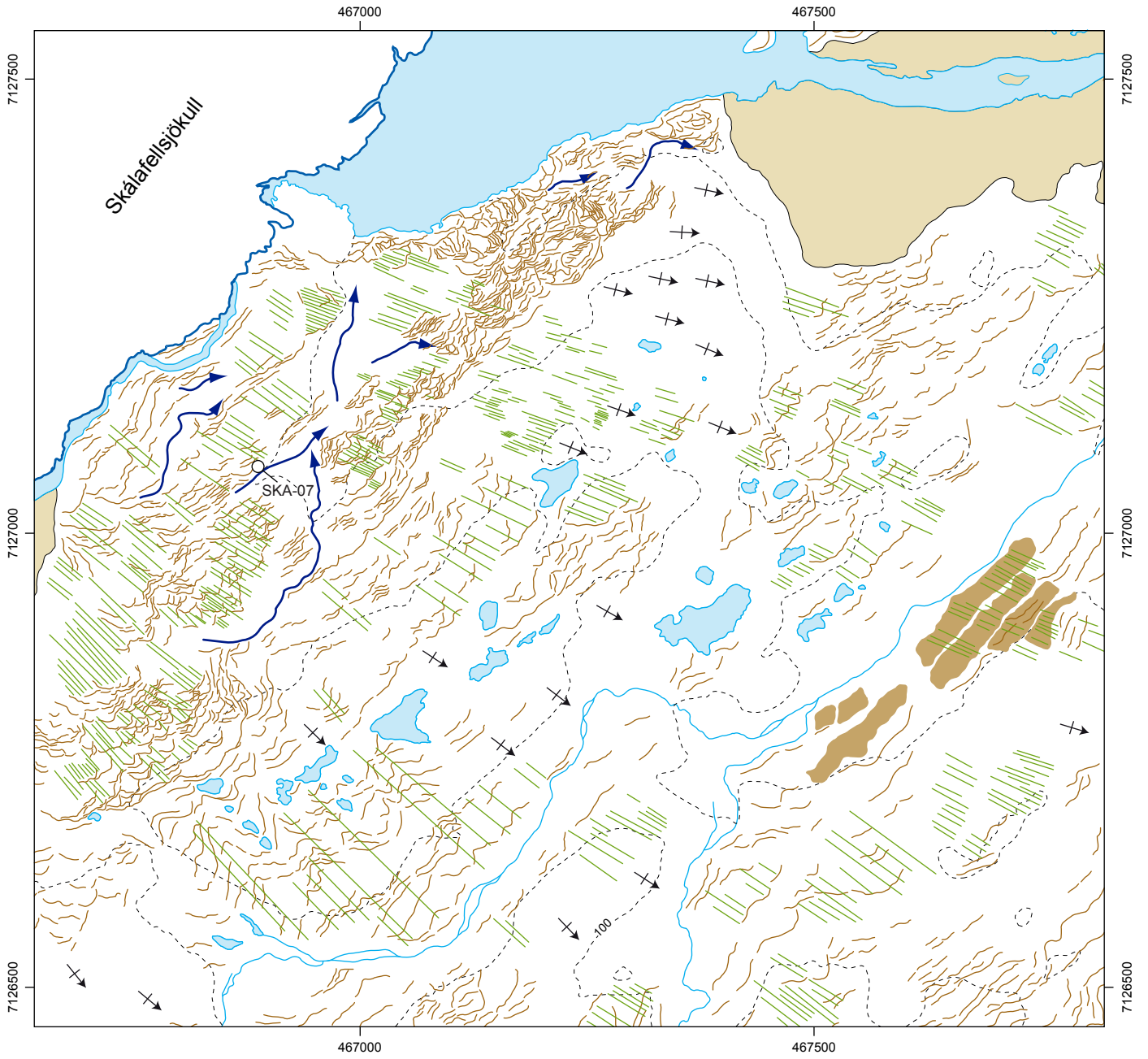
*Fines (<0.063 mm)*

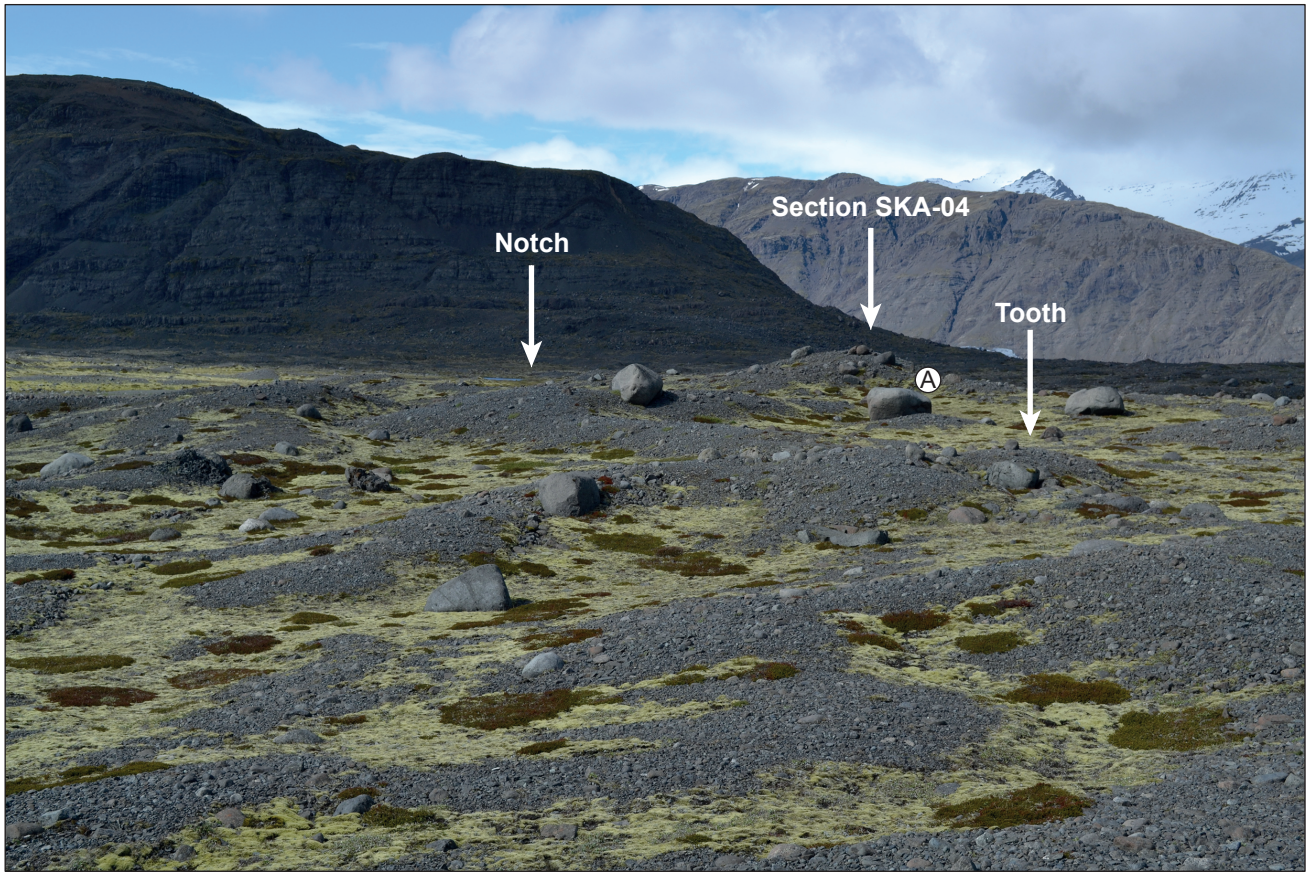
- Fl Laminated
- Fm Massive

**Symbols for section logs**

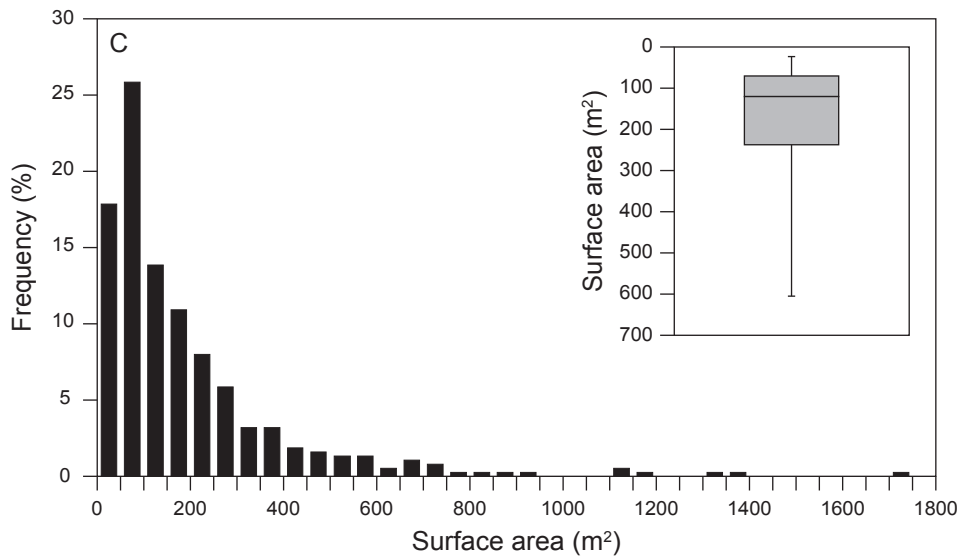
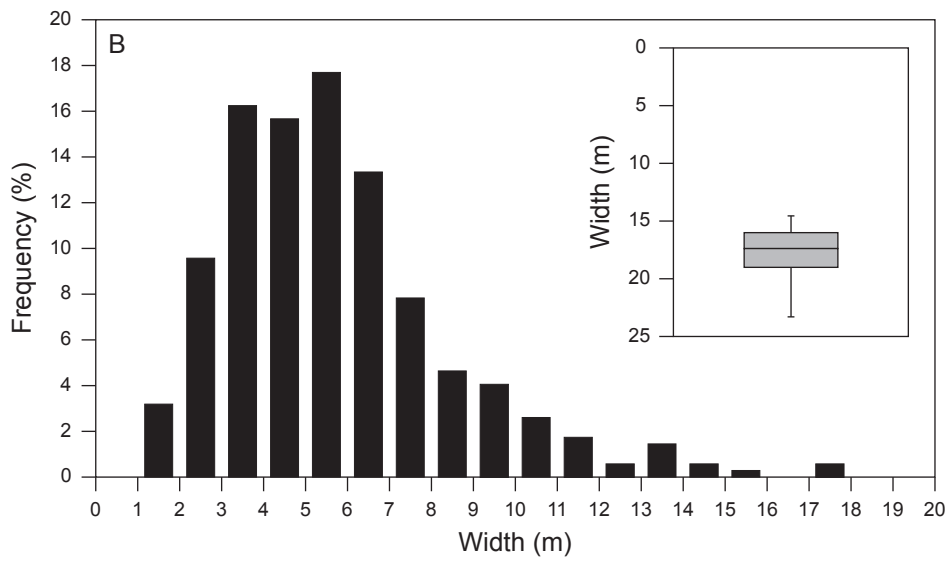
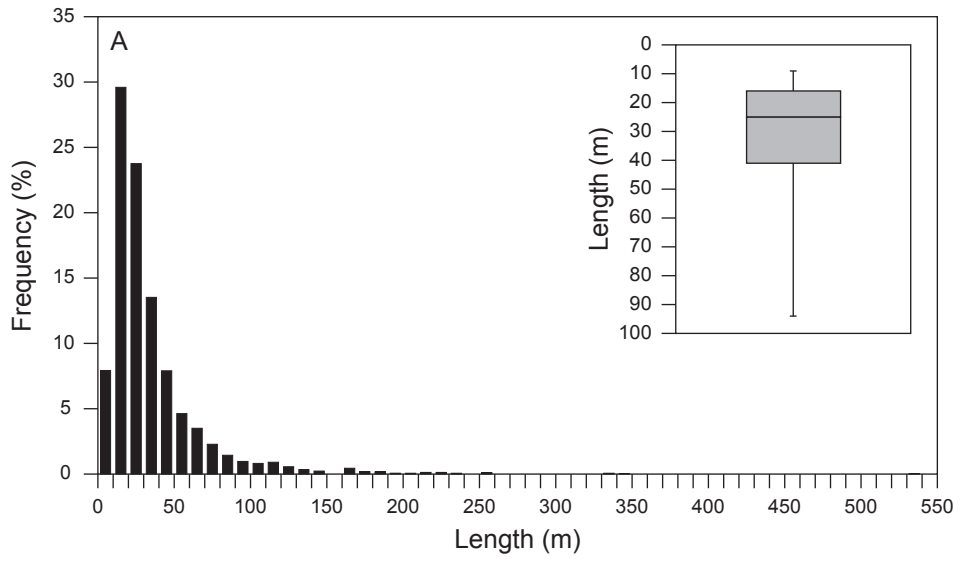


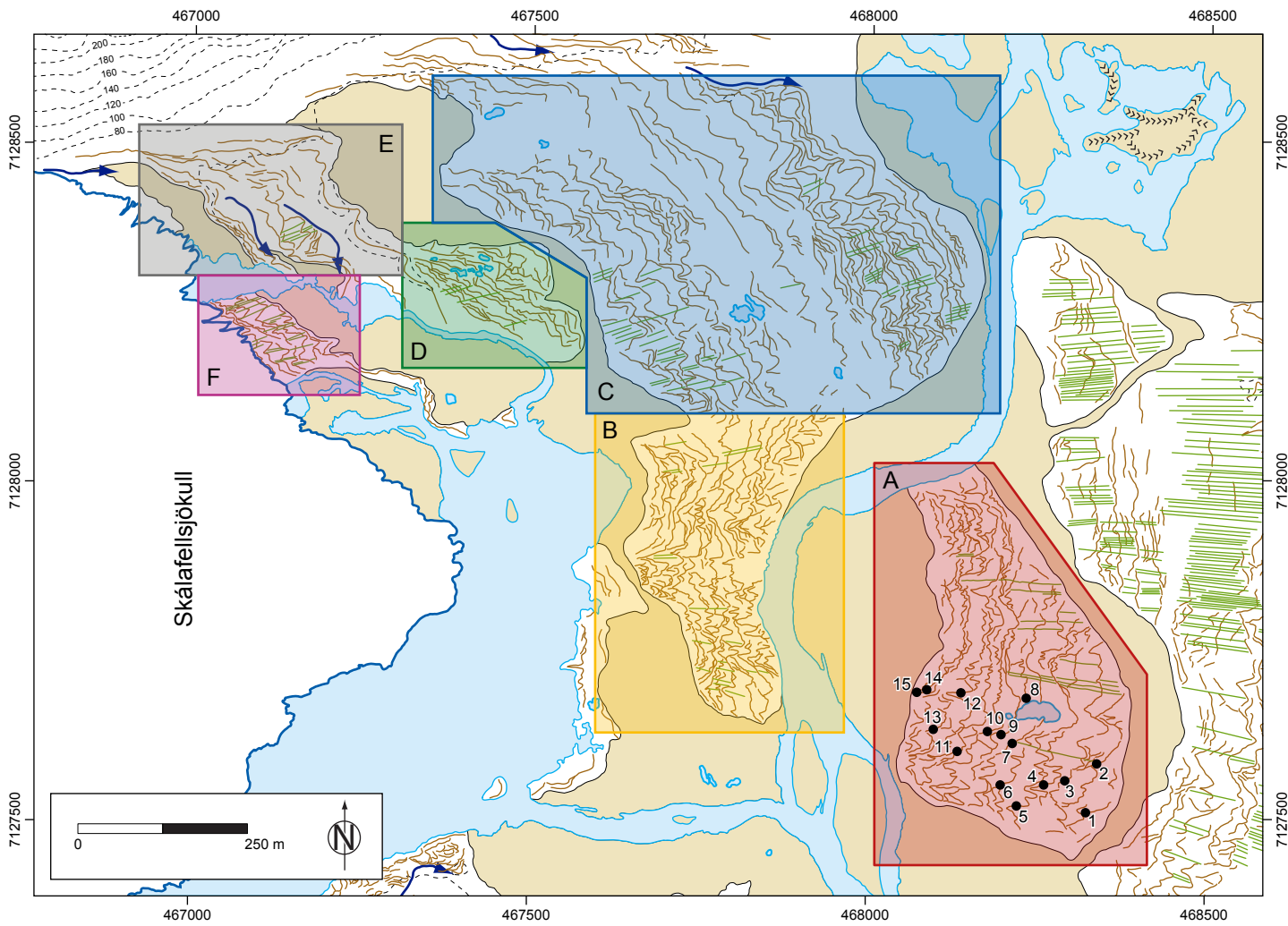


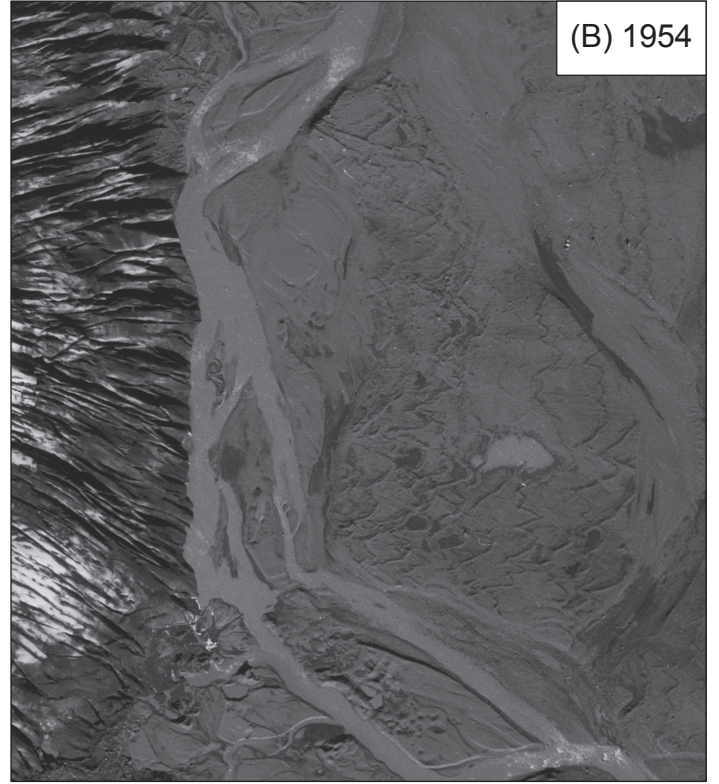
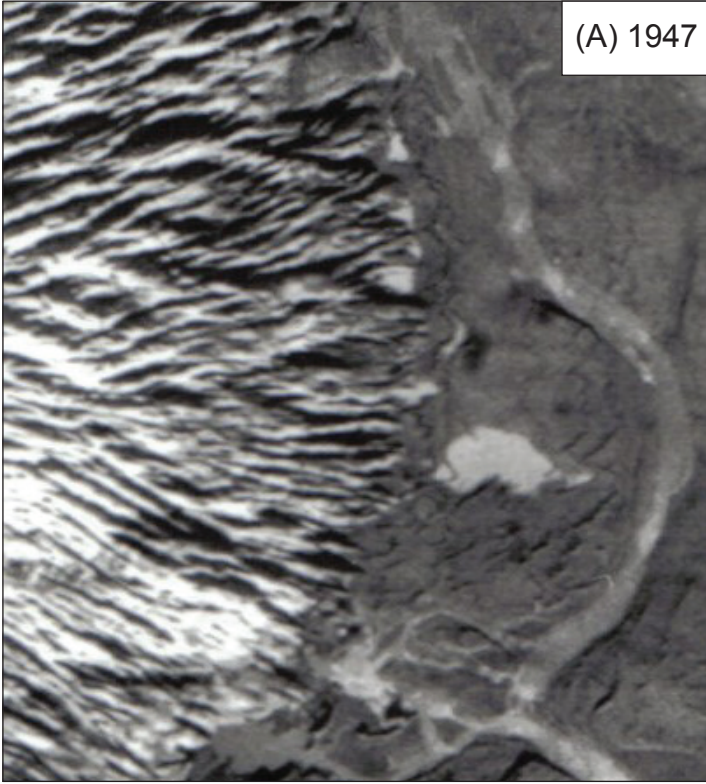


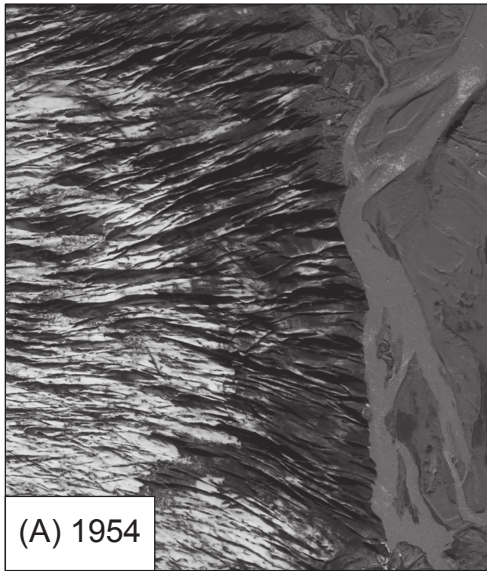




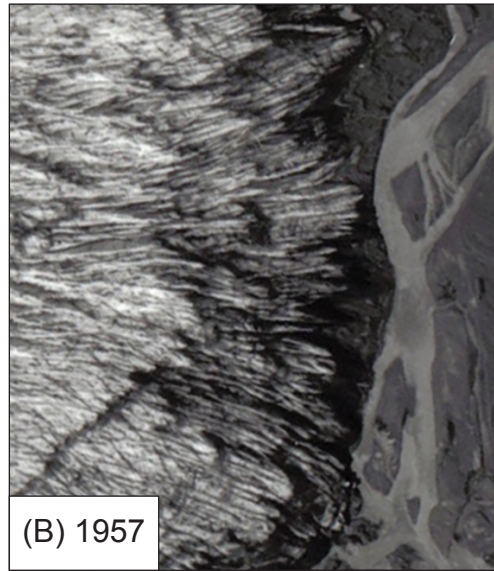




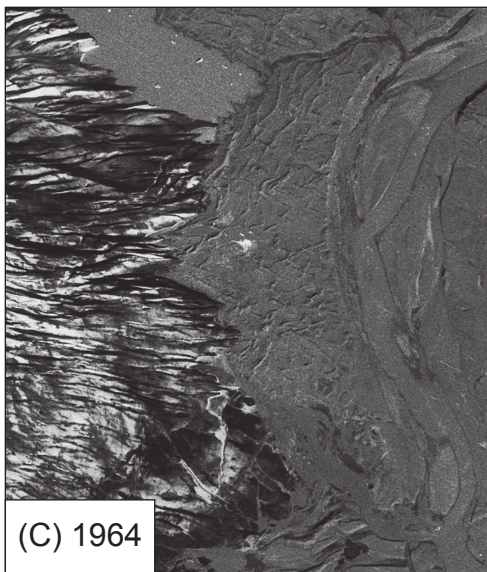




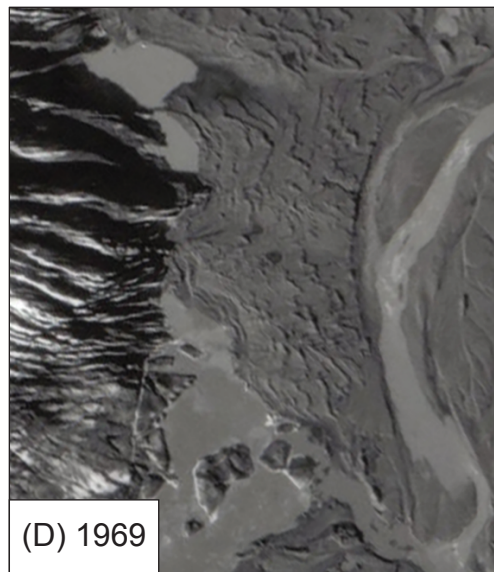
(A) 1954



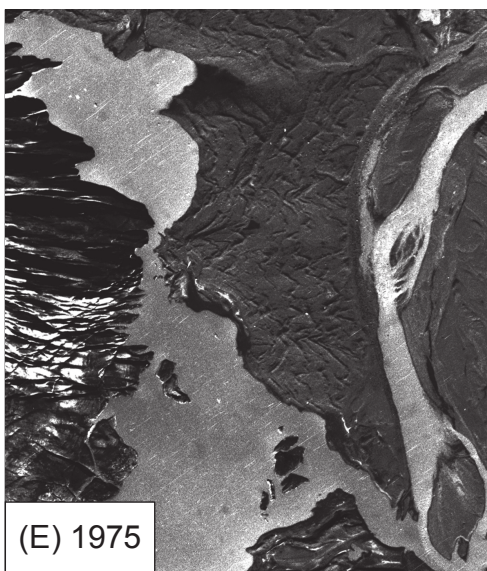
(B) 1957



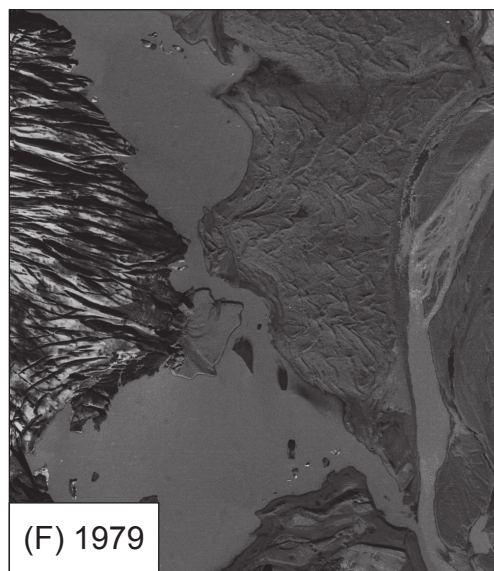
(C) 1964



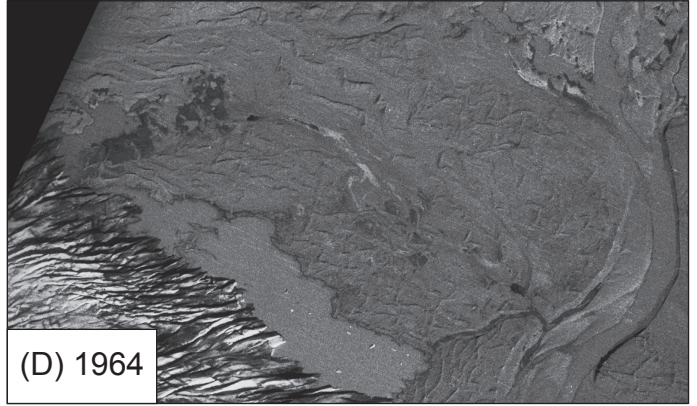
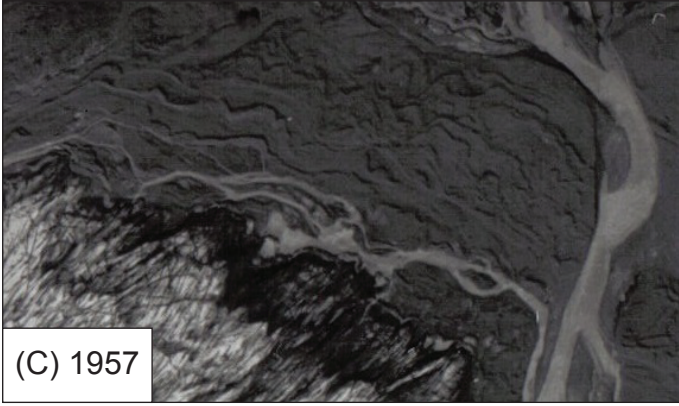
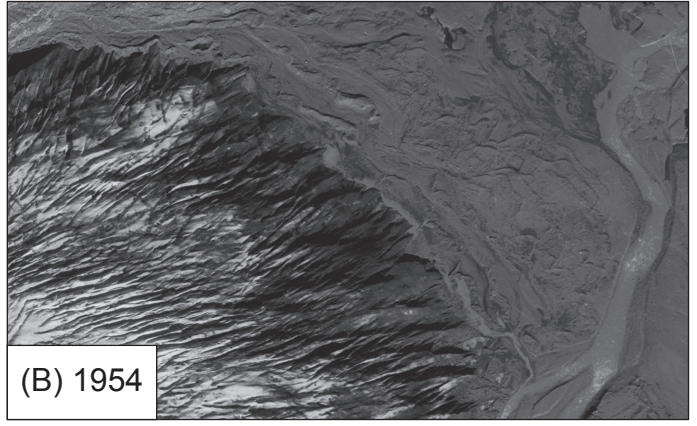
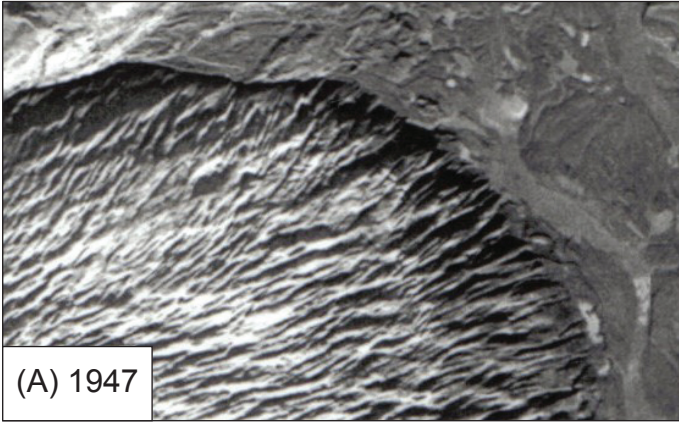
(D) 1969

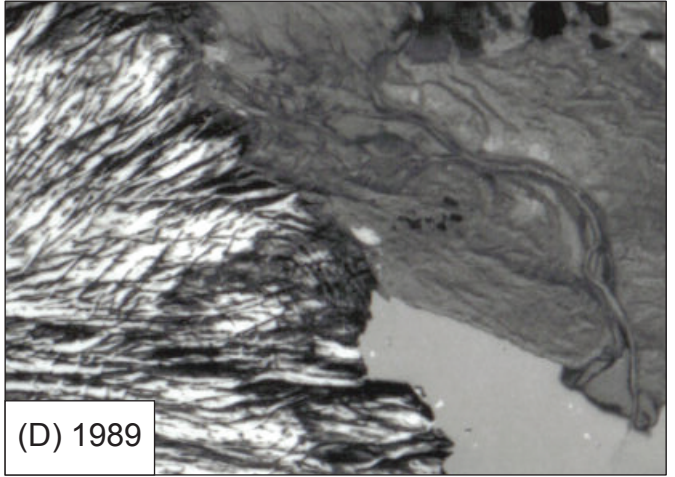
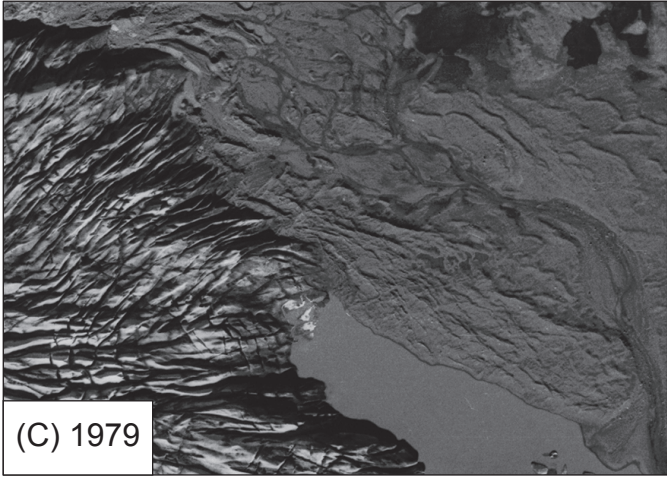
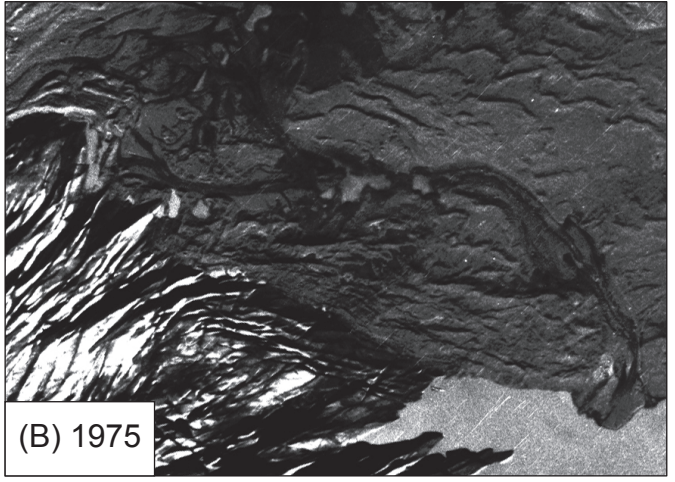
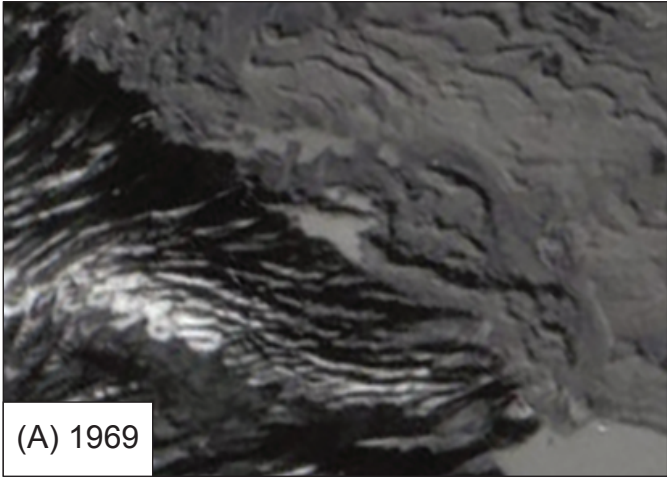


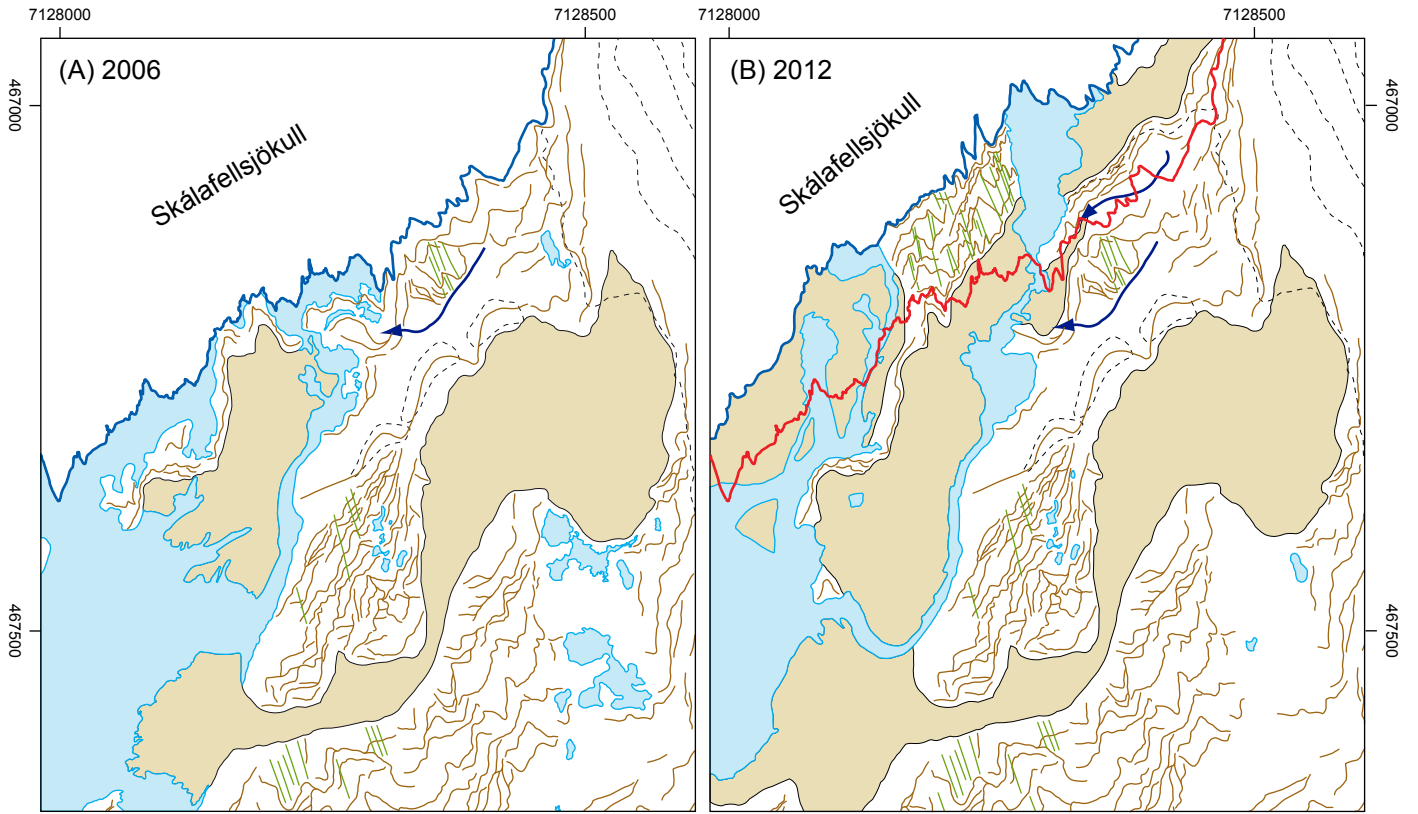
(E) 1975

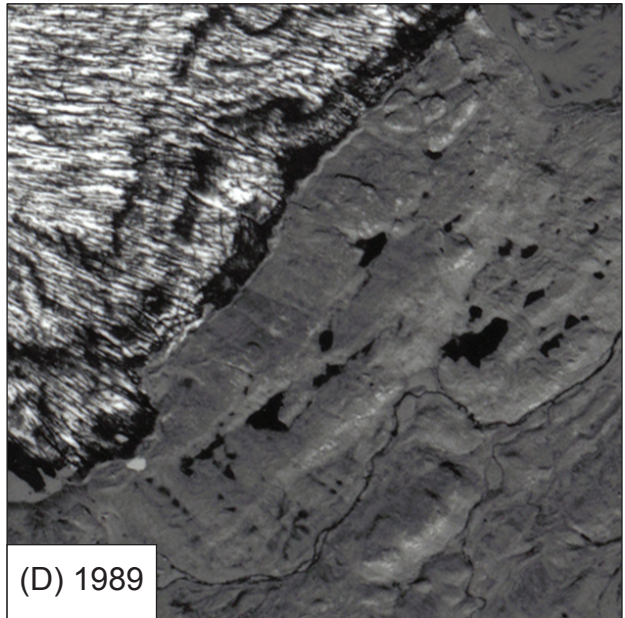
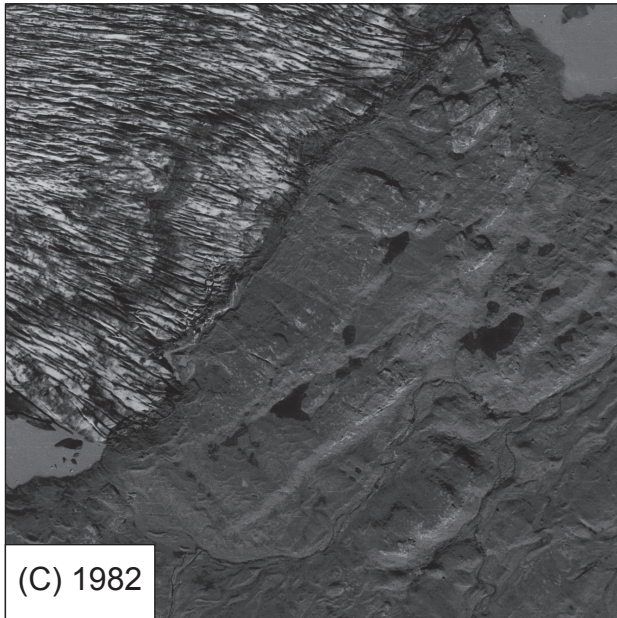
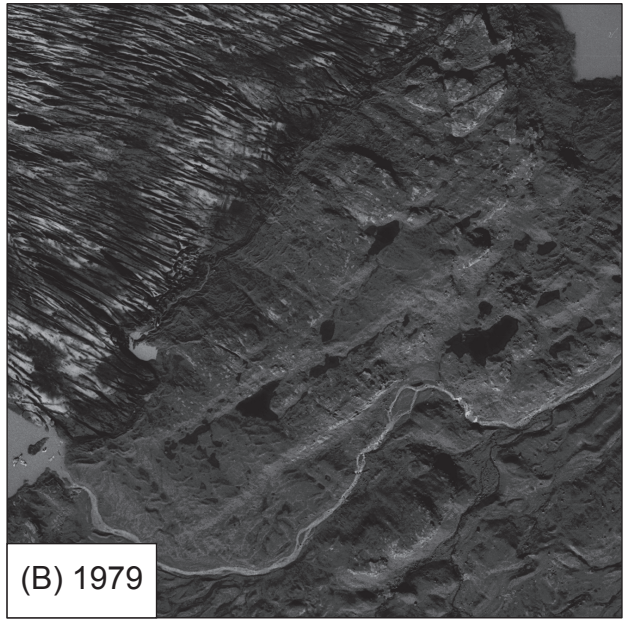
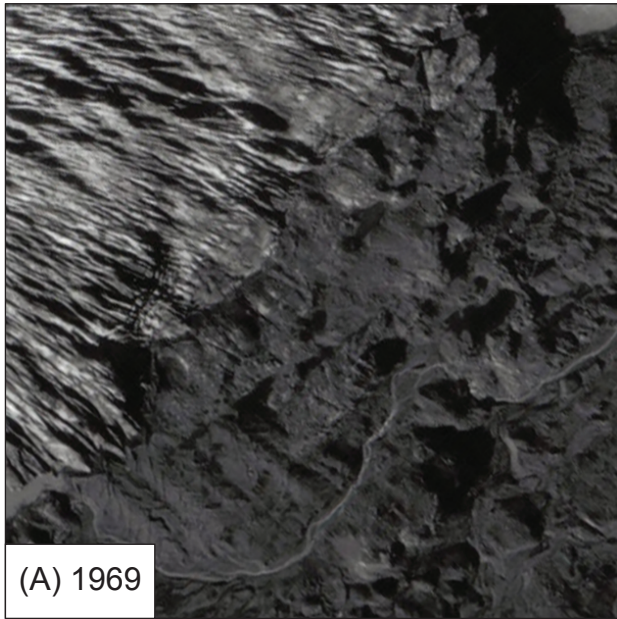


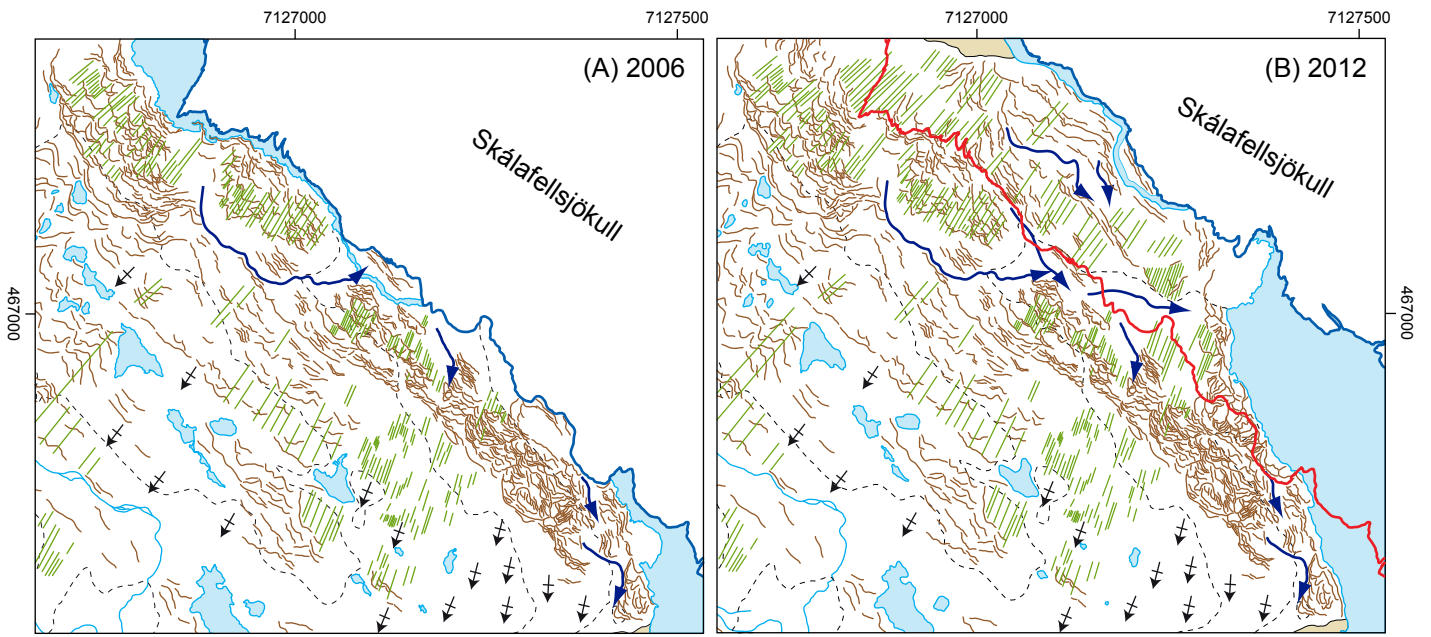
(F) 1979

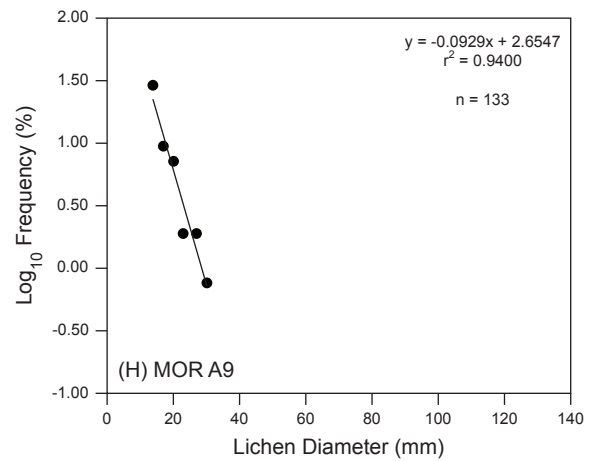
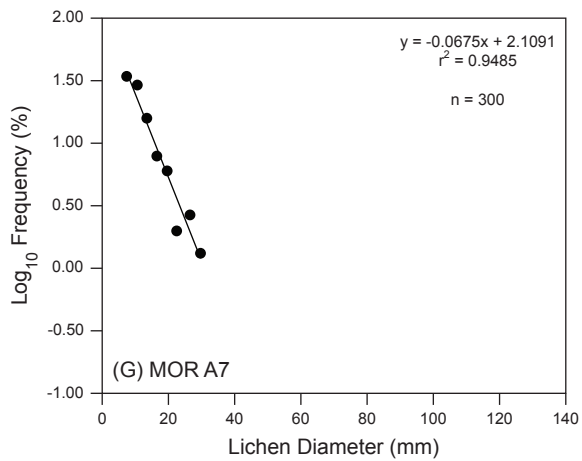
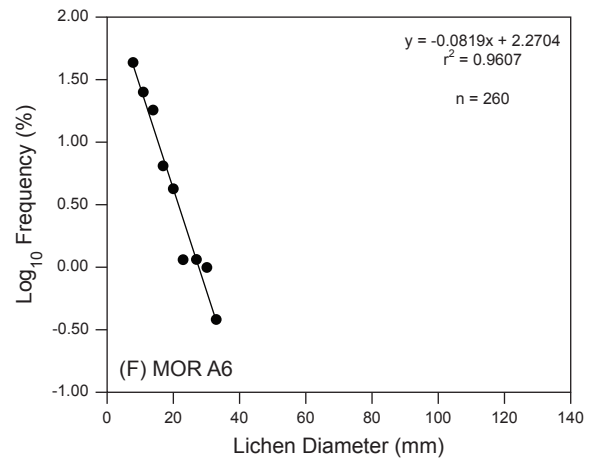
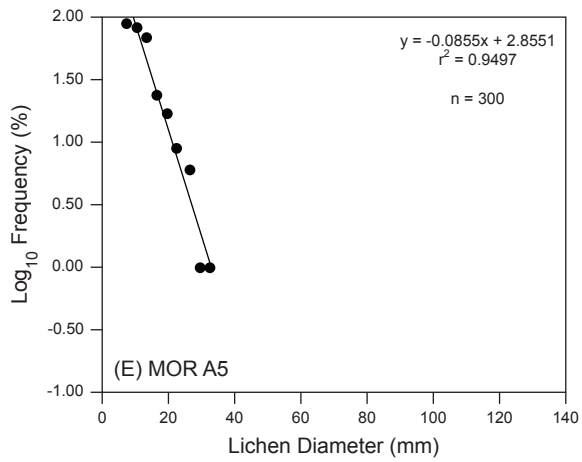
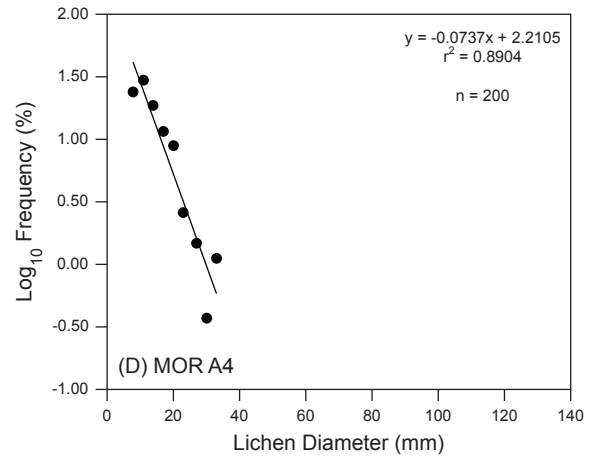
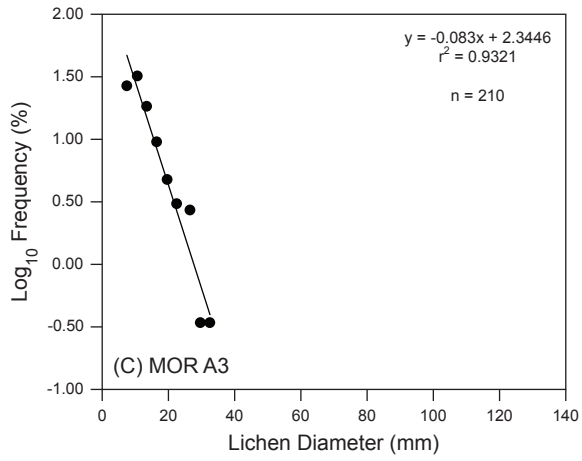
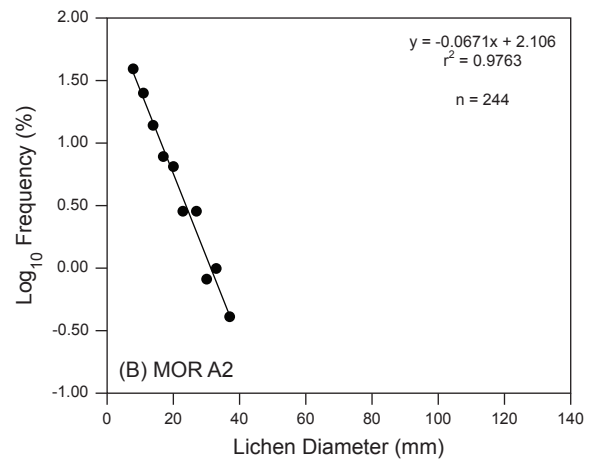
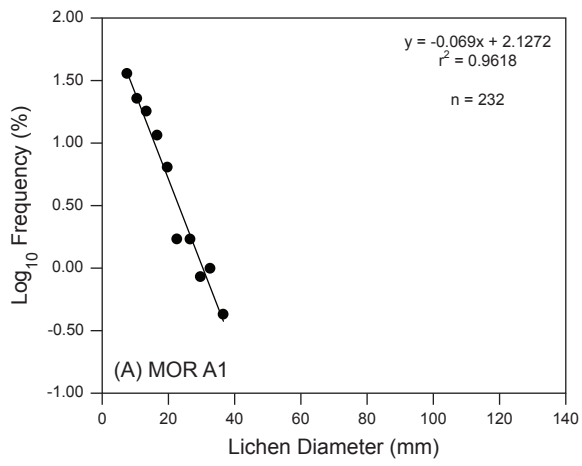


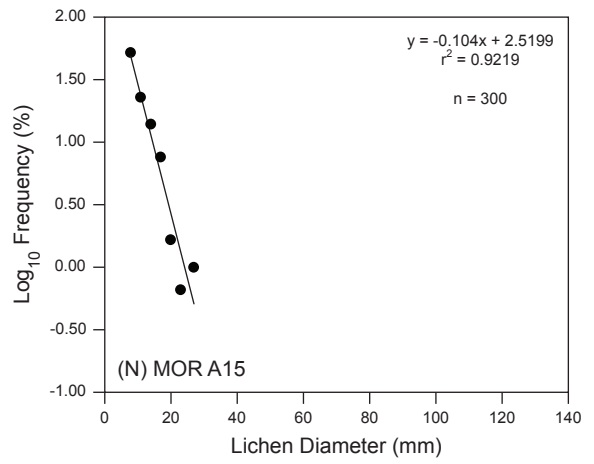
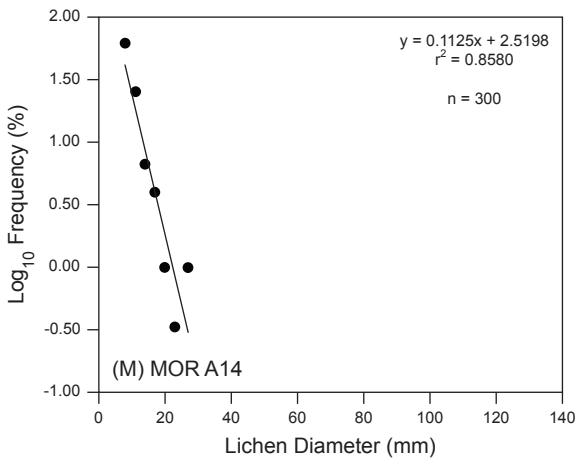
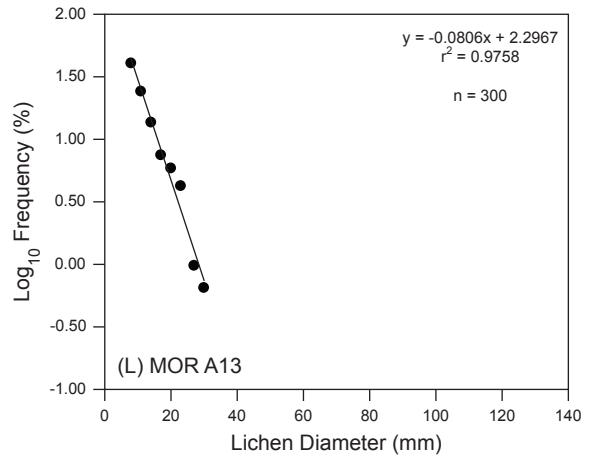
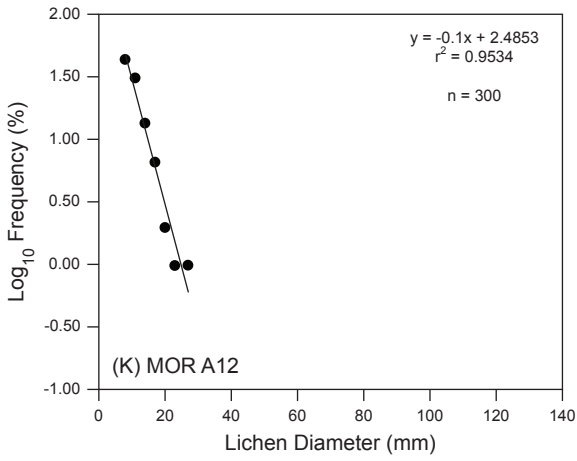
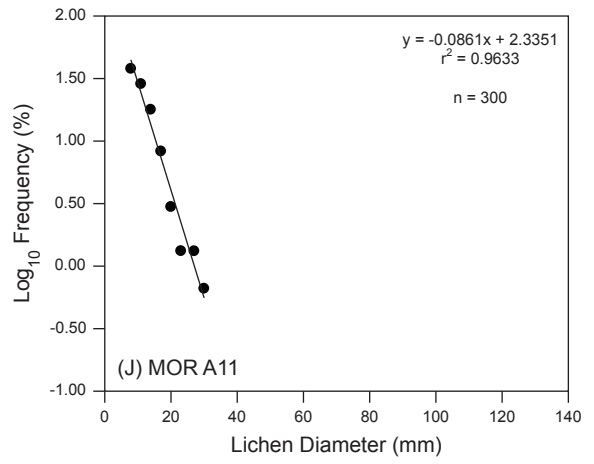
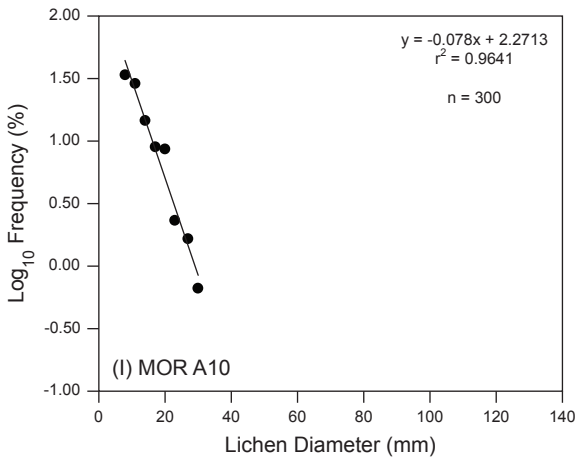


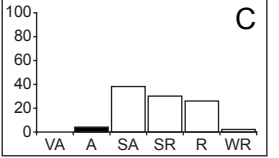
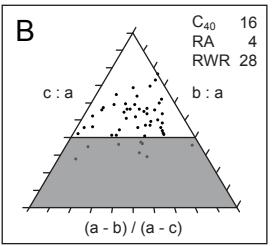
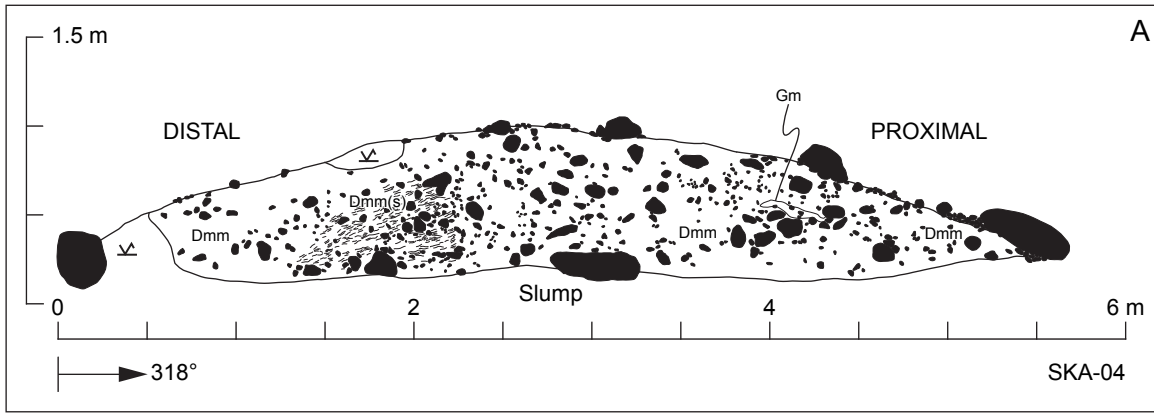


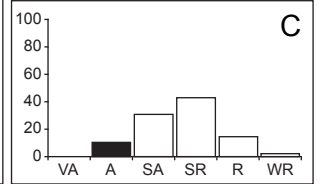
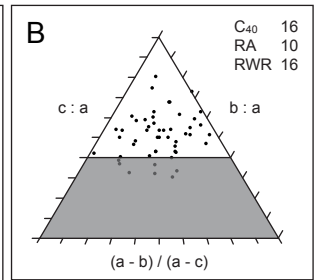
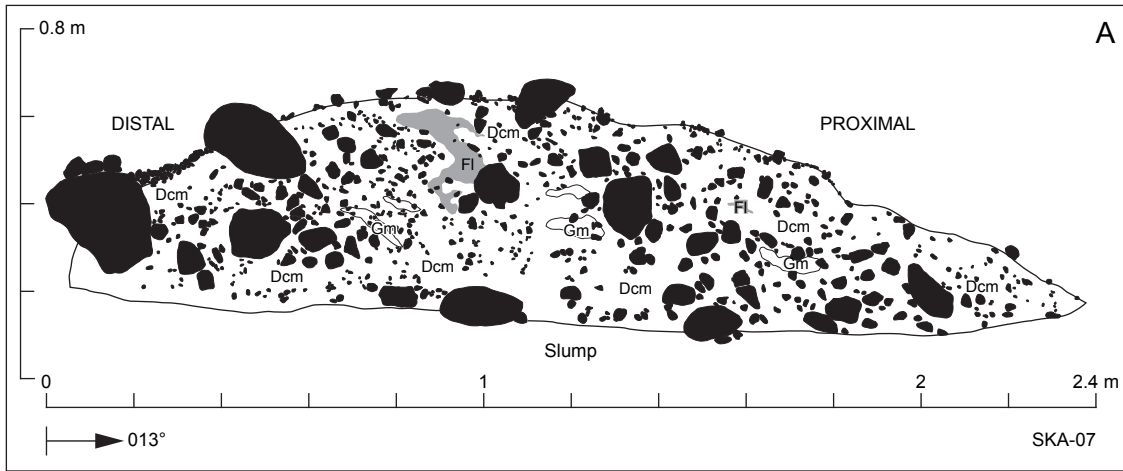




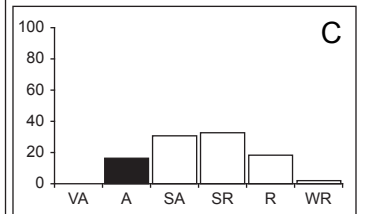
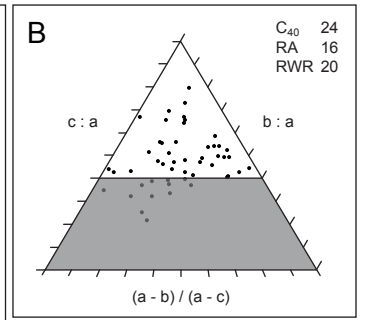
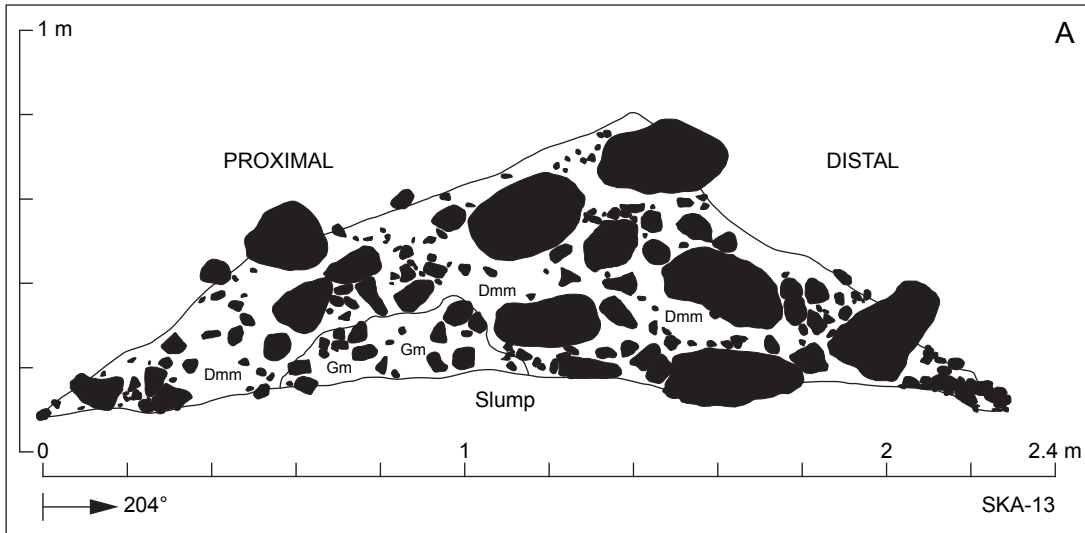


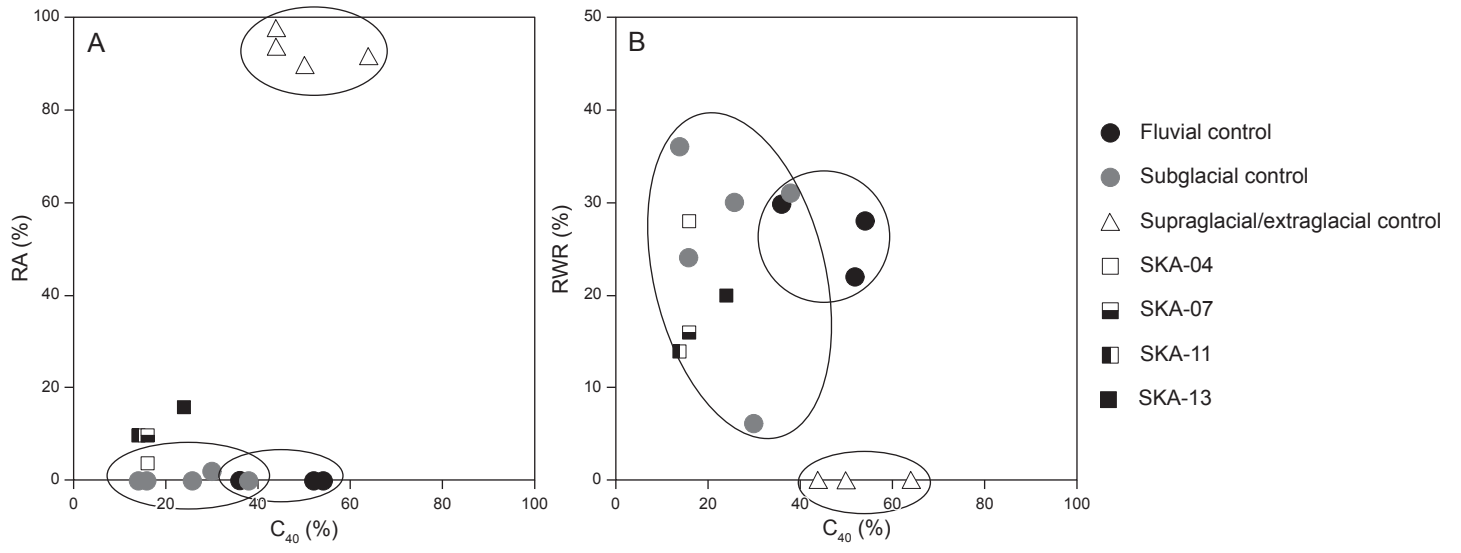






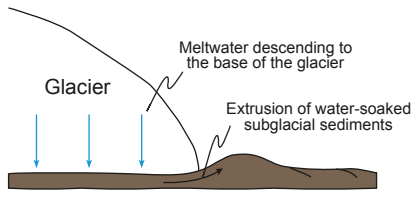




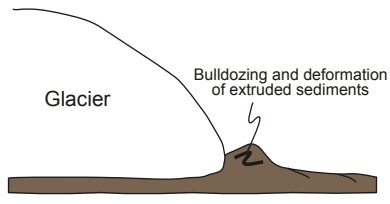


### (A) Squeezing and bulldozing

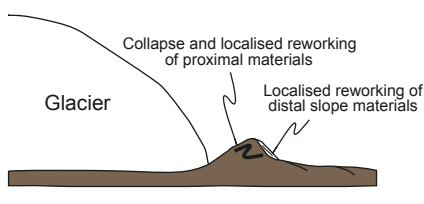
(1) summer



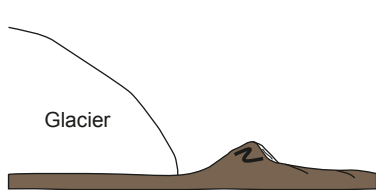
(2) winter



(3) spring

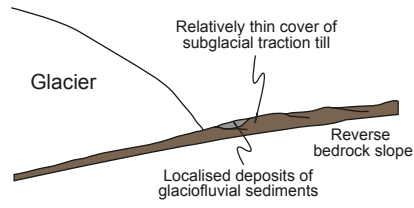


(4) summer

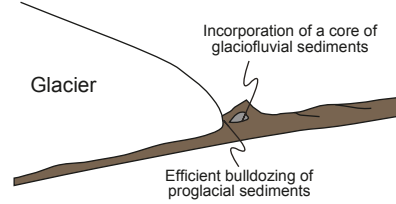


### (B) Bulldozing of proglacial material

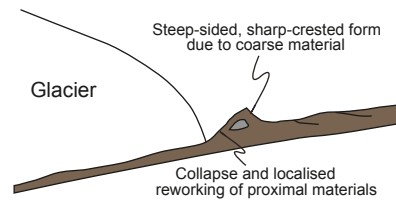
(1) summer



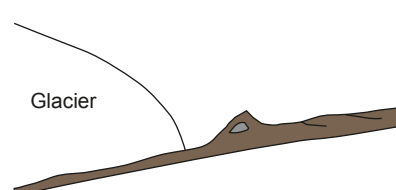
(2) winter



(3) spring

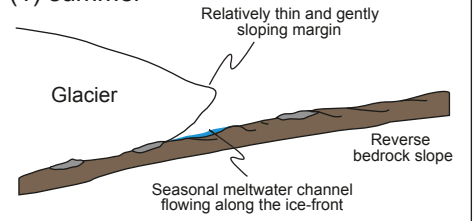


(4) summer

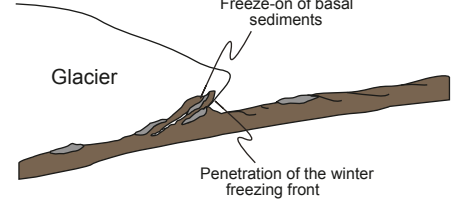


### (C) Submarginal freeze-on

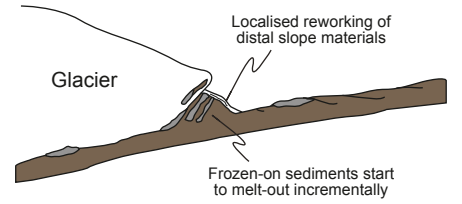
(1) summer



(2) winter



(3) spring



(4) summer

